THE EXPERIMENTAL AND THEORETICAL STUDY OF
METHANE SOLUBILITY IN AN OIL-BASE
DRILLING FLUID

A Thesis

Submitted to the Graduate Faculty of the
Louisiana State University and
Agricultural and Mechanical College
in partial fulfillment of the
requirements for the degree of
Master of Science

in

The Department of Petroleum Engineering

by
Patrick Leon O'Bryan
B.S., Mississippi State University, 1983
December 1985

ACKNOWLEDGEMENTS

TABLES OF CONTENTS

LIST OF TABLES

vi

LIST OF FIGURES

ABSTRACT

A blowout of a well being drilled is one of the most expensive
and potentially dangerous problems faced by the oil and gas produc-
ing industry. A tool that can be used in training personnel and
developing new equipment and well control procedures is a well con-
trol simulator. However, current well control simulators are over
simplified especially when the well is being drilled with an oil-
base drilling fluid.

Current well control simulators often do not take into account
the fact that under certain conditions, a gas kick taken while
drilling with an oil-base drilling fluid might completely dissolve
into the drilling fluid and thus going undetected at the surface un-
til the gas cut drilling fluid is circulated up the well annulus
and the gas rapidly evolves from the drilling fluid. This situa-
tion is very dangerous to rig personnel since there is little time
to implement the proper well control procedures before the well
flows out of control.

The purpose of this study is to perform an experimental study
to determine the solubility of methane, a gas commonly encountered
in the field, in an oil-base drilling fluid and then develop a
computer model to simulate this phenomena.

INTRODUCTION

One of the most expensive and potentially dangerous problems faced by the oil and gas producing industry is the control of high pressure formation fluids encountered while drilling for hydrocarbon reservoirs. If this is not accomplished, a blowout or uncontrolled discharge of formation fluids can occur. When this uncontrolled discharge occurs at the surface or seafloor, it frequently results in damage to the drilling equipment and environment, and sometimes results in personal injury or loss of life. In extreme cases, additional wells must be drilled in order to flood the high pressure formation causing the flow before the blowout can be stopped.

When this uncontrolled discharge from the wellbore is into a subsurface formation, it is difficult and very expensive to correct. Usually, subsurface control can be regained only by sealing off and abandoning the lower portion of the well. Many expensive wells have to be redrilled each year because of underground blowouts as well as surface blowouts.

It has been recognized that blowout prevention measures are the best approach towards reducing the hazard to drilling personnel, equipment, and the environment. Extensive blowout prevention activities

1

have been undertaken by the industry over the past two decades. These activities have included the development of improved equipment, procedures, and personnel training in the use of the equipment and procedures. As the search for petroleum reserves has continued to move to greater depths and more hostile environments, the blowout prevention problem has continued to increase in complexity.

A well control computer model package is a key tool which can be used in evaluating alternative equipment and procedures and in the training of rig personnel in effective well control contingency plans. However, current well control computer models are greatly over simplified and often do not accurately predict well behavior for certain well conditions. One of the greatest current shortcomings is the inability to accurately model well behavior when a gas kick (influx of gas into the well) is taken while drilling with an oil-base drilling fluid.

Figure 1.1 shows the most common kick behavior assumed by existing well control simulators (McKenzie). In this model the gas kick will exist as bubbles dispersed throughout the drilling fluid (assumed to be water-based) and the solubility of the gas in the drilling fluid, although taken into account, is relatively small. While this may be the case for water-

Annular
drilling
fluid
backflow.

Gas & drilling
fluid zone.
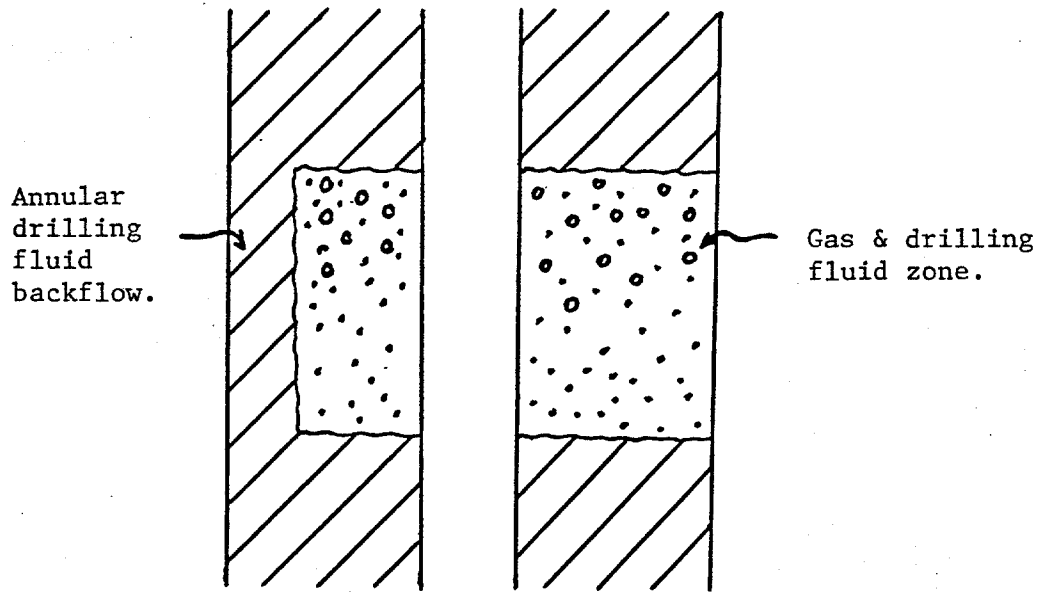
Figure 1.1 Commonly Assumed Gas Kick Behavior.In
Water-based Drilling Fluids.

Zone of rapid
gas evolution.

Dissolved gas
zone.
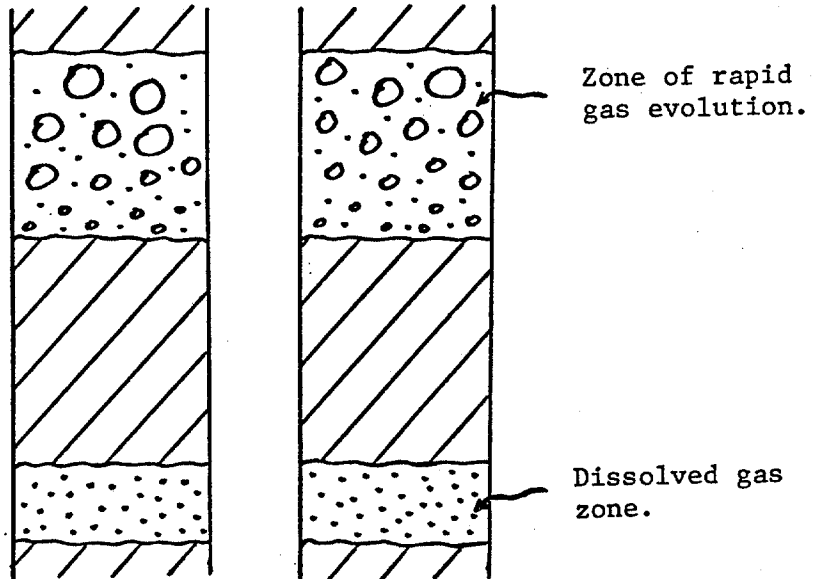
Figure 1.2 Possible Kick Behavior In Oil-based
Drilling Fluids.

based drilling fluids, this is probably not the case when a gas kick is taken while drilling with an oil-based drilling fluid.

Although it is recognized that reservoir gas mixes and dissolves in an oil-based drilling fluid, the mixing mechanism and subsequent events are poorly understood. From field experience, kick detection is thought to be much more difficult when the formation gas readily dissolves in the drilling fluid. Also, when the kick is circulated to the surface, the rapid evolution of gas from the drilling fluid makes proper operation of the well control choke much more difficult (Figure 1.2). An ability to fully understand and mathematically model this phenomenon is extremely desirable.

Even when a gas kick is not taken, gas which occupies the pore space of rock destroyed by the bit may enter the mud system. This is commonly called drilled gas. When drilled gas is pumped to the surface in an oil-based drilling fluid very rapid gas evolution and expansion is sometimes absent resulting in a dangerous situation occuring at the rig floor with the release of the drilled gas at the surface. It has been reported that in some cases, the rotary bushings have been knocked out of the rotary table by the violent release of gas from the well. Mathematical modelling of drilled gas in a well is also desirable.

The objectives of this study were: (1) to measure gas solubilities for several base-oils used to prepare oil-based drilling fluids, (2) to measure gas solubility in a typical oil-based drilling fluid, (3) to determine factors which affect the solubility of gas in oil-based drilling fluids, and (4) to develop a computer model for predicting gas/oil-based drilling fluid phase behavior.

CHAPTER II

LITERATURE REVIEW

O'Brien was the first to report the results of a
study on well control problems caused by gas solubility
in oil-based drilling fluids. In this 1981 study, the
differences between gas solubility in water-based and
oil-based drilling fluids were discussed. The author
stated that the solubility of gas in water-based drilling
fluids was so small that for all practical purposes it
was negligible. Although the author made no experimental
measurements he went on to state that at the same
temperature and pressure, the solubility of gas in an
oil-based drilling fluid would be 10 to 100 times greater
than the solubility in water-based fluids.

In order to more fully understand how much gas would
actually dissolve in an oil-based drilling fluid under
the influence of reservoir pressures and temperatures,
Thomas, Lea, and Turek presented experimental data on the
solubility of methane in diesel oil and in a 9.0 pound
per gallon (ppg) density, diesel oil-based drilling fluid
at 100 degree F. In practice, the most common
representation of the solubility of a gas in a liquid is
by the bubble point pressure of the gas/liquid mixture.
By definition, the bubble point pressure is the pressure
at which the first bubble of gas forms in the liquid

6

phase of a mixture. The authors presented nine bubble point pressures for varying mole fractions of methane and diesel oil and three bubble point pressures for varying weight fractions of methane and the oil-based drilling fluid.

A summary of the data obtained from the experiments of Thomas, Lea, and Turek are shown in Tables 2.1 and 2.2. They found that the bubble point pressures for the methane/oil-based-drilling-fluid systems were higher than those for the methane/diesel-oil systems having the same weight percent methane. This was expected since the drilling fluid contains components other than diesel oil in which methane does not readily dissolve. For example, a significant fraction of an oil-base drilling fluid is composed of brine and solids. To predict methane/oil-based drilling fluid bubble point pressures, the authors chose the Amoco Redlich-Kwong equation of state (ARKES). The ARKES is given as:

$$p = RT/(V_m - b) - a/[T^{.5}V_m(V_m + b)] \qquad (2.1)$$

where p = pressure, psia

R = universal gas constant, $10.73 \dfrac{psia \cdot ft^3}{lb\text{-}mol \cdot R}$

T = temperature, $^{\circ}R$

V_m = molar volume, $ft^3/lb\text{-}mole$

Table 2.1 Amoco experimental data for methane in diesel
(Thomas, Lea, and Turek).

Methane (mol %)	Bubblepoint Pressure at 100 F (psia)
19.08	805
23.92	1,000
28.76	1,320
34.28	1,682
39.01	2,065
44.24	2,405
54.26	3,635
61.23	4,820
66.45	5,790

Table 2.2 Amoco experimental data for methane in
oil-base drilling fluid
(Thomas, Lea, and Turek).

Methane (wt %)	Bubblepoint Pressure at 100 F (psia)
1.846	1,555
3.626	2,570
5.342	3,585

*Density of oil-based mud at 14.7 psia and
78 F = 1.0985g/cm .

$$b = \text{molecular repulsion parameter, } ft^3/\text{lb-mole}$$

$$a = \text{molecular attraction parameter, } psia \cdot \left(\frac{ft^3}{\text{lb-mole}}\right)$$

The a and b parameters were determined as functions of the critical properties of the individual components making up the mixture or phase (liquid or vapor below the bubble point, liquid above the bubble point) with equations given as:

$$a = \Omega_a R^2 T_c^{2.5}/P_c \tag{2.2}$$

and,

$$b = \Omega_b R T_c/P_c \tag{2.3}$$

where Ω_a = Yarborough dimensionless parameter

Ω_b = Yarborough dimensionless parameter

a = molecular attraction parameter, $psia \cdot \left(\frac{ft^3}{\text{lb-mole}}\right)$

b = molecular repulsion parameter, $ft^3/\text{lb-mole}$

P_c = critical pressure, psia

T_c = critical temperature, $^{\circ}R$

R = universal gas constant, $10.73 \frac{psia \cdot ft^3}{\text{lb-mol} \cdot R}$

Once the a and b parameters had been determined for the pure components making up the mixture or phase, the overall a and b parameters for the entire mixture or phase were determined from equations given as:

$$a_m = \underset{ij}{\Sigma\Sigma} x_i x_j (1 - C_{ij})(a_i a_j)^{.5} \tag{2.4}$$

and,

$$b_m = \underset{i}{\Sigma} x_i b_i \tag{2.5}$$

where C_{ij} = binary interaction coefficient

x_i = mole fraction of component i in the phase

x_j = mole fraction of component j in the phase

a_i = molecular attraction parameter of component i

a_j = molecular attraction parameter of component j

a_m = molecular attraction parameter of phase

b_i = molecular repulsion parameter of component i

b_m = molecular repulsion parameter of phase

In order to predict methane/drilling fluid bubble point pressures with the ARKES, the authors had to account for methane solubility in the brine, surfactants, and solids in the drilling fluid. To account for the solubility of methane in the sodium chloride brine used in their drilling fluid, the authors used the work of O'Sullivan and Smith. To model the effects of the surfactants and solids in the drilling fluid, the authors treated these as equivalent amounts of diesel fuel and used the EOS to predict adsorption isotherms. The final adjustment to the ARKES was the use of a nonzero binary interaction coefficient. The value was 0.061 and was used in Equation 2.4 with all methane and diesel component binaries. Figures 2.1 and 2.2 show the equation of state match with their experimental data.

In 1984, Matthew published work on how to handle acid gas (hydrogen sulfide and carbon dioxide) kicks in
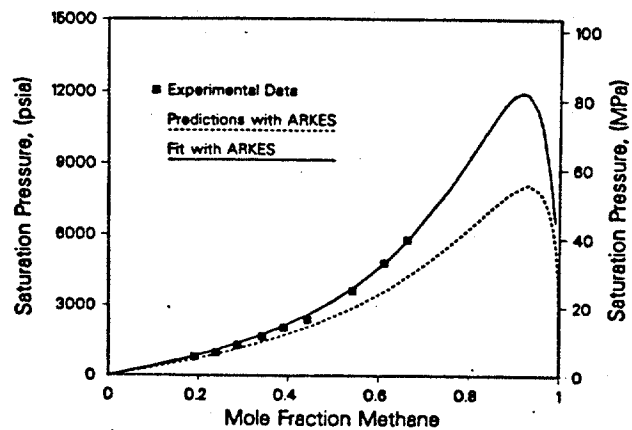
Figure 2.1   ARKEOS fit of methane/diesel
            experimental data (Thomas,
            Lea, and Turek).
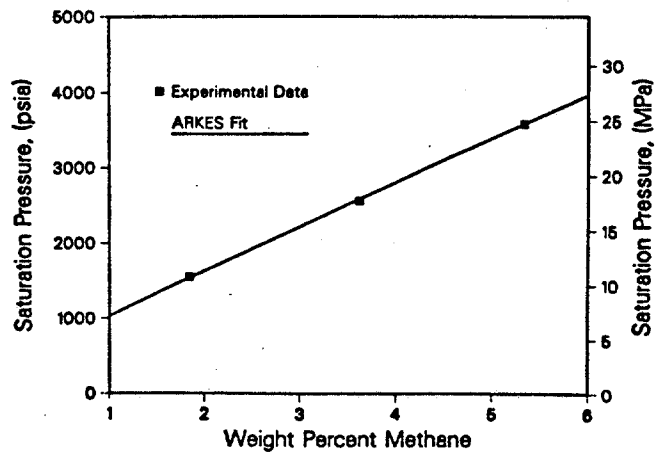
Figure 2.2   ARKEOS fit of methane/drilling
            fluid experimental data (Thomas,
            Lea, and Turek).

oil-based drilling fluids. Experimentally determined solubility curves for methane as well as carbon dioxide and hydrogen sulfide in diesel oil at 250.0 degree F were presented. Chemicals used to build oil-based drilling fluids were not taken into account and fluid compressibilties were neglected. Also it was assumed that all solution gas was liberated at the bubble point. It was concluded that the relative solubilities of gases entering the wellbore are different and that of the three gases studied, methane will break out of solution first. As the pressure is further reduced, carbon dioxide will be next to break out and hydrogen sulfide will be the last.

CHAPTER III

EXPERIMENTAL STUDY

After reviewing the literature it was evident that more experimental data was needed. In addition to a need for more bubble point pressure data, there was a need for density measurements for gas/oil-based-drilling-fluid systems. Knowledge of the densities of the fluids occupying the wellbore after a gas kick has occurred is critical to the success or failure of well control simulation predictions to adequately describe actual well conditions. Also these phase behavior data were required over a wider range of temperatures than those studied in previous investigations in order to more closely represent actual well conditions. Finally, an expansion to previous investigations was needed to determine whether the new low toxic oils (Salisbury) recently developed for use in oil-based drilling fluids affect gas solubility in the drilling fluid.

This chapter discusses the experiments that were performed in this study. Covered are the experimental apparatus and calibration, experimental procedures, presentation of the data, and discussion of the data obtained.

3.1 Experimental Apparatus and Calibration

To measure the bubble point pressures of gas/liquid

systems at elevated temperatures, a laboratory apparatus was designed and constructed as shown in Figure 3.1. The system has a 250 ml positive displacement pump used to displace mercury into a blind pressure-volume-temperature (PVT) cell. The PVT cell is constructed of stainless steel, has a capacity of about 1000 ml, and has a maximum operating pressure of 10,000 psia. Pressure is monitored using a 10,000 psig bourdon tube gauge. The PVT cell is heated with a heating mantle and heat losses to the atmosphere are minimized by the addition of extra insulation. The temperature of the system is controlled by a dual set point temperature controller connected to the heating mantle. The temperature of the cell is monitored using a digital thermometer with a platinum resistance probe placed between the PVT cell and heating mantle. The PVT cell is mounted on a stand that allows rotation of the cell during experiments which facilitates mechanical mixing of the fluids being studied.

Loading of the PVT cell is done with the aid of sample bottles and a burret. The sample bottles are 500 ml, stainless steel bottles connected at the bottom to the positive displacement pump, and at the top to a manifold which allows access to either the gas storage bottles or the PVT cell. These sample bottles are used to load the gas into the PVT cell. The burret is a 1000 ml, glass burret with a teflon stop cock. It is
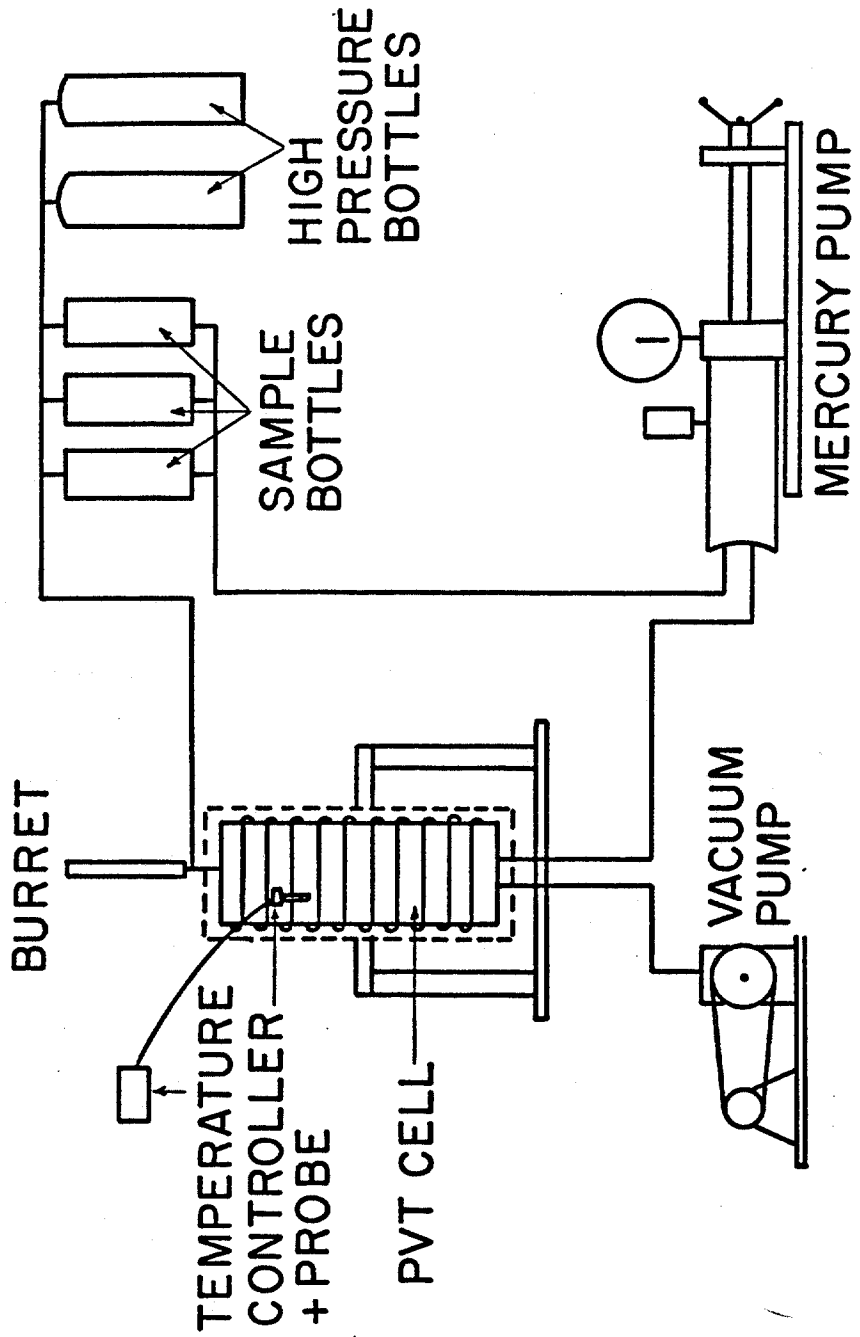
Figure 3.1 Experimental Apparatus

connected to the PVT cell and is used to load the liquids into the cell.

Communication between various parts of the system is controlled with 19 valves placed at various points throughout the system. All the valves used have a 10,000 psia, maximum pressure rating. The large number of valves allows isolation of any part of the system preventing down time of the rest of the system should any system component need repair or cleaning.

Once the laboratory apparatus was operational, calibration of the system over the expected experimental range of pressures and temperatures was performed. To calibrate the system, the manifold and cell were filled with mercury and compressibilities were measured at several temperatures. A calibration computer program was then used to generate an equation describing the PVT cell capacity as a function of temperature and pressure. This equation takes into consideration the expansion of the cell due to pressure and temperature and also accounts for variations in the volume of mercury in the cell due to pressure and temperature. A listing of the calibration program, data used for calibration of the system, and the cell equation can be found in Appendix A.

3.2 Experimental Procedures

Experiments were conducted in two parts. The first part was experiments with gas and pure oil and the second

was with gas and an oil-based drilling fluid. In order to use the work of Thomas, Lea, and Turek as a basis for comparison, methane was chosen as the gas for this study. In addition, communication between the author and various industry personnel has shown that methane is the most common and troublesome gas in the field and a study with this gas was most desirable. Diesel, Mentor 28, and Conoco LVT oils were used as the liquid phases for the methane/pure-oil study and a 13.0 pound per gallon (ppg) oil-based drilling fluid was used in the methane/drilling -fluid study.

3.2.1 Methane/pure-oil Systems

As a means of characterizing the mixtures used in these experiments, a molar percentage of each component in the mixture for a given experiment was determined. The procedure followed to accomplish this is outlined in Appendix B.1.

Once the PVT cell was loaded, the system was allowed at least four hours to heat up to the experimental temperature while compressibilities of the positive displacement pump and associated tubing were remeasured. This was done at the beginning of each experiment due to fluctations in the room temperature, the possibility of gas being trapped in the pump or pressure gauge, and as a check for system leaks.

When the system had reached run temperature and the

system compressibilities had been measured, mercury was pumped into the PVT cell in small increments. At each increment, the pump volume, the cell pressure, and the cell temperature were recorded. The cell was periodically rotated and the pressure readings were checked and recorded until the pressure was stabilized, indicating equilibrium in the cell. This procedure was repeated for various cell volumes until a pressure-volume isotherm was defined.

Once the experiment had been completed, the raw data was entered into the calibration computer program listed in Appendix A. The program generated the bulk volume of the methane/oil sample mixture for a given pressure, temperature, and indicated pump volume. Appendix C provides the raw data, calibrated data, and plots of the data before and after calibration for a typical experiment.

After each experiment, more methane was added to the PVT cell, as described in Appendix B.1, and the procedures just described were repeated. After the desired number of data points had been obtained at a given temperature, the system was cleaned with toluene and hexane, dried, reloaded, and heated to the new experimental temperature.

3.2.2 Methane/oil-based-drilling-fluid Systems

The methane/oil-based-drilling-fluid experimental

procedure was the same as just described for the methane/oil experiments except for the way the mixtures were characterized. Since an oil-based drilling fluid has no readily measureable molecular weight, methane/drilling fluid mixture components were reported as weight fractions of the total mixture weight. The procedure for determining these weight fractions and loading the PVT cell for the methane/drilling-fluid experiments is outlined in Appendix B.2.

3.3 Experimental Results

Experiments were performed at temperatures of 100, 200, and 300 degree F. It was felt that these temperatures would adequately represent most well conditions encountered in the field while making data obtained more systematic for analysis.

The methane/pure oil study was broken up into three separate studies: (1) methane/diesel - oil, (2) methane/Mentor 28-oil, and (3) methane/Conoco LVT-oil. Only the methane/Mentor 28 system was studied at all three above mentioned temperatures. This was because it has been stated that Mentor 28 is one of the more commonly used oils in mixing oil-based drilling fluids at this time (Billingsley). The other systems were studied at 100 degree F for reasons stated later in this text.

The final set of experiments were performed with the methane/13.0 ppg oil-based drilling fluid system. This

study was also conducted at the above mentioned temperatures.

3.3.1 Methane/diesel-oil Study

This set of experiments were conducted for three reasons:

1. To get familiar with the laboratory apparatus and make sure it was working properly,

2. To check the experimental procedure by trying to match data presented in the work of Thomas, Lea, and Turek, and

3. To compare bubble point pressures for methane/low - toxic - oil (Mentor 28 and Conoco LVT) systems.

Figure 3.2 shows the current study's experimentally determined bubble point pressures for methane/diesel oil systems at 100 degree F and those of Thomas, Lea, and Turek plotted as bubble point pressure vs mole percent methane soluble in diesel at that pressure (Table 2.1 shows the experimental data of Thomas, Lea, and Turek). The agreement between the two sets of data is excellent. It was concluded that this study's experimental methods and procedures were correct and work proceeded.

Table 3.1 is a summary of the experimental data for

Table 3.1:   Methane/diesel Experimental Data

Mole % Methane	Bubble Point Pressure, psia
19.50	720.0
30.26	1220.0
32.45	1475.0
46.46	2545.0
56.35	3795.0
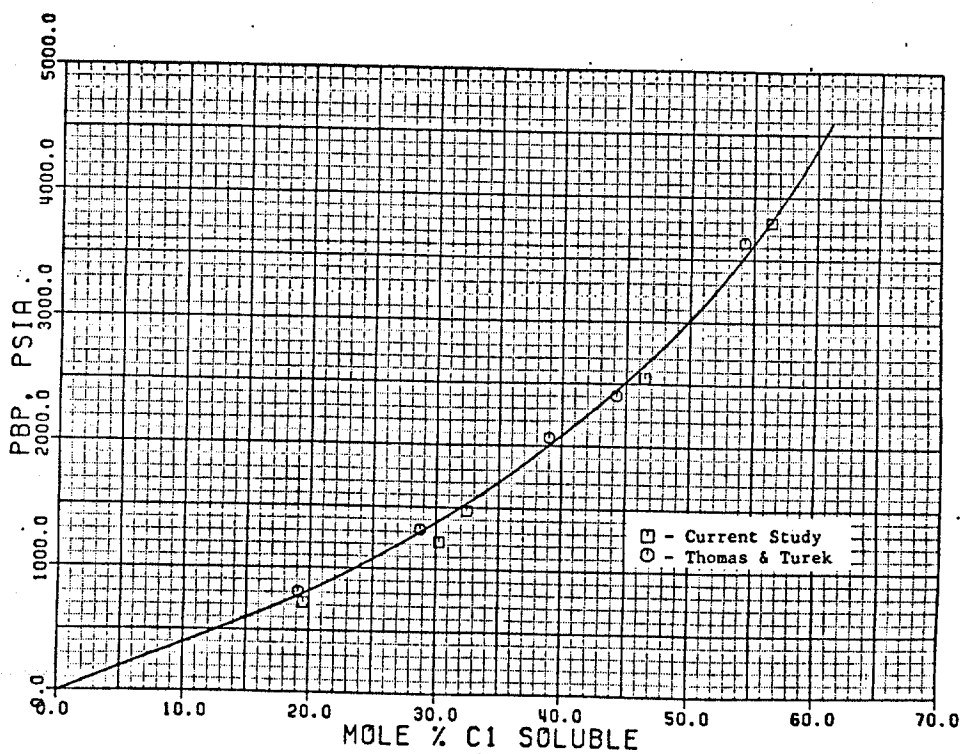
Figure 3.2:   Current Study vs Thomas, Lea, and Turek Experimental Data for Methane/diesel (T = 100 deg F).

this particular study. The calibrated data for each individual experiment is shown in Appendix D.1.

3.3.2 Methane/Mentor 28 Study

Five experiments were performed at each temperature. The number of experiments conducted was governed by the pressure limits of the laboratory apparatus and the accuracy with which the bubble point pressure could be determined. As the mole percent methane in the system increases, the distinct break in the pressure versus volume plot which indicates the bubble point pressure diminishes (Figure C.2). Therefore, the upper limit for the gas composition in the system was set at 50.0 mole percent.

Figure 3.3 shows the experimental data plotted as bubble point pressure verus mole percent methane soluble in Mentor 28 at that pressure. A summary of the experimental data for this study can be found in Table 3.2 and the actual calibrated data for each experiment can be found in Appendix D.2.

3.3.3 Methane/Conoco LVT-oil Study

This study was conducted to make available data for more than just one methane/low-toxic-oil system for comparison to the methane/diesel-oil study. The reason for this will be pointed out later in this text. Four experiments were performed at 100 degree F for this

23
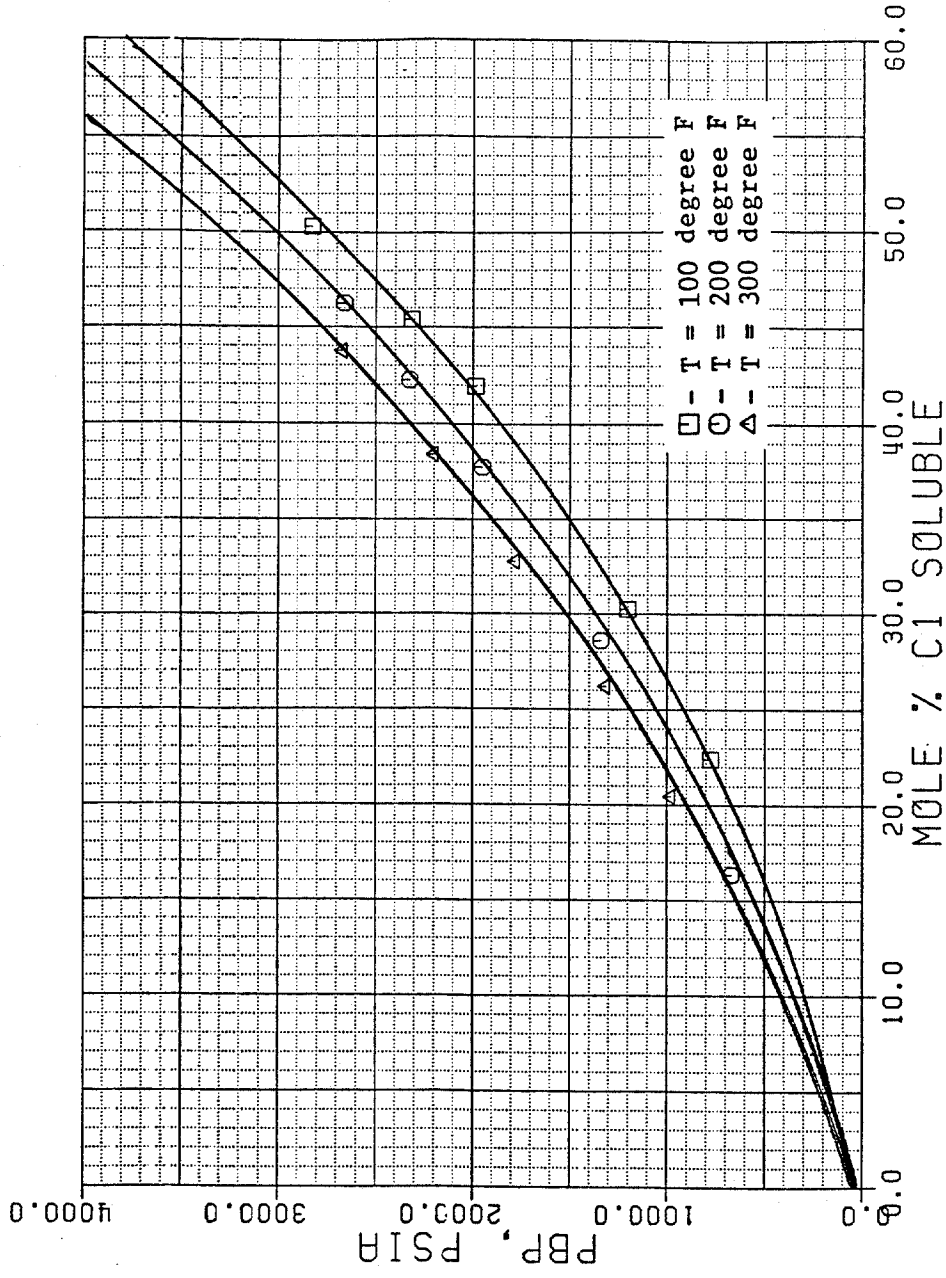
Figure 3.3: Experimental Data For Methane/Mentor 28
Oil Systems.

Table 3.2: Methane/Mentor 28 Experimental Data

Mole % Methane	Bubble Point Pressure, psia	Temperature, deg F
22.42	775.0	100.0
30.24	1200.0	100.0
41.95	1985.0	100.0
45.38	2315.0	100.0
50.29	2825.0	100.0
16.33	670.0	200.0
28.58	1340.0	200.0
37.73	1950.0	200.0
42.27	2325.0	200.0
46.25	2660.0	200.0
20.43	980.0	300.0
26.19	1315.0	300.0
32.73	1780.0	300.0
38.39	2199.0	300.0
43.75	2670.0	300.0

study. Figure 3.4 shows a plot of the experimental data obtained as bubble point pressure versus mole percent methane soluble in Conoco LVT at that pressure. Table 3.3 is a summary of the experimental data and Appendix D.3 contains the actual calibrated data for each experiment.

3.3.4 Methane/oil-based-drilling-fluid Study

The oil-based drilling fluid used in this study was 80 volume percent oil, 20 volume percent brine, and had a density of 13.0 ppg. The fluid was mixed with Mentor 28 as the base oil and the brine was a 300,000 ppm calcium chloride solution. Table 3.4 shows a summary of the formulation used to mix this drilling fluid.

One of the problems with using a drilling fluid mixed in a laboratory for experiments is that they do not adequately represent a drilling fluid in the field. To overcome this problem, the drilling fluids used in these experiments were mixed with a homogenizer or high shear mixer, to give the drilling fluid a shear representative of a fluid that has been run through a drilling bit in the field. Also, the drilling fluids were dynamically temperature aged at 300 degree F for 24 hours in a roller oven. This aging would aid in simulating an actual field drilling fluid while providing a means of checking the stability of the drilling fluid emulsion and removing any air trapped in the fluid during

Table 3.3: Methane/Conoco LVT Experimental Data

Mole % Methane	Bubble Point Pressure, psia
9.91	395.0
21.49	875.0
29.88	1345.0
42.84	2080.0
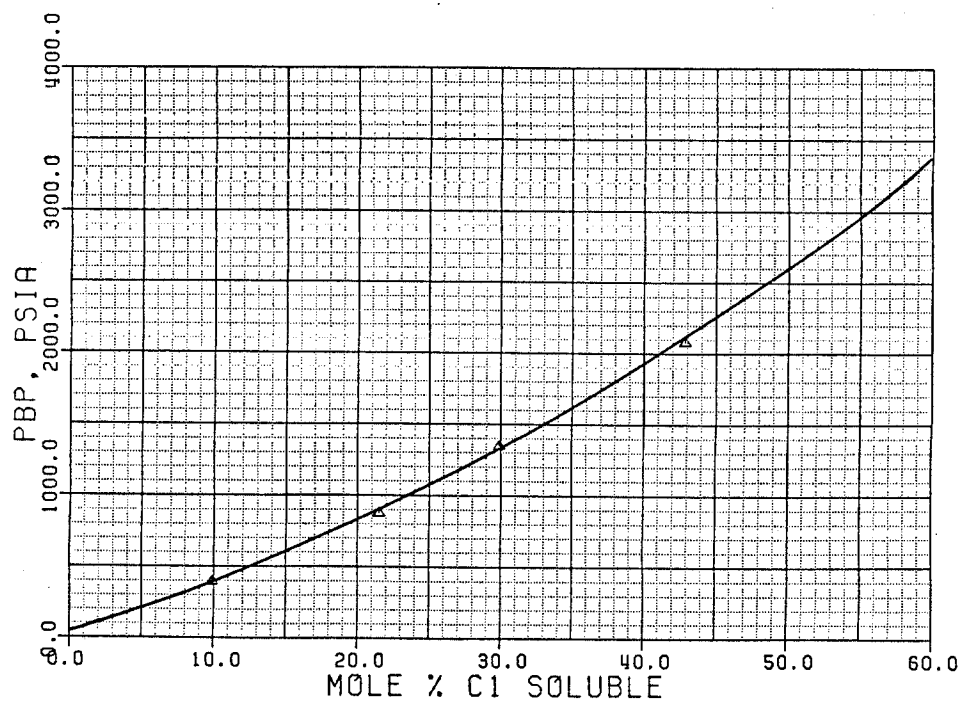
Figure 3.4: Experimental Data For Methane/Conoco
LVT Oil Systems.

Table 3.4: 13.0 ppg Drilling Fluid Formulation

Component	Volume, cc	Weight, gm
Mentor 28	225.0	--
lime	--	4.5
primary emulsifier	12.0	--
filtration agent	--	5.0
fresh H20	50.0	--
gelling agent	--	4.5
secondary emulsifier	6.0	--
CaCl2	--	23.0
Barite	--	292.0

mixing.

Table 3.5 summarizes the bubble point pressures determined for this study. Figure 3.5 shows this data plotted as bubble point pressure versus weight percent methane soluble in the drilling fluid at that pressure. A summary of the actual calibrated data for each experiment can be found in Appendix D.4.

3.4 Discussion of the Results

In this section a comparison of the methane/diesel-oil and methane/low-toxic-oil studies is presented. In addition, the results for methane/drilling-fluid versus methane/oil systems are contrasted. A discussion of system densities and the effect of temperature on bubble point pressures is also presented.

3.4.1 Methane/diesel-oil and Methane/low-toxic-oil Comparison

Low toxic oils differ from diesel oils in the aromatic hydrocarbon content of each. Aromatic hydrocarbons are very toxic to the environment and because diesel oils have a high content of these, their use in the environment is very restricted. Low toxic oils have recently been developed in an attempt to reduce the risk of environmental damage caused by the use of oil-based drilling fluids. Their aromatic content has been reduced while their paraffinic (straight and branched

Table 3.5: Methane/13.0 ppg Drilling Fluid Experimental Data

Weight % Methane	Bubble Point Pressure psia	Temperature deg F
2.9	2925.0	100.0
3.4	3605.0	100.0
4.3	4425.0	100.0
0.57	780.0	200.0
1.70	2135.0	200.0
2.32	2875.0	200.0
1.07	1600.0	300.0
2.32	3080.0	300.0
2.52	3275.0	300.0
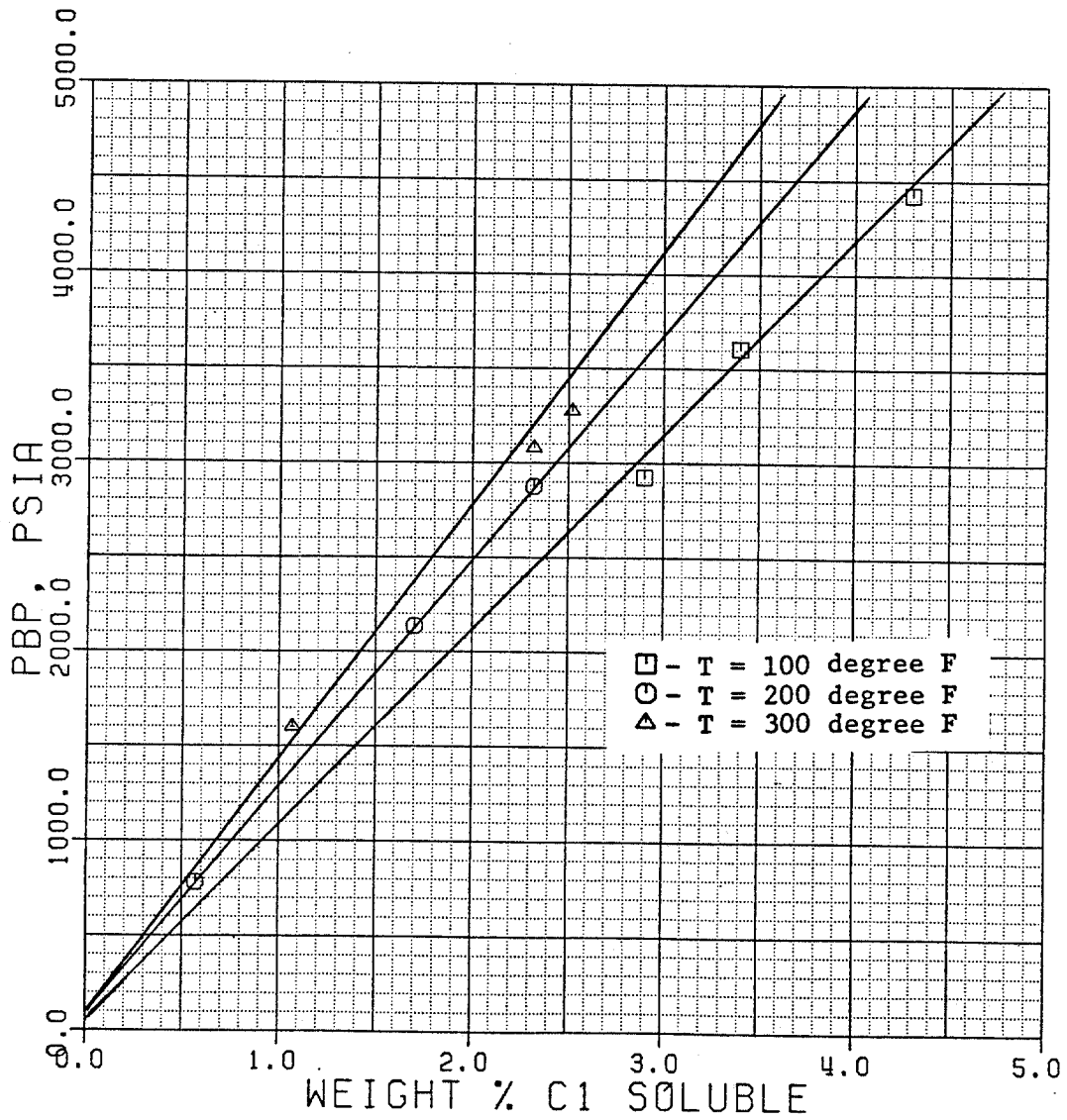
Figure 3.5:   Methane/drilling fluid Experimental Data

chain alkanes) and napthenic (cyclic alkanes) content has been increased. A detailed discussion of the chemical and physical properties of low toxic oils is beyond the scope of this study, however, the reader is refered to Bennett, Boyd, et.al., and Salisbury and Jachnik.

Figure 3.6 shows a plot of bubble point pressure versus mole percent methane soluble in the oil at that pressure for the methane/diesel, Mentor 28, and Conoco LVT oil studies at 100 degree F. All three sets of data appear to lay along the same curve with the methane/Conoco LVT data showing slightly higher bubble point pressures. The minor variations evident in the experimental data are considered negligible for the field since the type of oil is one of many chemical variations in a drilling fluid which can affect the bubble point pressure. This is significant for mathematical modeling purposes because a generalized oil can be derived from the compositions of the three oils tested which would allow adequate representation of most oils used in the field for mixing oil-based drilling fluids. The advantage of having this generalized oil composition will be pointed out in the mathematical modeling section of this text. For now, the composition of the new generalized oil is introduced.

Tables 3.6 - 3.8 show the molar composition of the diesel, Mentor 28, and Conoco LVT oils as determined from

32
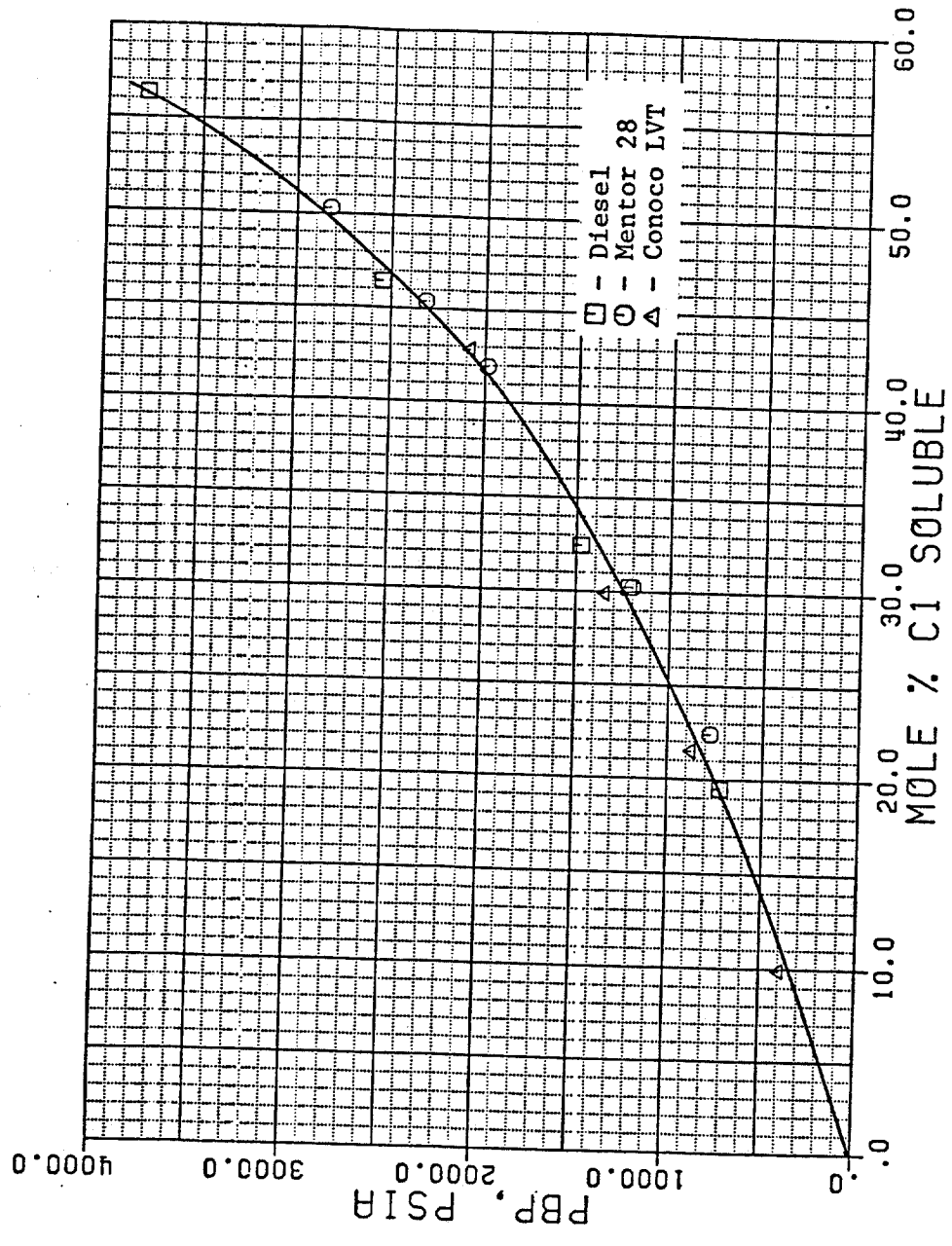
Figure 3.6: Methane Dissolved In Diesel, Mentor 28, and Conoco LVT Comparison (T = 100 $^\circ$F).

Table 3.6: No. 2 Diesel Oil Molar Composition

Carbon Number	Mole Percent
9	1.3997
10	2.5340
11	4.0720
12	6.5313
13	11.6477
14	12.2027
15	16.0007
16	14.3790
17	11.8823
18	8.9947
19	4.2977
20	1.7457
21	2.5613
22	1.1000
23	0.4487
24+	0.2013
	Σ = 100.00

Molecular Weight = 204.2 lb/lb-mole

Density @ 60.0 deg F = 6.9358 ppg

Table 3.7: Mentor 28 Molar Composition

Carbon Number	Mole Percent
13	1.4187
14	2.2240
15	6.0817
16	11.6920
17	9.4953
18	31.8370
19	28.1870
20 +	10.0710
	Σ = 100.00

Molecular Weight = 252.0 lb/lb-mole

Density @ 60.0 deg F = 7.1168 ppg

Table 3.8: Conoco LVT Molar Composition

Component Number	Mole Percent
9	1.1736
10	11.2037
11	24.1092
12	16.5396
13	11.8951
14	17.6742
15	15.2455
16	1.4253
17+	0.7333

$$\Sigma = \overline{100.00}$$

Molecular Weight = 177.35 lb/lb-mole

Density @ 60.0 deg F = 6.7426 ppg

gas chromatographic analysis performed as part of this study. The molecular weights of the oils are also shown. The Conoco LVT oil was included in this study because the molecular weight of this oil is lower than that of the other two oils. This gives added confidence that the compositional range of most oils used in the field for mixing oil-based drilling fluids has been covered. Table 3.9 shows the molar averaged, generalized oil composition and the corresponding molecular weight as determined from the compositions of the three oils used in this study.

3.4.2 Methane/oil and Methane/drilling-fluid Comparison

Figure 3.7 shows a comparison of the methane/oil and methane/drilling - fluid experiments. For comparison purposes, the mole percent methane soluble in pure oil has been changed to weight percent methane soluble. As you can see, the bubble point pressures for the methane/drilling-fluid systems are much higher than those for the methane/oil systems. The higher bubble point pressures mean that the methane is less soluble in the drilling fluid than it is in the oil. Air also could cause higher bubble point pressures in the methane and drilling fluid systems if air was trapped in the drilling fluid.

Extrapolation of the bubble point curves to zero weight percent is one test that can be made to determine if air was being trapped in the sample. This test was

Table 3.9: Generalized Base Oil Composition

Component Number	Mole Percent
9	0.8578
10	4.5792
11	9.3937
12	7.6903
13	7.9872
14	10.7003
15	12.4426
16	9.1654
17	7.3703
18	13.6106
19	10.8282
20	3.9389
21	0.8538
22	0.3667
23	0.1496
24 +	0.0671
	$\Sigma = \overline{100.00}$

Molecular Weight = 209.8 lb/lb—mole

Density @ 60.0 deg F = 6.9357 ppg
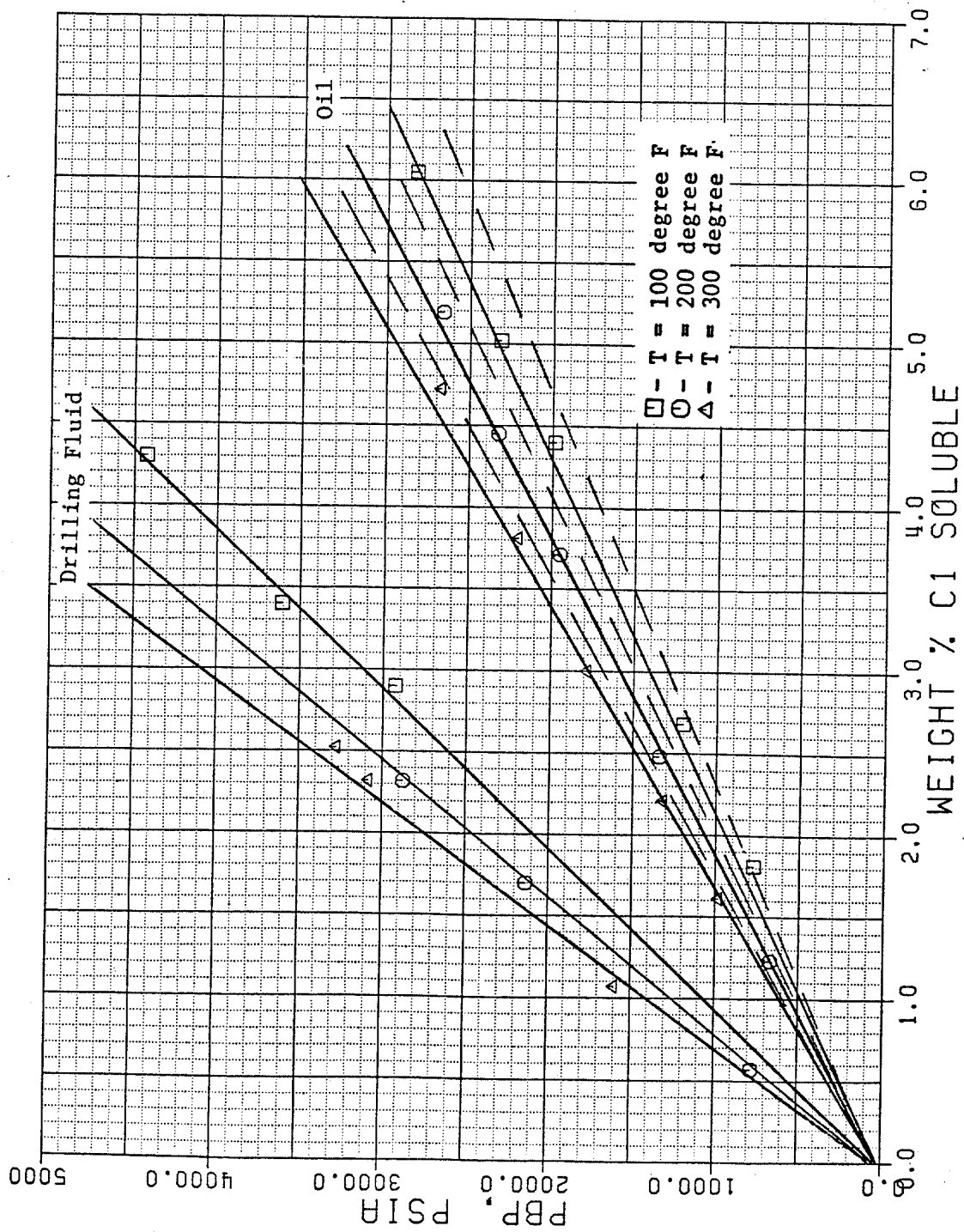
Figure 3.7: Methane/oil and drilling-fluid Systems Comparison

first done using data presented previously by Thomas, Lea, and Turek for methane dissolved in drilling fluid. Extrapolating the bubble point curve back to 0.0 weight percent methane soluble (Figure 3.8), one obtains a bubble point pressure of 500 psia. At this point, the bubble point pressure should be approximately 15.025 psia or one atmosphere. Referring now to Figure 3.5, which is the plot of the experimental data for the current study, the bubble point pressure is close to 15.025 psia at 0.0 weight percent methane soluble indicating that no significant amount of air was trapped in the drilling fluid.

Refering again to Figure 3.7, the dashed lines below the bubble point curves for the methane/oil systems are the curves generated if one takes the volume of oil in a given volume of drilling fluid and dissolves all of the methane in the methane/drilling fluid system into that volume of oil. The differences between the dashed line and the experimentally measured bubble points for methane and oil indicate that at the bubble point for a given methane/drilling fluid system some of the methane dissolves in other components within the drilling fluid.

As shown in Table 3.4 there are three main liquid components in the drilling fluid used in this study: 1.) oil (Mentor 28), 2.) emulsifiers and 3.) water (the 23.0 gm of CaCl2 added when mixing make this a 300,000 ppm
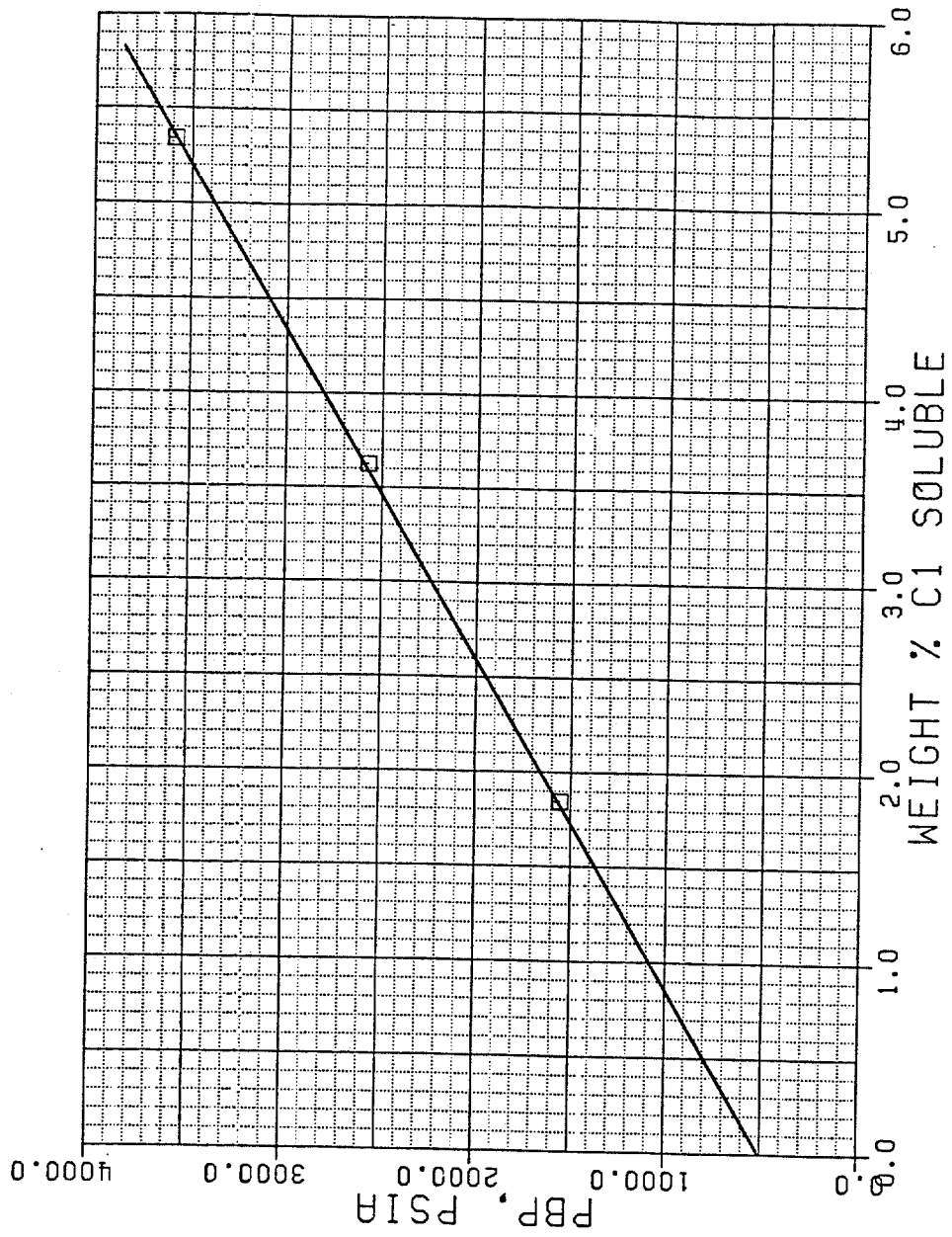
Figure 3.8: Thomas, Lea, and Turek Methane/drilling-fluid Experimental Data (T = 100 deg F).

brine). If the solubility of methane in each of these liquid components was known, the relative amount of methane dissolved in each liquid component at the bubble point pressure of the methane/drilling fluid mixture could be estimated. Once the amount of methane dissolved in each is known, they can be summed up and subtracted from the total amount of methane dissolved in the drilling fluid. If any methane remains then it can be safely assumed that this amount adsorbs on the drilling fluid solids. On the other hand, if none remains then the solids will affect methane/drilling fluid bubble point pressures only by diluting the liquid components in the drilling fluid with all the methane dissolving into the three main liquid components of the drilling fluid.

In order to make the required observations, the solubity of methane in the emulsifiers and brine had to be determined. Since no experimental data was available for methane solubility in emulsifiers, additional experiments had to be performed. Solubility of methane in brine was determined from published data.

Three experiments each at 100, 200, and 300 degree F were performed with varying weight fractions of methane. The procedures for loading and running the experiments were the same as those previously described for the methane/drilling fluid systems(Appendix B.2). Table 3.10

Table 3.10: Methane/emulsifier Experimental
Data

Weight % Methane	Bubble Point Pressure psia	Temperature deg F
1.104	800.0	100.0
2.454	1840.0	100.0
4.03	2590.0	100.0
0.965	770.0	200.0
2.074	1725.0	200.0
4.030	3215.0	200.0
.878	750.0	300.0
2.074	1800.0	300.0
3.600	3200.0	300.0

is a summary of the data generated from these experiments and Figure 3.9 is the data plotted as bubble point pressure versus weight percent methane dissolved into the emulsifier at that pressure.

To determine the solubility of methane in brine, the correlation presented by Culberson and McKetta for methane solubility in pure water was used and corrected for salinity by using curves developed by Frick and Taylor. These are shown in Figures 3.10 and 3.11.

For calculation purposes, all experimental data for methane dissolved in drilling fluid, oil, and emulsifier were curve fitted to a straight line equation using linear regression. The equations for the methane/drilling-fluid systems give the bubble point pressure for the mixture as a function of weight percent methane dissolved in the drilling fluid. The methane/oil and methane/emulsifier equations give the weight percent methane dissolved in the oil and emulsifier as a function of the bubble point pressure of the methane/drilling-fluid system in question.

The curves for methane solubility in brine were also curve fitted by linear regression to a polynomial of 2 degrees. These equations give the standard cubic feet of methane dissolved in a barrel of pure water as a function of the bubble point pressure of the methane/drilling fluid system. The number is then corrected for the
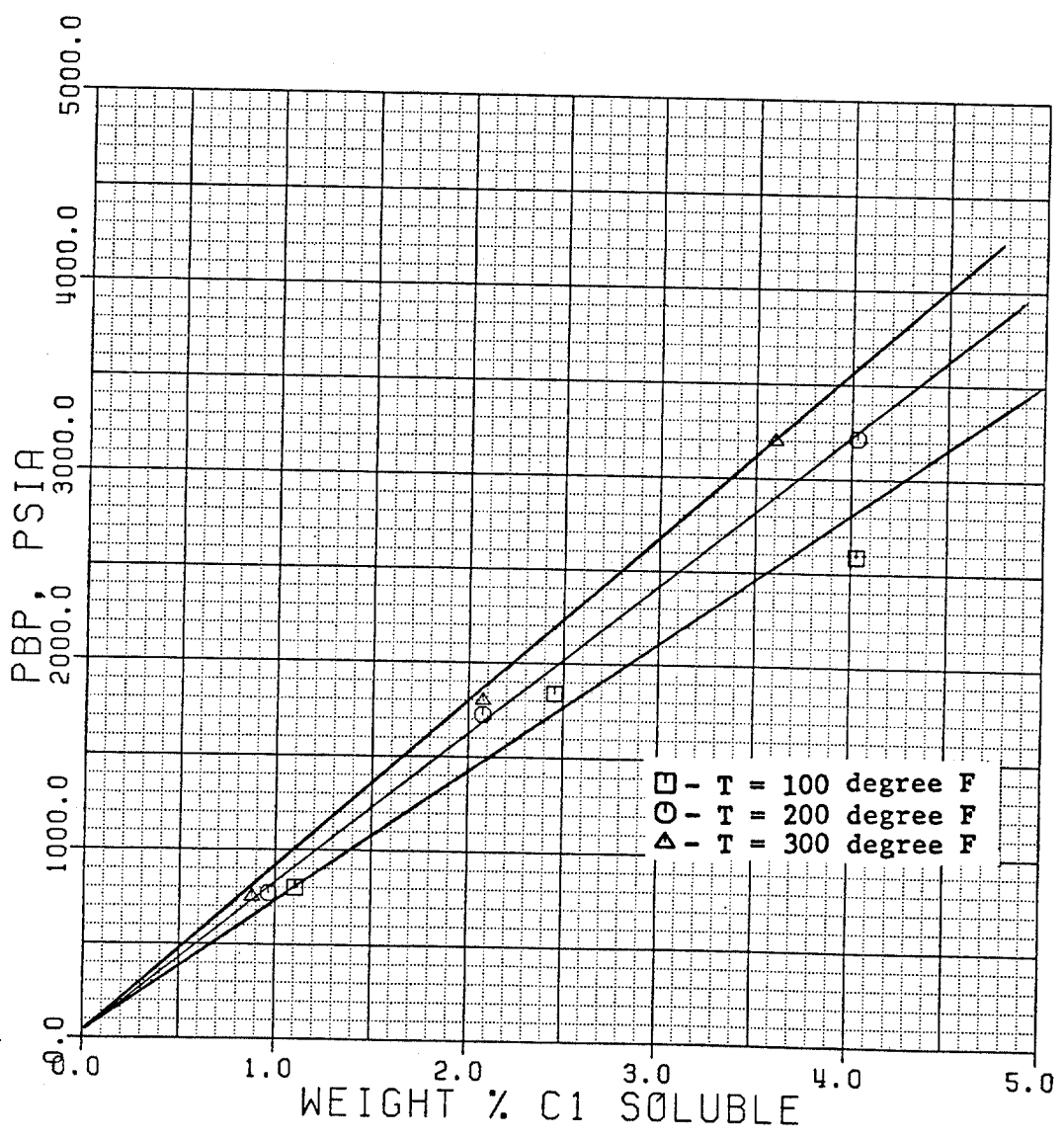
Figure 3.9:   Methane/emulsifier Experimental Data
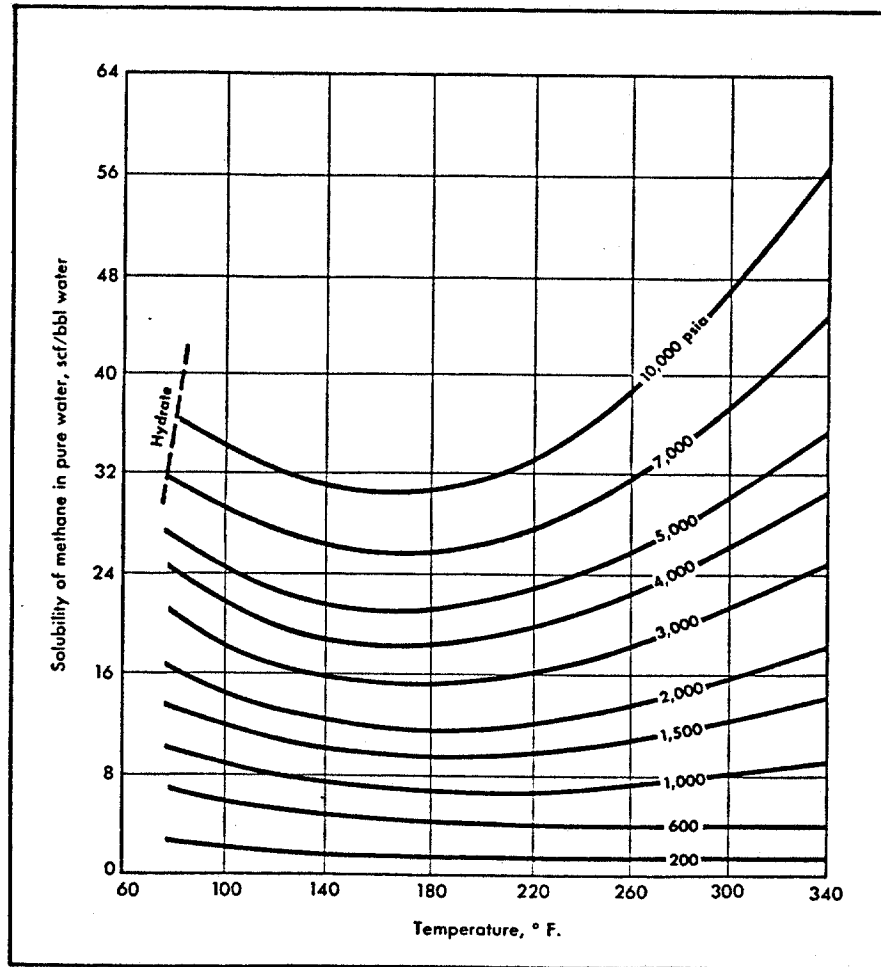
Figure 3.10: Solubility of Methane in Pure Water
(Culberson and McKetta).
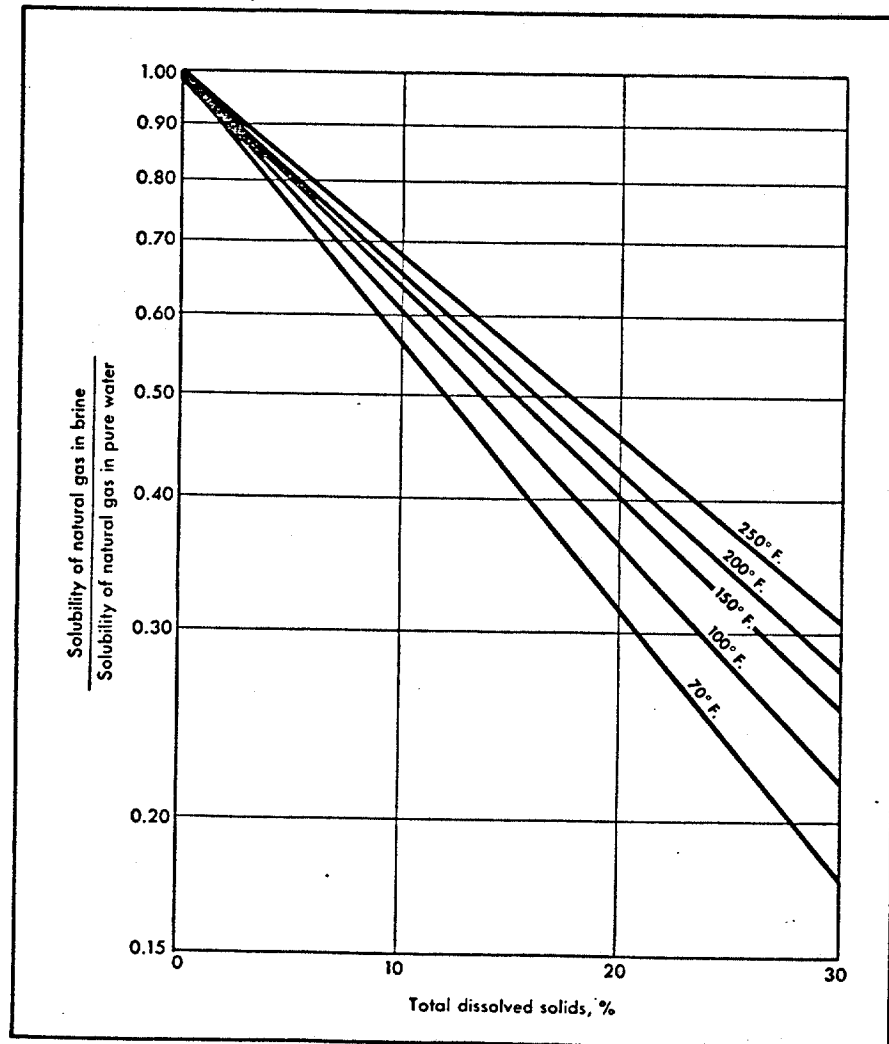
Figure 3.11: Effect of Salinity On The Amount of Gas In Solution When Fully Saturated With Gas (Frick and TAylor).

salinity of the brine using a correction factor obtained from linear regression fitting of the curves in Figure 3.11.

When using linear regression developed equations, it is necessary to take into account errors in the estimates made by these equations due to the failure of the estimates to perfectly fit the experimental data. In order to compensate for these errors, confidence intervals are determined. The confidence interval frequently used for experimental studies is 90% (Wojtanowicz). This was the confidence interval used in this study. All of the equations, along with their confidence intervals, are presented in Appendix E.

Once all the information needed for the determination of the effects of solids on the solubility of methane in the drilling fluid was obtained, the analysis was performed. The procedure followed for this analysis is presented in Appendix F. This procedure determines the amount of gas which could be adsorbed by the solids as the total gas dissolved in the drilling fluid minus the gas which was dissolved in each of the pure liquid phases (oil, brine, and emulsifier). The analysis was performed with 1.0, 2.0, and 3.0 weight percent methane dissolved in the drilling fluid at 100, 200, and 300 degree F. These weight percents were chosen because data in this range was available for each of the

Table 3.11: Average Maximum and Minimum Percent
Methane Not Accounted for.

Temperature, degree F	Maximum Average, %	Minimum Average, %
100.0	26.64	3.83
200.0	15.55	-6.21
300.0	24.65	-34.34

Maximum average over temperature range = 22.28%

Minimum average over temperature range = -12.24%

pure liquid phases.

Table 3.11 is a summary of the maximum and minimum error in methane solubility obtained as discussed above at the temperature indicated. Since a 90% confidence interval was used in determining these values, there is 90% confidence that the error lies within these limits. Taking the average of these limits over the range of temperatures indicated, you will note that the maximum error is 22.28 % and the minimum is -12.24 %. Since 0.0 % error lies within these limits, it is concluded that solids do not significantly adsorb any methane. Thus, solids will affect methane solubility in an oil-base drilling fluid by only diluting the volume of liquids within the drilling fluid in which methane can dissolve. The solids apparently act as an inert ingredient from the standpoint of methane solubility. It was also found that about 95 % of the methane dissolved in the drilling fluid was dissolved in the oil phase with 4.5 % dissolving in the emulsifier and .5 % in the brine. It can then be stated that brine and emulsifiers in the drilling fluid will also reduce methane solubility in the drilling fluid via dilution of the oil.

The significance of these conclusions for this study will be brought out later in this text. However it is felt that these conclusions can be applied in field practice from the standpoint that in order to reduce the

possibility of a gas kick completely dissolving in the drilling fluid at bottom hole conditions and the resulting slower detection time, adjustment in the solids, brine, and emulsifier content can be made to dilute the oil phase of the drilling fluid and create a bottom hole situation closer to that for a water-base drilling fluid (Figure 1.1). This would increase the kick detection time and allow the proper procedures to be implemented resulting in a much safer and calmer situation on the rig floor.

3.4.3 System Densities

As shown in Appendix D, the density of each system at the bubble point pressure was determined and values are presented for each experiment. The densities above and below the bubble point pressure for each methane/drilling-fluid experiment are shown in Appendix D.4.

The experimental data for the methane/drilling-fluid systems, particularly data at and above the bubble point pressure, often yield densities abnormally high compared to the density of the unsaturated drilling fluid (13 ppg @ 60 deg F). This is especially evident for the densities determined at 200 degree F which at pressures slightly above the bubble point pressure are as much as 2.5 ppg higher than the unsaturated drilling fluid density. In other cases, the density determined for saturated

drilling fluid was less than that for unsaturated drilling fluid. For example, data for the 1.07 weight % methane dissolved in 98.93 weight % drilling fluid at 300 degree F indicates that the density of the unsaturated drilling fluid is not reached until the methane/drilling-fluid system is compressed almost 1000 psia above the bubble point pressure. This discrepancy in density behavior prompted additional investigation.

The procedure for loading the PVT cell with the drilling fluid called for the fluid to be transferred from the burret (shown in Figure 3.1) to the PVT cell through a connecting hose clamped to both the PVT cell and burret. Before introducing the drilling fluid to the PVT cell, a vacuum was placed in the cell to aid in pulling the viscous drilling fluid into the PVT cell. However, this procedure was abandoned because of continuous plugging of expensive valves with the barite in the drilling fluid. The new procedure called for removing the top assembly from the PVT cell and pouring the drilling fluid directly into the cell. During the course of the research, individual files were maintained for each experiment performed. Upon reviewing these files, it was found that all the experiments performed, except the 1.07 weight % methane/98.93 weight % drilling fluid experiment at 300 degree F, utilized the old procedure for loading the drilling fluid into the PVT

cell. The 1.07 weight % methane experiment used the new method of pouring the drilling fluid into the PVT cell. It was concluded that when the drilling fluid was loaded by placing a vacuum in the cell and pulling the drilling fluid into the cell from the burret a small amount of air was entrained into the drilling fluid between the hose connector on the cell valve and the clamped hose. The small amount of trapped air may not have effected the measured bubble point pressures but was felt to have been enough to effect system densities.

To confirm that the measured bubble point pressures were not affected and to generate more accurate density data for later use in the study, three experiments were repeated at 100 degree F with varying weight percents of methane dissolved in a 13.0 ppg oil-based drilling fluid. The new method of loading the drilling fluid into the PVT cell was used. The calibrated data is shown in Appendix D.6, with Table 3.12 summarizing the bubble point pressures measured and Figure 3.12 showing this data along with the data generated at 100 degree F using the old cell loading method plotted as bubble point pressure vs weight percent methane dissolved in the drilling fluid. Figure 3.12 shows that the new data lays along the same trend as the old data. It can therefore be concluded that the small amount of air trapped in the drilling fluid was not enough to significantly affect the

Table 3.12: New Experimental Bubble Point Pressures
and Densities For Methane/drilling
Fluid At 100 Deg F.

Weight % Methane	Bubble Point Pressure, psia	Bubble Point Density, ppg
1.254	1360.0	12.74
2.950	3050.0	12.14
4.180	4250.0	11.85
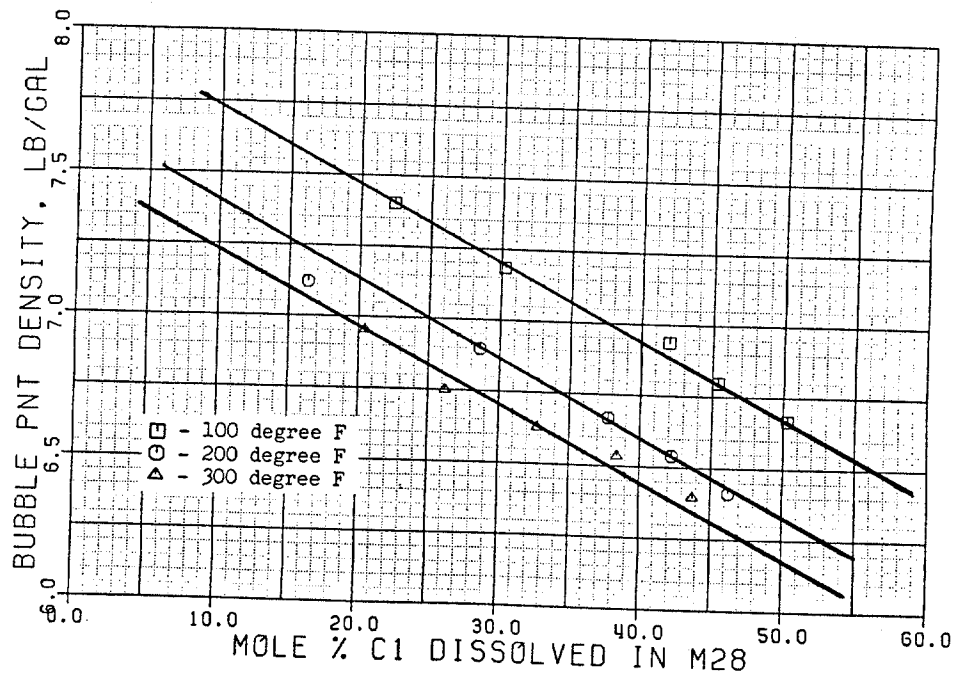
Figure 3.13: Bubble Point Density vs Mole %
Methane Dissolved.
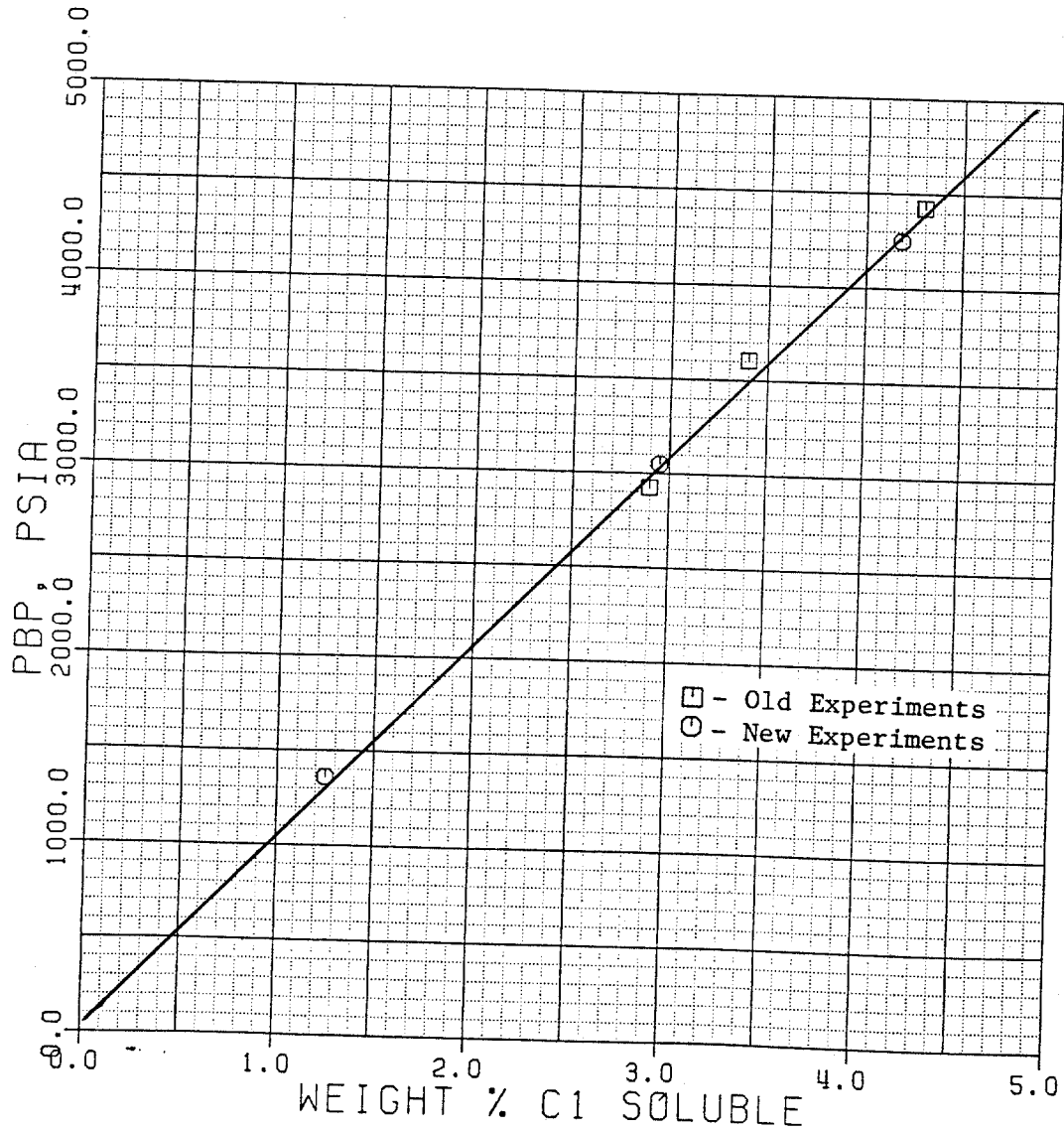
Figure 3.12: Old vs New Experimental Procedure For Methane/drilling Fluid Systems (T = 100 °F).

measured bubble point pressures and they are therefore valid. However, the density data generated using the old method of loading the PVT cell with drilling fluid should be considered too high and not representative of the actual phenomena.

For convenience, the densities at the bubble point pressure for the new experiments have been tabulated in Table 3.12. These data show that the densities decrease with increasing weight percents of methane dissolved in the drilling fluid. Figure 3.13 is a plot of the bubble point density versus mole percent methane dissolved for the methane/Mentor 28 experiments. Figure 3.13 indicates that as the mole percent methane dissolved in the Mentor 28 increases, the density decreases. Furthermore, as the temperature increases, the density decreases. We can conclude that as the amount of methane dissolved in the drilling fluid increases, the oil in the drilling fluid will swell and cause an increase in the volume of drilling fluid thus reducing its density. In addition, an increase in the temperature will also tend to swell the oil in the drilling fluid and in turn reduce the density. It should be noted that the conclusions formed are not meant to rule out possible swelling of the brine and emulsifier in the drilling fluid due to temperature and dissolved methane. It is recognized that this probably occurs, but it is felt that brine and emulsifier

CHAPTER IV

COMPUTER MODEL

As pointed out in the introduction of this text, one of the short comings of current well control simulators is their inability to adequately model gas/oil-base-drilling-fluid phase behavior. The basis of many phase behavior calculations is the vapor-liquid equilibrium constant or K-value given as,

$$K_i = y_i/x_i \qquad (4.1)$$

Where K_i = vapor-liquid equilibrium ratio for component i

y_i = mole fraction of component i in the vapor phase

x_i = mole fraction of component i in the liquid phase.

For bubble point pressure calculations, we introduce the following relationship,

$$\Sigma K_i z_i = 1.0 \qquad (4.2)$$

Where K_i = vapor-liquid equilibrium ratio for component i

z_i = mole fraction of component i in the total mixture.

The bubble point pressure is reached when this equality has been satisfied.

K-values can be determined in several ways, but the most common method is from K-value charts similar to the

57

one shown in Figure 4.1 for methane. You will notice that all the curves converge to a pressure of 5000 psia. This pressure is known as the convergence pressure and is the pressure at which the K-value is equal to one. This unity in the K-value occurs at or near the critical point for a particular mixture in which methane is a component. The critical point, by definition, is the point at which the compositions of the vapor and liquid phase become identical in a mixture.

The problem encountered by using K-value charts is that for a mixture, the convergence pressure must be determined and the appropriate K-value chart selected. Figure 4.2 again shows the K-value chart for methane for a convergence pressure of 1000 psia. At 500 psia and 100 degree F, the K-value is 3.2 for a 1000 psia convergence pressure but at the same conditions using a 5000 psia convergence pressure, the K-value is 6.6. It should now be evident how critical it is to know the correct convergence pressure before making bubble point pressure calculations. However, to try and model mixture phase behavior using K-value charts would be impractical, especially in computer applications since the convergence pressure would have to be determined for each methane/drilling-fluid mixture and K-values obtained. With all the possible combinations of methane dissolved in drilling fluid that can occur in the process of

swelling effects have less impact on the density of the drilling fluid since the relative volumes of these components in the drilling fluid are small compared to the volume of oil in the drilling fluid.

3.4.4 Temperature Effects On Methane Solubility

Referring to Figures 3.3 and 3.5, you will note that as the temperature increases, the bubble point pressure for a given percent methane (mole or weight) increases. It can therefore be concluded that as temperature increases, the solubility of methane in oil and oil-based drilling fluids decreases.
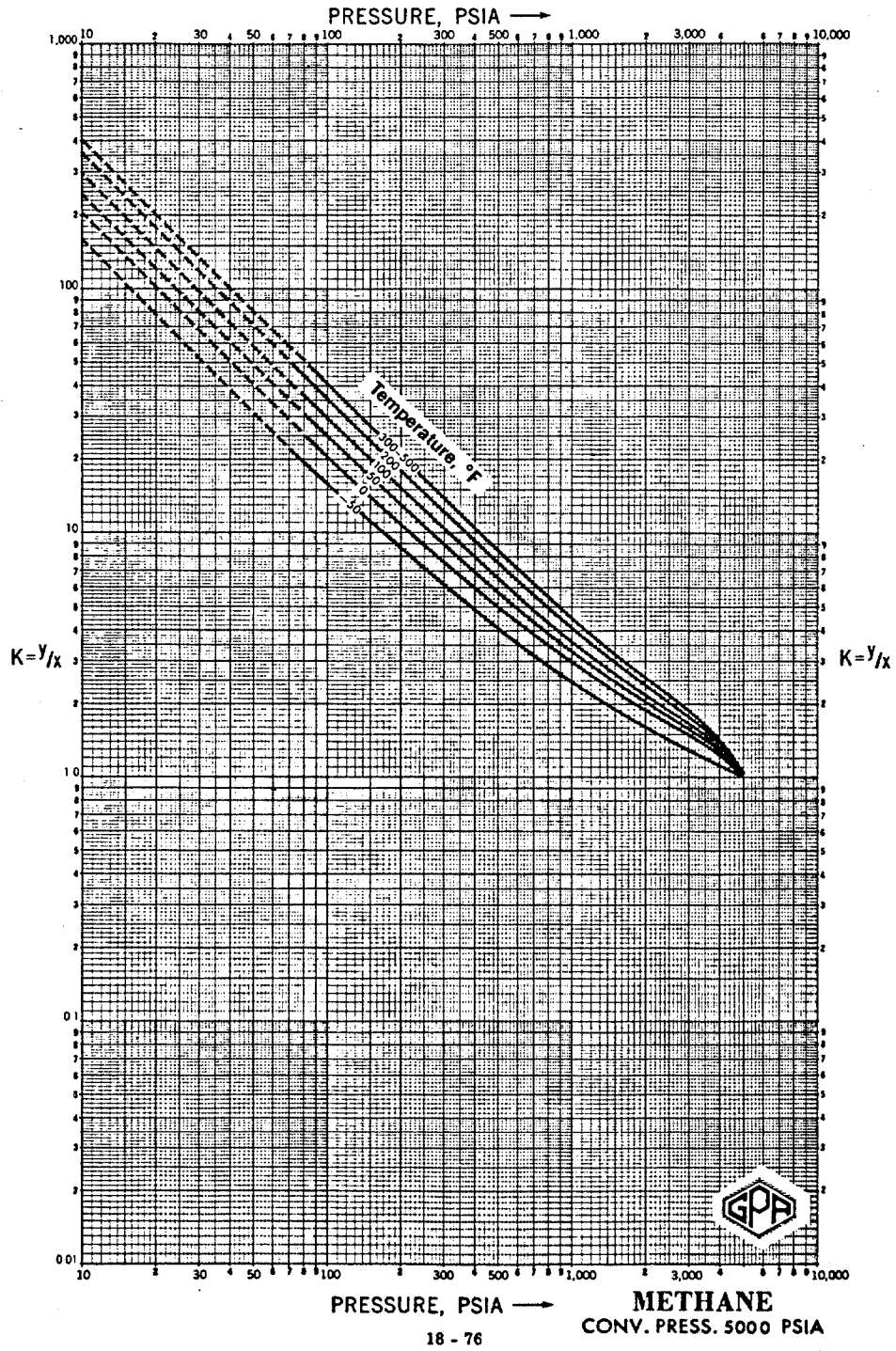
Figure 4.1: K-value Chart For
Methane
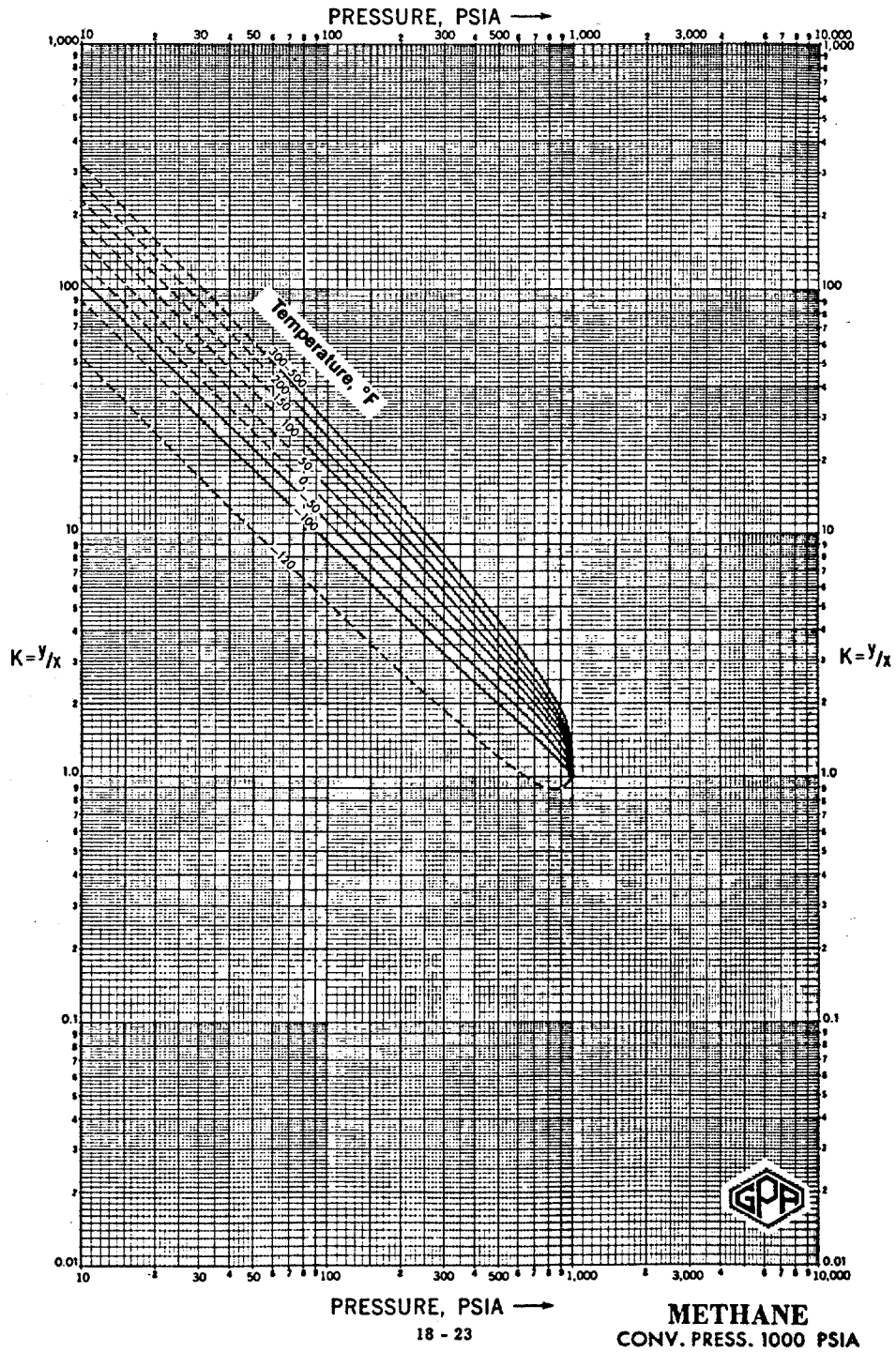
Figure 4.2:   K-value Chart For
Methane

circulating a kick out of the well and the fact that the phase behavior model will eventually be expanded to cover all gas kick compositions it is quite clear that an attempt to store K-value tables for several hydrocarbon components and many different convergence pressures is undesirable.

Equations of state are a very efficient tool for determining K-values for computer model applications. In this chapter, a computer model will be outlined that is based on an equation of state and is used to model methane/drilling-fluid system bubble point pressures and to predict densities above and below the bubble point. To do this, the model will have to predict methane phase behavior with oil, emulsifier, and brine components in the drilling fluid. A general discussion of the model will be presented followed by sample predictions made with the model compared to experimental data.

4.1 Methane/oil Model

It has already been mentioned in the literature review of this text that Thomas, Lea, and Turek used the Amoco Redlich-Kwong equation of state to predict methane/oil bubble point pressures. However, Walas states that for vapor-liquid equilibria calculations, the Amoco Redlich-Kwong equation of state is "not at all satisfactory". In 1979, Daubert, et.al. performed a detailed comparison of nine methods for calculating

vapor-liquid equilibria. It was found that of the nine methods studied the Soave and Peng-Robinson equations of state were best for vapor-liquid equilibria calculations with the Peng-Robinson equation of state predicting better liquid phase densities. Thus, the Peng-Robinson equation of state was chosen for the current study's computer model.

In basic form, the Peng-Robinson equation of state is given as,

$$P = \frac{RT}{v - b} - \frac{a(t)}{v(v + b) + b(v - b)} \qquad (4.3)$$

where P = pressure, psia

R = universal gas constant, $10.73 \frac{psia \cdot ft^3}{R \cdot lb\text{-}mol}$

T = temperature, ^{o}R

v = molar volume, $ft^3/lb\text{-}mol$

b = molecular repulsion parameter, $ft^3/lb\text{-}mol$

a(t)= molecular attraction parameter, $psia \cdot (\frac{ft^3}{lb\text{-}mol})^2$

Parameters a(t) and b can be calculated with equations given as,

$$a(t)_i = a(t_c)_i \cdot \alpha(t_r,\omega)_i \qquad (4.4)$$

where $a(t)_i$ = molecular attraction parameter for comp. i

$a(t_c)$ = $0.45724R^2T_c^2/P_c$, $psia \cdot (\frac{ft^3}{lb\text{-}mol})^2$

$\alpha(t_r,\omega)$ = $[1+.37464+1.54226\omega-.26992\omega^2(1-T_r^{.5})]^2$

$$R \qquad = \text{universal gas constant, } 10.73 \; \frac{\text{psia} \cdot \text{ft}^3}{\text{R} \cdot \text{lb-mol}}$$

$$T_c \qquad = \text{pure component critical temperature, } {}^o\text{R}$$

$$P_c \qquad = \text{pure component critical pressure, psia}$$

$$T_r \qquad = \text{pure component reduced temperature, } T/T_c$$

$$\omega \qquad = \text{pure component acentric factor}$$

and,

$$b_i = 0.07780 R T_c / P_c \tag{4.5}$$

where b = molecular repulsion parameter for comp. i

R = universal gas constant, $10.73 \; \frac{\text{psia} \cdot \text{ft}^3}{\text{R} \cdot \text{lb-mol}}$

T_c = pure component critical temperature, ${}^o\text{R}$

P_c = pure component critical pressure, psia.

For mixtures, parameters a(t) and b can be calculated from pure component a(t)i and bi parameters using the mixing rules given by equations 2.4 and 2.5. Once these parameters have been determined for a particular mixture, two new parameters, A and B, can be

calculated as a function of the pressure and temperature

of interest with equations given as,

$$A = a(t)P/R^2T^2 \tag{4.6}$$

where A = cubic equation of state parameter

$a(t)$ = molecular attraction parameter of mixture

P = pressure, psia

R = universal gas constant, $10.73 \frac{psia \cdot ft^3}{R \cdot lb\text{-}mol}$

T = temperature, ^oR

and

$$B = bP/RT \tag{4.7}$$

where B = cubic equation of state parameter

b = molecular repulsion parameter of mixture

P = pressure, psia

R = universal gas constant, $10.73 \frac{psia \cdot ft^3}{R \cdot lb\text{-}mol}$

T = temperature, ^oR

Knowing that,

$$v = zRT/P \tag{4.8}$$

where   v = molar volume, ft^3/lb-mol

z = compressibility factor

R = universal gas constant, $10.73 \frac{psia \cdot ft^3}{R \cdot lb\text{-}mol}$

T = temperature, ^{o}R

P = pressure, psia

and solving equations 4.6 for a(t) and equation 4.7 for b, substitution of these functions into equation 4.3 gives,

$$z^3 - (1-B)z^2 + (A - 3B^2 - 2B)z - (AB - B^2 - B^3) = 0.0 . \qquad (4.9)$$

This is the cubic form of equation 4.1 and is the form of the Peng-Robinson equation of state used in the computer model. All parameters are calculated as described for a given phase, liquid or vapor, and equation 4.9 is solved for its roots. If calculations are being made for a vapor phase, the largest positive root is the gas deviation factor of the vapor phase. If on the other hand, parameters were determined for a liquid phase then the smallest positive root will be the deviation factor of the liquid phase.

Once the deviation factors of the respective phases have been determined, the fugacity coefficient of each component in a given phase can be calculated using,

$$\ln\phi_k = \frac{b_k}{b}(z-1) - \ln(z-B) - \frac{A}{2.414B}[\frac{2\sum_i x_i a_{ik}}{a} - \frac{b_k}{b}]\ln(\frac{z+2.414B}{z-0.414B})$$

$$(4.10)$$

where ϕ_k = fugacity coefficient of component k

b_k = molecular repulsion parameter of component k in phase

b = phase molecular repulsion parameter

z = compressibility factor of phase

B = cubic equation of state parameter

A = cubic equation of state parameter

x_i = mole fraction of component i in phase

a_{ik} = molecular attraction parameter for components i and k in phase

a = molecular attraction parameter for phase.

Once the fugacity coefficient is determined for each phase, they can related as,

$$K_i = \phi_{iL}/\phi_{iV} \qquad (4.11)$$

where K_i = vapor-liquid equilibrium ratio for component i

ϕ_{iL} = fugacity coefficient of component i in the liquid phase

ϕ_{iV} = fugacity coefficient of component i in the vapor phase.

$$K_i = F_i y_i / x_i \qquad\qquad (4.12)$$

where K_i = vapor-liquid equilibrium ratio for

component i

y_i = mole fraction of component i in the

vapor phase

x_i = mole fraction of component i in the

liquid phase

$F_i = f_{iL}/f_{iV}$

f_{iL} = fugacity of component i in liquid phase, psia

f_{iV} = fugacity of component i in vapor phase, psia.

Using the Peng-Robinson equation of state to predict bubble point pressures requires the method of successive substitution in order to achieve the relationship of equation 4.2. The procedure followed was presented by Baker and Luks. One simplifying assumption was made in this procedure namely that methane would be the only component in the vapor phase. It was felt that this would be a reasonable assumption since the oils used in drilling fluids have very low volatile fractions with the lightest hydrocarbon present being C9. Also chemicals

are added to oil-base drilling fluids to make them temperature stable. A flow chart of the bubble point pressure model is shown in Figure 4.3.

In chapter three a generalized oil composition was introduced in Table 3.9 for use in this model. If this had not been developed, the composition of the oil used in the field would have to be entered into the program each time it is ran and this information is generally not known in the field. The critical properties of each oil component have also been assigned in the model and these are summarized in Table 4.1.

Once the computer model for predicting bubble point pressures of methane/oil systems was operating, the model had to be calibrated using a binary interaction coefficient in the mixing relationship for the molecular attraction parameter given in equation 2.4. It was found that a value of 0.065 was sufficient to adjust predictions to match experimental data. Figures 4.4 - 4.6 show predictions of bubble point pressures for varying mole fractions of methane dissolved in Mentor 28 oil at 100, 200, and 300 degree F compared with the experimental data. The results indicate that there is good agreement between experimental and predicted bubble point pressures.

The next step was to predict oil densities with the model when methane is dissolved in the oil. To do this

Figure 4.3: Methane/oil Phase Behavior Model
Flow Chart.
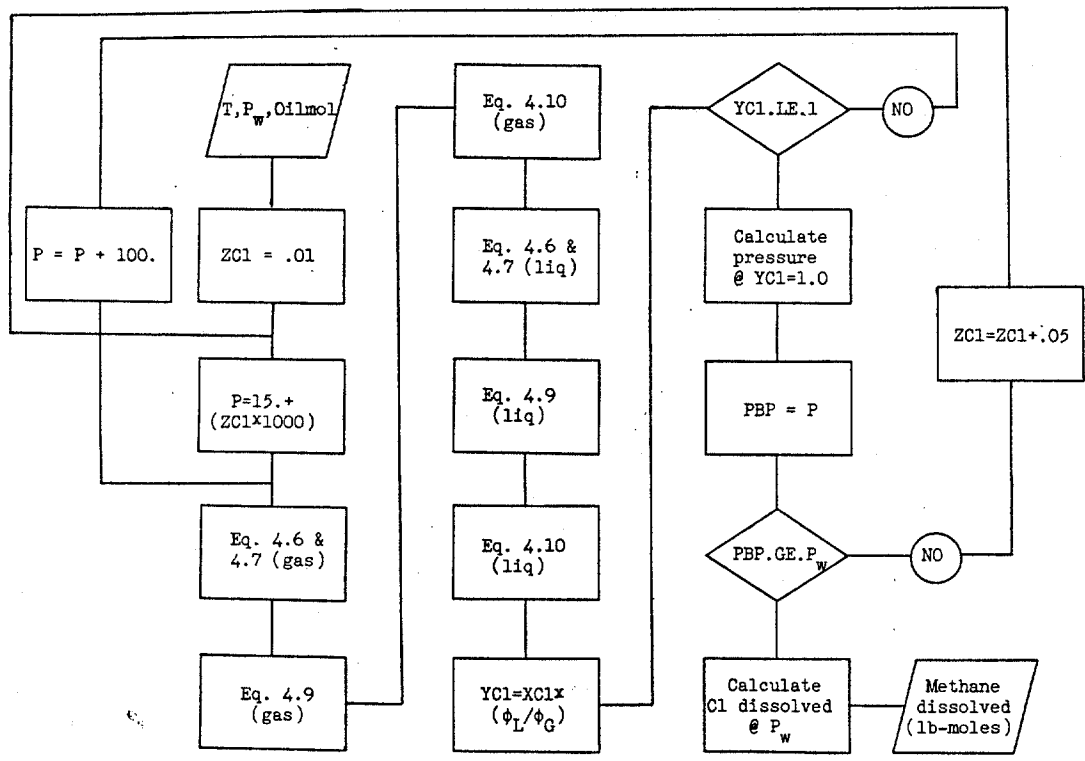
Nomenclature: T = temperature, ^{O}F

P_W = well pressure, psia

Oilmol = moles of oil, lb-moles

PBP = bubble point pressure, psia

Table 4.1: Oil Component Critical Properties

Component Number	Tc, Deg R	Pc Psia	Acentric Factor
9	1085.0	383.0	0.348
10	1128.0	351.0	0.385
11	1166.0	325.0	0.419
12	1203.0	302.0	0.454
13	1236.0	286.0	0.484
14	1270.0	270.0	0.516
15	1304.0	255.0	0.550
16	1332.0	241.0	0.582
17	1360.0	230.0	0.613
18	1380.0	222.0	0.638
19	1400.0	214.0	0.662
20	1421.0	207.0	0.690
21	1442.0	200.0	0.717
22	1461.0	193.0	0.743
23	1480.0	188.0	0.768
24	1497.0	182.0	0.793
45	1747.0	101.0	1.048
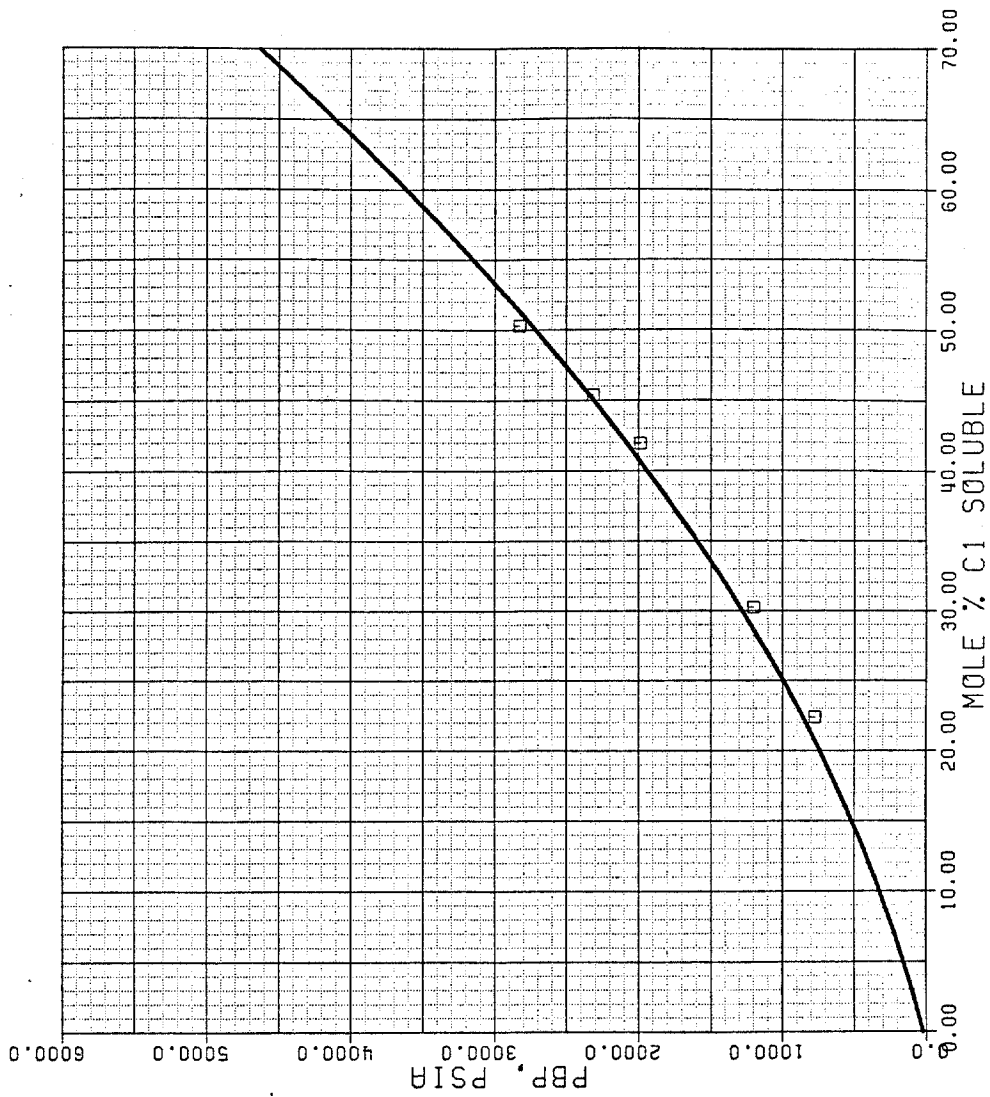
Figure 4.4: Experimental vs Predicted Pbp
For Methane/Mentor 28 @ 100 °F.
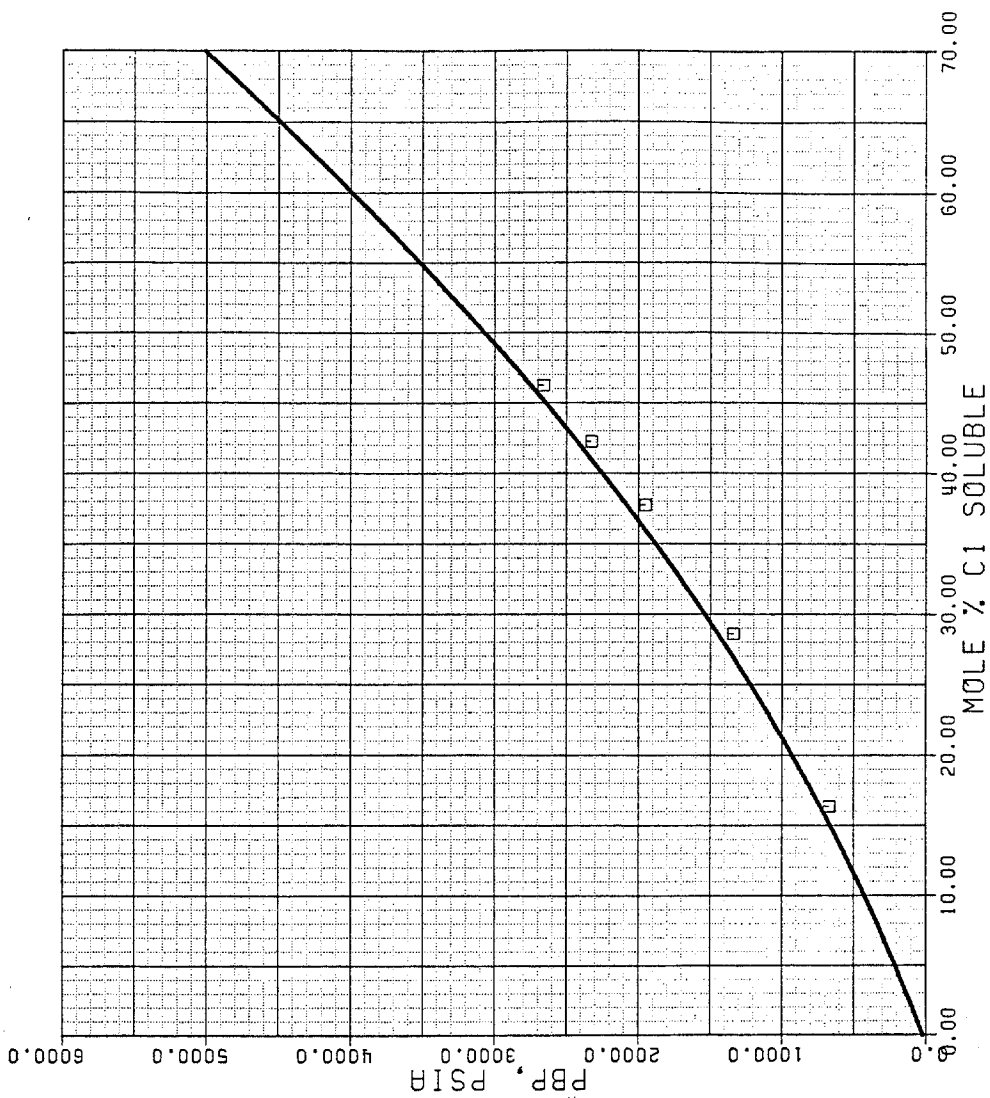
Figure 4.5: Experimental vs Predicted P_{bp} For Methane/Mentor 28 @ 200 °F.
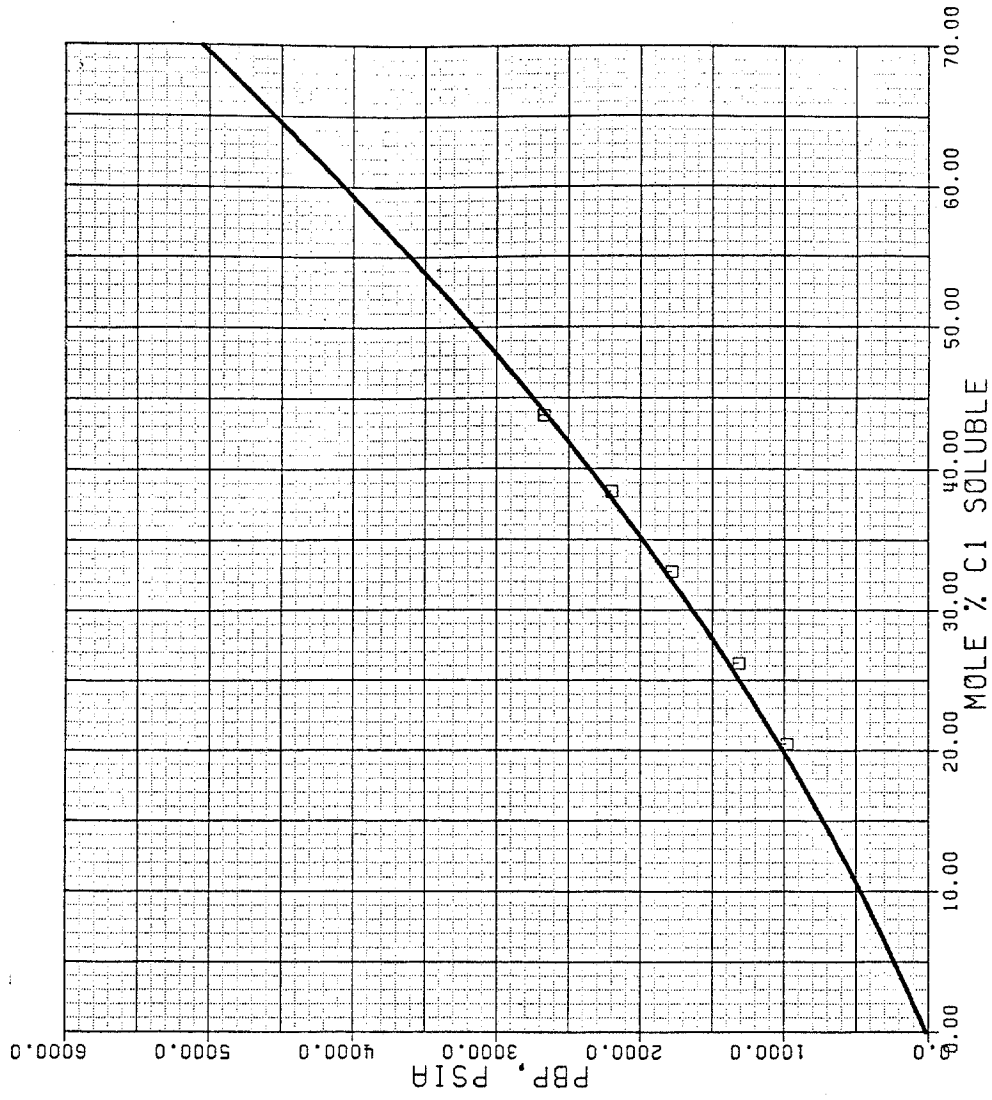
Figure 4.6: Experimental vs Predicted Pbp
For Methane/Mentor 28 @ 300 °F.

the following relationship is used,

$$V = zRT/P \qquad (4.13)$$

where V = molar volume, gal/lb-mole

   z = liquid compressibility

   R = universal gas constant, $80.3 \frac{\text{gal} \cdot \text{psia}}{\text{lb-mol} \cdot \text{R}}$

   T = temperature, $^{\circ}R$

   P = pressure, psia

At a given pressure and temperature, we can find the lb-moles of methane dissolved in the oil from our equation of state model and the resulting lb-moles of liquid from

$$n_{Ltot} = n_{C1} + n_{oil} \qquad (4.14)$$

where n_{Ltot} = total lb-moles of liquid

   n_{C1} = lb-moles of C_1 dissolved in oil

   n_{oil} = lb-moles of oil.

The average molecular weight of the methane/oil liquid phase can then be found by

$$MW_{liq} = MW_{C1}x_{C1} + MW_{oil}x_{oil} \qquad (4.15)$$

where MW_{liq} = liquid molecular weight, lb/lb-mole

   MW_{C1} = C_1 molecular weight, lb/,b-mole

MW_{oil} = oil molecular weight, lb/lb-mole

x_{C1} = mole fraction C_1 in liquid

x_{oil} = mole fraction oil in liquid

and the density can then be determined as,

$$\rho_o = MW_{liq}/V \qquad\qquad (4.16)$$

where ρ_o = density of liquid mixture, lb/gal

MW_{liq} = liquid molecular weight, lb/lb-mole

V = molar volume of the liquid, gal/lb-mole

Figure 4.7 shows experimental and predicted methane/Mentor 28 bubble point densities.

One problem was encountered when trying to predict methane/Mentor 28 bubble point densities and that was that the molar averaged composition molecular weight presented in Table 3.9 could not be used in equation 4.15 to calculate the molecular weight of the oil and dissolved methane. This was because the molecular weight of the Mentor 28 oil was 252 lb/lb-mole, as determined from gas chromatographic analysis, and the molar averaged molecular weight was 209 lb/lb-mole. If the molecular weight of the oil and dissolved methane was in error then subsequent use of equation 4.16 would introduce error in
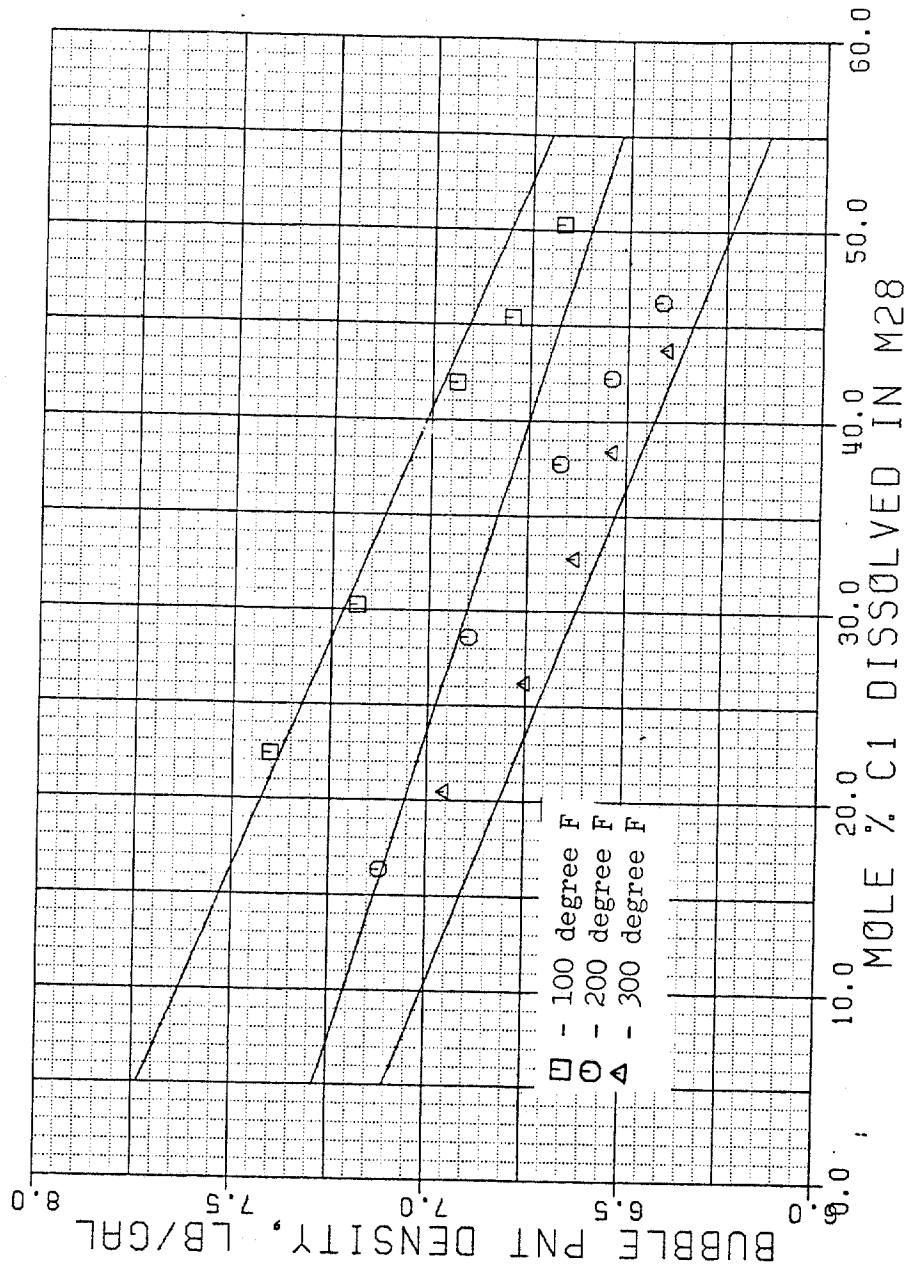
Figure 4.7: Experimental vs Predicted Bubble
            Point Densities.

the calculated density. Therefore density calculations for oil and dissolved methane should be made with the experimentally determined molecular weight of the oil in question (252 lb/lb-mole for Mentor 28, 204.2 lb/lb-mole for diesel, and 177.35 lb/lb-mole for Conoco LVT). For convenience, these molecular weights are stored in the program.

4.2 Methane/emulsifier Model

Trying to model methane/emulsifier systems phase behavior presented several problems. First it was not known what the emulsifier was composed of so it could not be modeled directly with the Peng-Robinson equation of state. Secondly, if the methane/emulsifier system could not be modeled with the equation of state, then the flexibility of the entire phase behavior model for methane/drilling-fluid systems would be limited by the amount of experimental data available.

In order to overcome these problems, a trial and error process was conducted to select a heavy hydrocarbon component that could interact with methane to yield results similar to the methane/emulsifier experimental data. It was found that a C45 component could reproduce the experimental data reasonably well when used in the equation of state model outlined for methane/oil using 0.065 as the binary interaction coefficient. Figures 4.8-4.10 show the predicted solubility of methane in
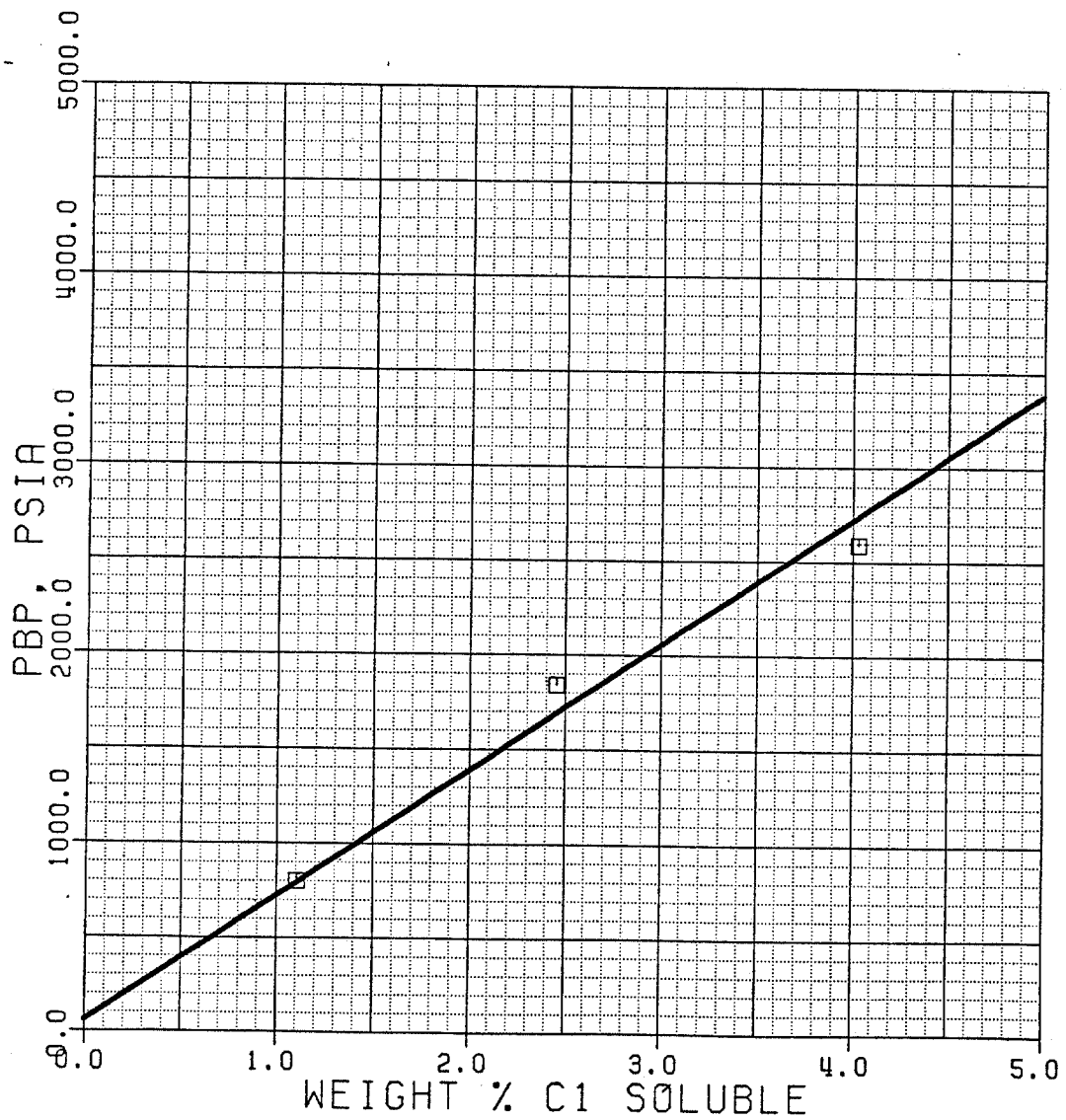
Figure 4.8: Experimental vs Predicted
Pbp For Methane/Emulsifier
@ 100 °F.

Figure 4.9: Experimental vs Predicted
Pbp For Methane/Emulsifier
@ 200 °F.
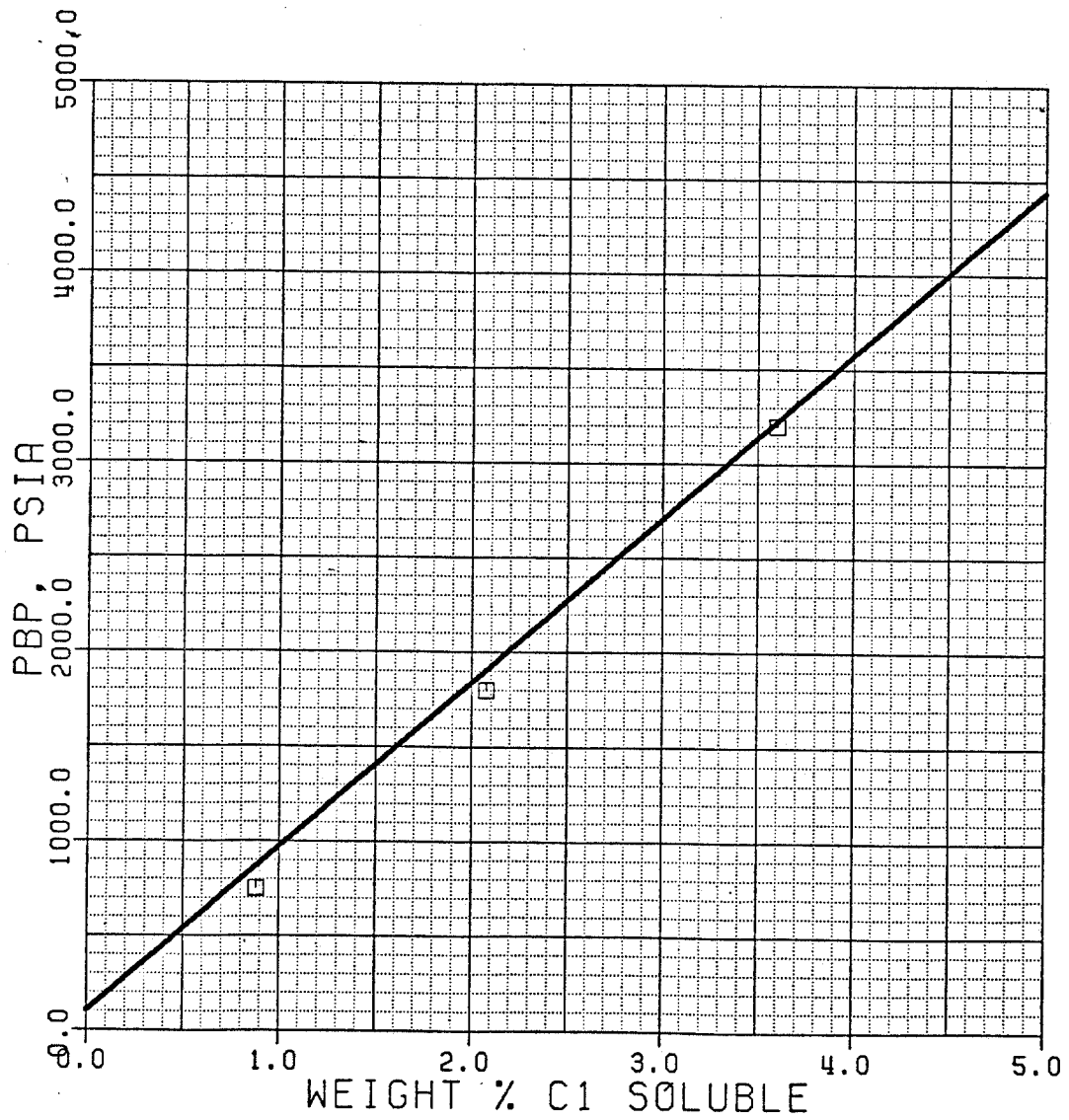
Figure 4.10: Experimental vs Predicted
Pbp For Methane/Emulsifier
@ 300 °F.

emulsifier as bubble point pressure versus weight percent methane soluble at that pressure. The flow chart for the methane/emulsifier bubble point pressure model is the same as the one shown in Figure 4.3 for the methane/oil model. Table 4.1 summarizes the critical properties of the component used to represent the emulsifier.

4.3 Methane/brine Model

To model the methane reaction with brine in the drilling fluid, the correlations presented by Culberson and McKetta along with the salinity correction presented by Frick and Taylor were used (Figures 3.10 and 3.11). The linear regression curve fits of these correlations presented in Appendix E were used in the computer model.

4.4 Methane/drilling-fluid Model

Figure 4.11 shows the flow chart for the methane/drilling fluid model. The first step in the model is to break the drilling fluid into components. The relative volumes of oil, brine, emulsifier, and barite are calculated using standard material balance calculations for oil-based drilling fluids as presented in the many drilling fluid technology handbooks. Those presented by Milchem Industries was used in this study.

Oil and brine volumes are calculated as a function of the oil-to-brine ratio of the drilling fluid and the density of the oil and brine mixture. The density of the

Figure 4.11: Methane/oil-base-drilling-fluid Phase Behavior Model Flow Chart.
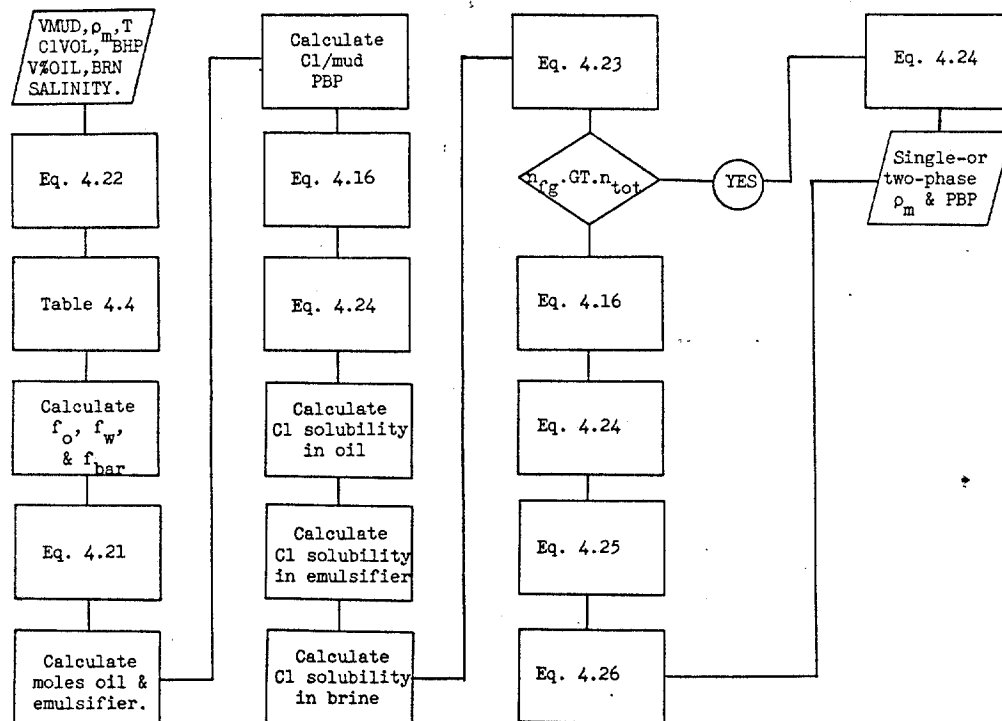
Nomenclature: VMUD = volume of drilling fluid mixed with methane, bbl

T = temperature, ^{O}F

ρ_m = drilling fluid density, lb/gal

C1VOL = volume of methane mixed with VMUD, cubic feet

BHP = bottom hole pressure, psia

V%OIL = volume % oil in drilling fluid

BRN SALINITY = brine in drilling fluid salinity, ppm

PBP = bubble point pressure, psia

oil and brine mixture is calculated as,

$$\rho_{ob} = f_o \rho_o + f_{brn} \rho_{brn} \qquad (4.17)$$

where ρ_{ob} = oil & brine density, lb/gal

ρ_o = oil density, lb/gal

ρ_{brn} = brine density, lb/gal

f_o = volume fraction of oil

f_{brn} = volume fraction of brine

The volume of oil and brine in a given volume of drilling fluid is determined as,

$$V_{ob} = [(35 - \rho_m)/(35 - \rho_{ob})]V_m \qquad (4.18)$$

where V_{ob} = volume of oil & brine, bbl

ρ_m = drilling fluid density, lb/gal

ρ_{ob} = oil & brine density, lb/gal

V_m = drilling fluid volume, bbl.

The individual volumes of oil and brine can now be calculated as,

$$V_o = f_o V_{ob} \qquad (4.19)$$

and,

$$V_{brn} = f_{brn} V_{ob} \qquad (4.20)$$

where V_o = volume of oil, bbl

V_{brn} = volume of brine, bbl.

In field practice, the oil-to-water ratio is often reported as the ratio of oil-to-pure water (salt free). It is necessary to correct this ratio for the increase in the pure water volume due to dissolved salt. This is accomplished by multiplying the percent water by a correction factor determined as a function of brine salinity. Also the water density has to be corrected for dissolved salt. Table 4.2 summarizes the brine densities and volume percent correction factors as functions of brine salinity for calcium chloride brines. This table has been curve fitted by linear regression and is included in the model.

The volume of barite in the given volume of drilling fluid is now calculated as,

$$V_{bar} = V_m - V_o - V_{brn} \qquad (4.21)$$

where V_{bar} = barite volume, bbl

V_m = drilling fluid volume, bbl

V_o = oil volume, bbl

V_{brn} = brine volume, bbl.

The volume of emulsifier is calculated as a function of the oil-to-water ratio and the temperature stability of the drilling fluid. To do this the gallons of emulsifier that must be added to 100 bbls of drilling fluid are determined from Table 4.3. This table has been included in the computer model.

Table 4.2: Brine Densities and Volume
            Correction Factor For Calcium
            Chloride Brine

Dissolved CaCl2, ppm	Brine Density, lb/gal	Volume Correction Factor
10,000	8.41	1.003
20,000	8.49	1.004
40,000	8.62	1.010
60,000	8.77	1.016
80,000	8.91	1.020
100,000	9.06	1.029
120,000	9.21	1.036
140,000	9.38	1.042
160,000	9.55	1.049
180,000	9.71	1.058
200,000	9.89	1.066
220,000	10.05	1.077
240,000	10.24	1.086
260,000	10.42	1.097
280,000	10.60	1.109
300,000	10.80	1.121
320,000	10.98	1.136
340,000	11.17	1.152
360,000	11.36	1.169
380,000	11.56	1.187
400,000	11.76	1.207

Table 4.3: Emulsifier Volumes

Oil: Water Ratio	Bottom Hole Temperature, Deg F				
	250	300	350	400	450
80:20	122.5	155.0	232.5	245.0	315.0
80:15	97.5	125.0	175.0	230.0	292.0
90:10	82.0	95.0	120.0	215.0	270.0

Values are reported as gallons of emulsifier/100 bbl of drilling fluid.

Now the lb-moles of oil and emulsifier are determined for use in the equation of state models previously outlined for methane/oil and emulsifier systems. Here the molecular weight of the molar averaged composition molecular weight presented in Table 3.9 is used for the oil lb-moles determination and a molecular weight of 539.0 lb/lb-mole (Whitson) was used for the molecular weight of the emulsifier. Next the lb-moles of methane for a given temperature is determined as,

$$n_g = PV/zRT \qquad (4.22)$$

where n_g = lb-moles of methane

           P = pressure, psia

           V = volume, ft^3

           z = compressibility factor

           R = universal gas constant, $10.73 \frac{ft^3 \cdot psia}{lb\text{-}mol \cdot R}$

           T = temperature, $^\circ R$.

Increasing lb-moles of methane are dissolved in the oil, emulsifier, and brine at increasing pressures until the total lb-moles of methane that are in the methane/drilling fluid system is exceeded. The pressure at which the given lb-moles of methane in the system will saturate the drilling fluid can then be determined by linear interpolation. This pressure is the bubble point pressure for the methane/drilling fluid system. Figures

4.12 - 4.14 show the predicted bubble point pressures compared to the experimental values at 100, 200, and 300 degree F.

The next part of the model is density calculations. To do this, the lb-moles of methane that can dissolve in each component of the drilling fluid at the pressure and temperature of interest is determined. The lb-moles of free gas can then be determined as,

$$n_{fg} = n_g - n_{og} - n_{brng} - n_{eg} \qquad (4.23)$$

where n_{fg} = free lb-moles of methane

n_{og} = lb-moles of methane dissolved in oil

n_{brng} = lb-moles of methane dissolved in brine

n_{eg} = lb-moles of methane dissolved in emulsifier.

The density of the drilling fluid is then calculated as,

$$\rho_{mg} = f_{og}\rho_{og} + f_{brn}\rho_{brn} + f_{bar}\rho_{bar} \qquad (4.24)$$

where ρ_{mg} = drilling fluid & dissolved C_1 density, lb/gal

ρ_{og} = oil & dissolved C_1 density, lb/gal

ρ_{brn} = brine density, lb/gal

ρ_{bar} = barite density, lb/gal

f_{og} = volume fraction oil & dissolved C_1

f_{brn} = volume fraction brine

f_{bar} = volume fraction barite
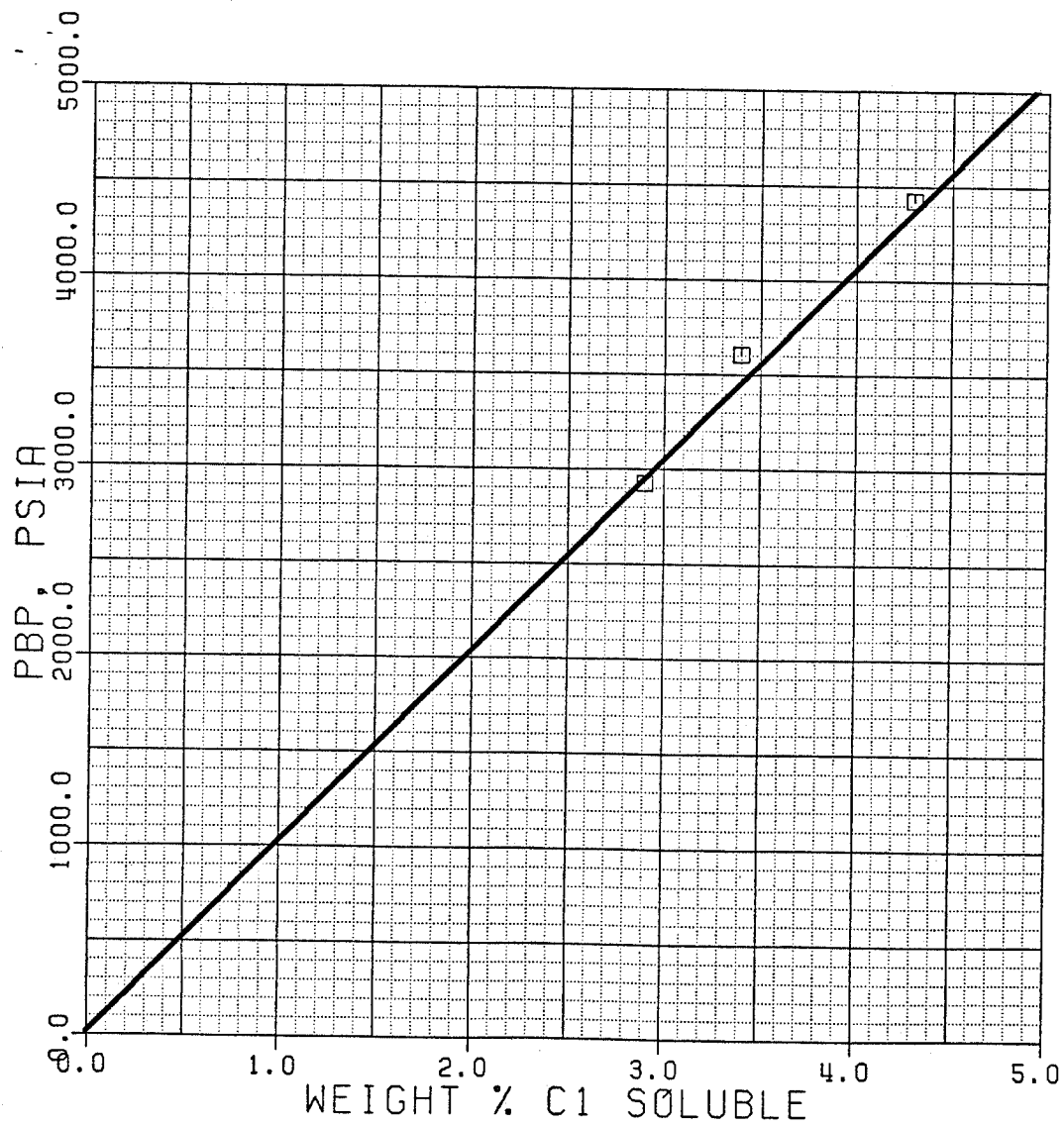
Figure 4.12: Experimental vs Predicted
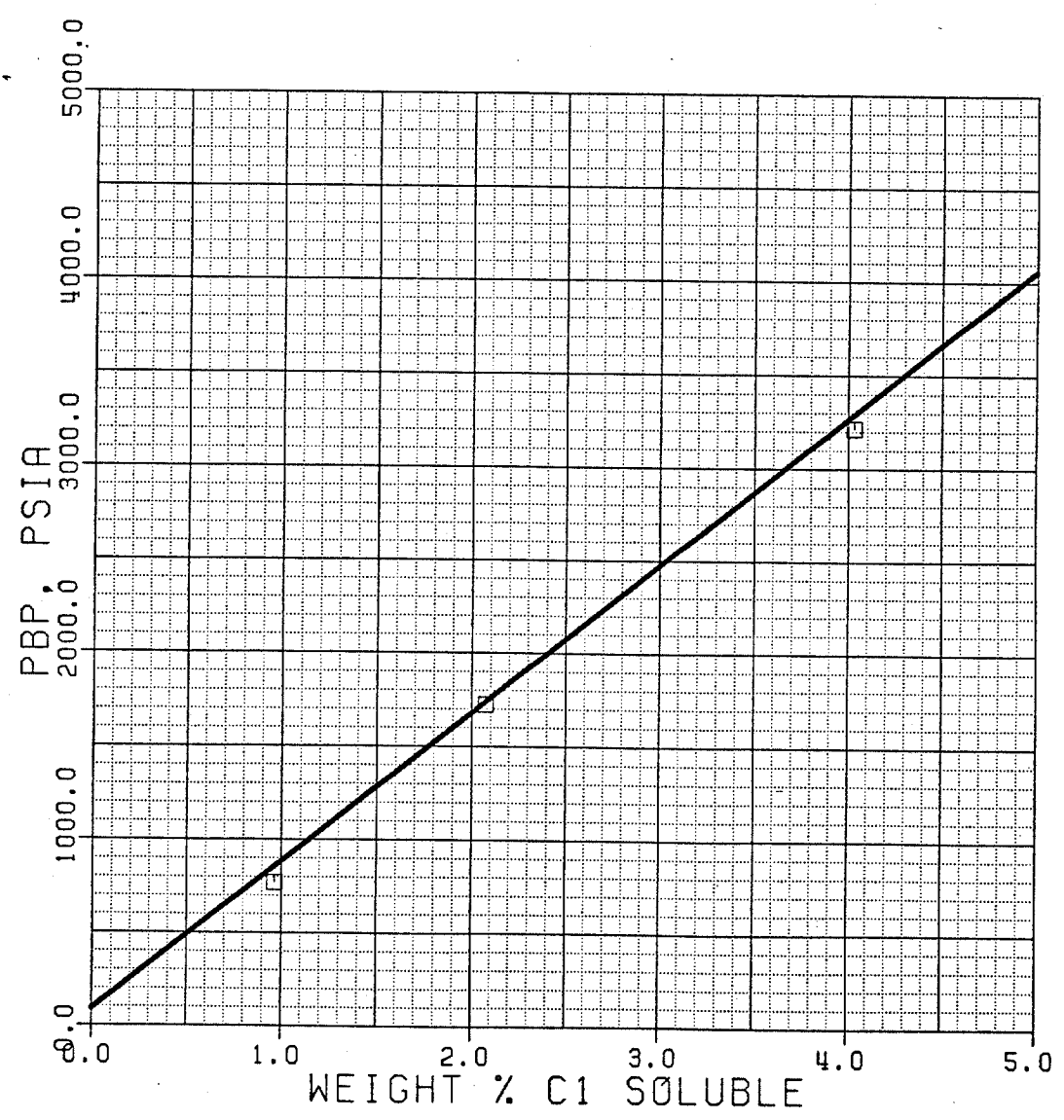Pbp For Methane/drilling
Fluid @ 100 $^{\circ}$F.
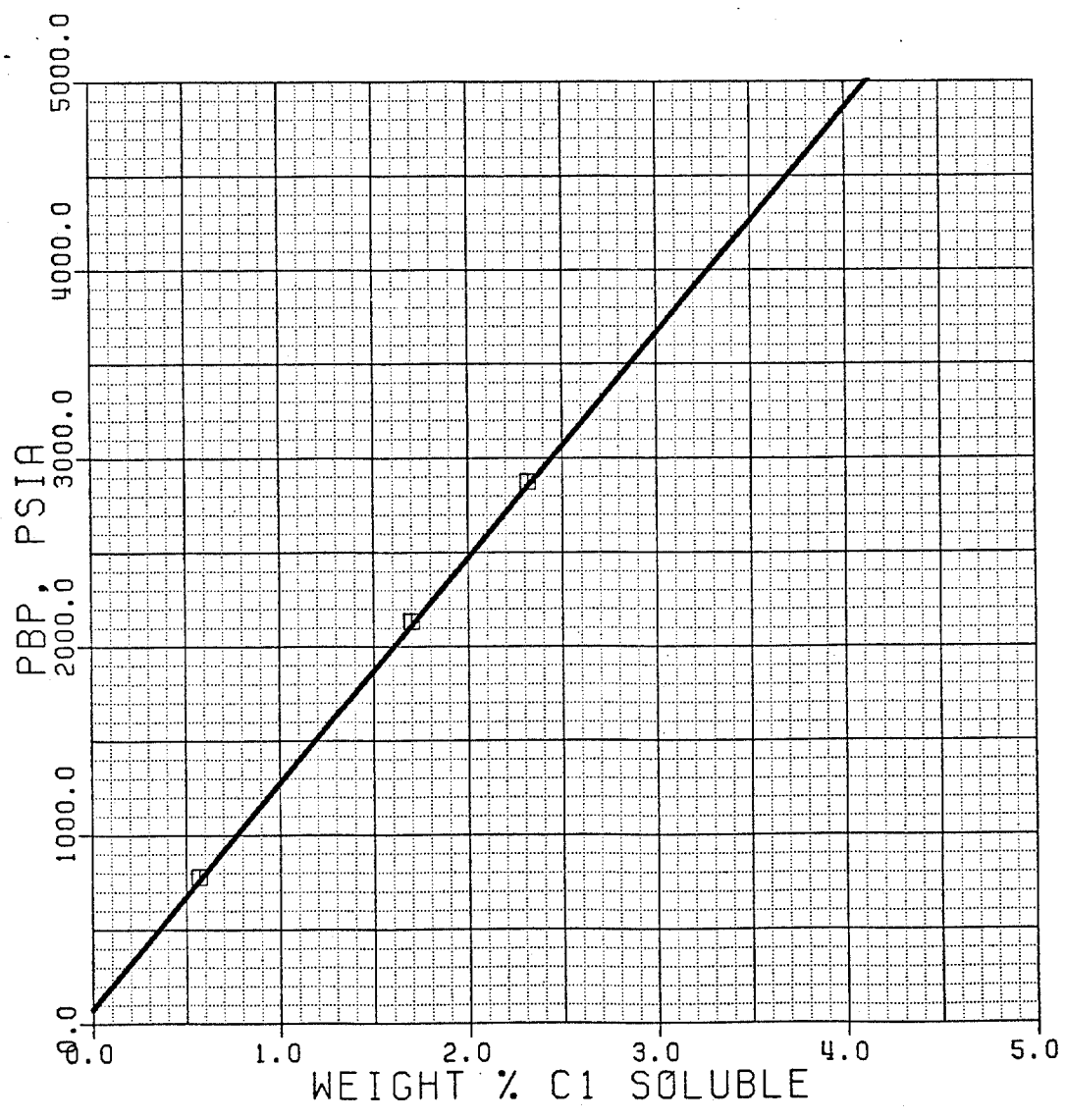
Figure 4.13: Experimental vs Predicted Pbp For Methane/drilling Fluid @ 200 °F.
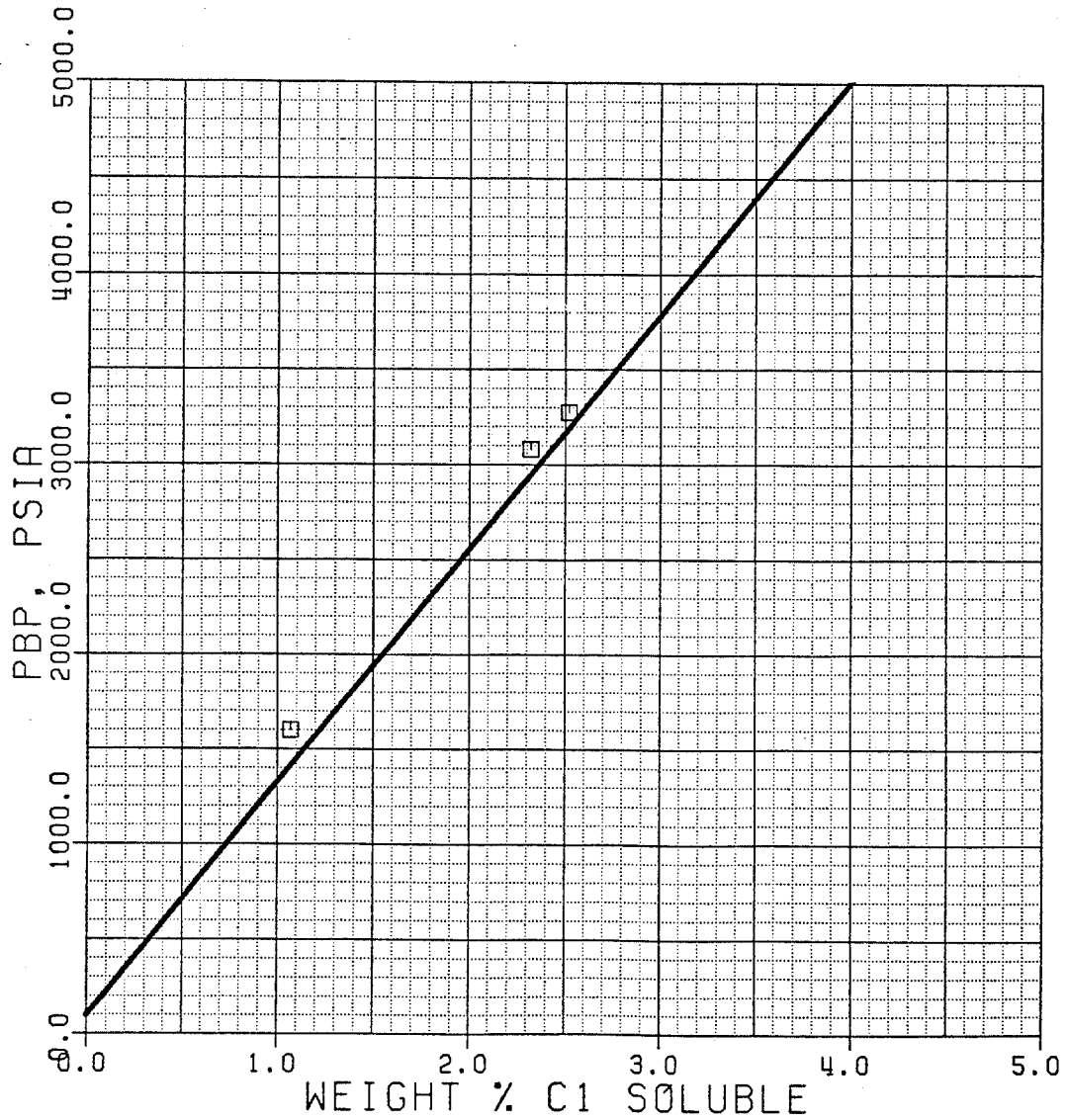
Figure 4.14: Experimental vs Predicted
Pbp For Methane/drilling
Fluid @ 300 $^{\circ}$F.

It should be noted that the emulsifier was not taken into account in equation 4.24. This is because emulsifier effects on drilling fluid density are negligible and generally not taken into account in practice. Also it is assumed here that since methane solubility in brine is so small, that the effects of any dissolved methane on the density of the brine can be neglected.

The density and volume of the oil and dissolved methane are calculated with the equation of state model previously outlined and the volume fractions of oil, brine, and barite recalculated because of the swelling of the oil due to dissolved methane.

The density of the free methane is calculated as,

$$\rho_{fg} = 16.04P/zRT \qquad (4.25)$$

where ρ_{fg} = free methane density, lb/gal

P = pressure, psia

z = compressibility factor

R = universal gas constant, $80.3 \frac{psia \cdot gal}{lb\text{-}mol \cdot R}$

T = temperature, ^{o}R.

The two-phase density can then be calculated as,

$$\rho_{tp} = f_{mg}\rho_{mg} + f_{fg}\rho_{fg} \qquad (4.26)$$

where ρ_{tp} = two-phase density, lb/gal

ρ_{mg} = drilling fluid & dissolved C_1 density, lb/gal
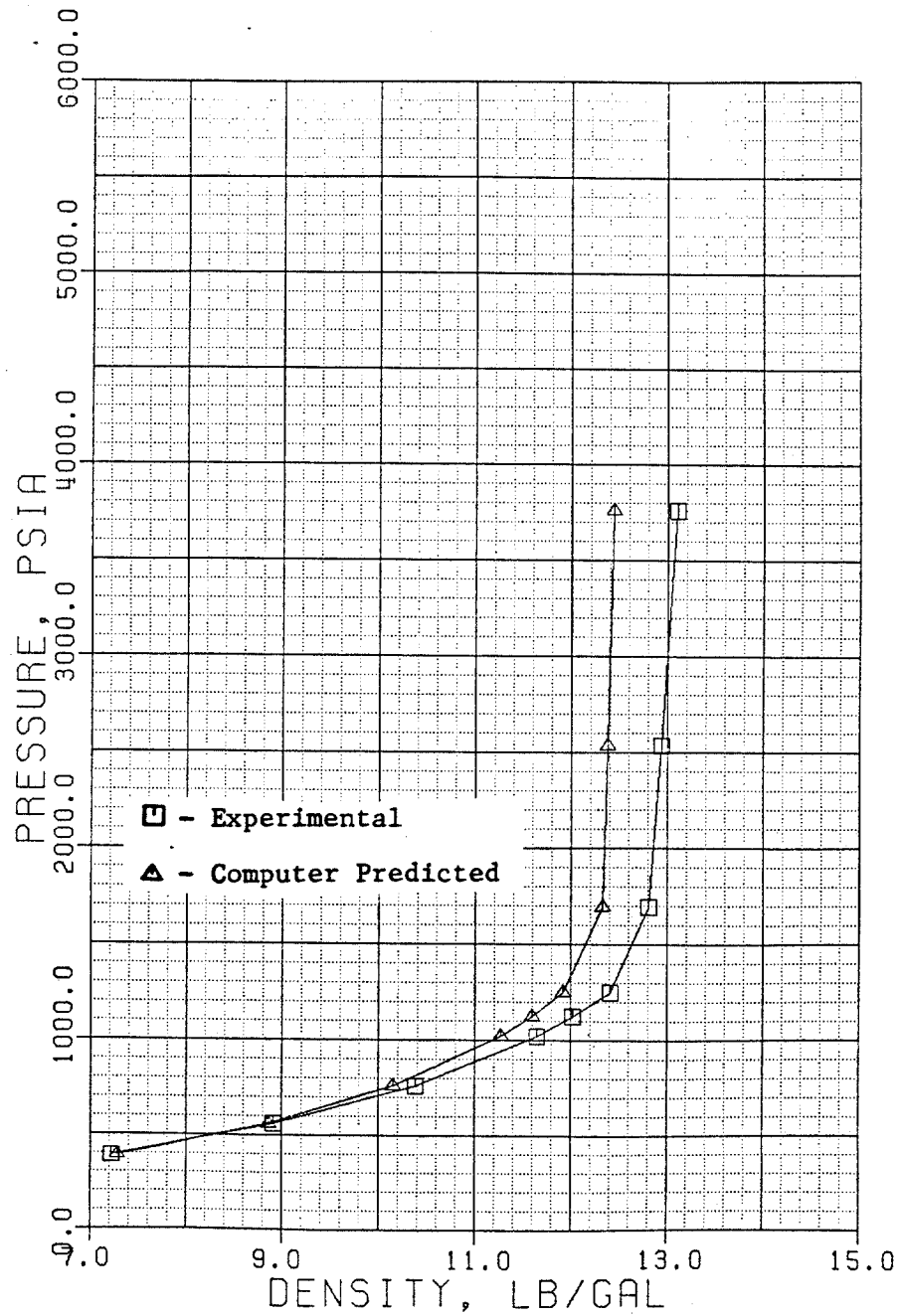
Figure 4.15: Experimental vs Predicted Densities
For 1.254 Wt % C_1 In 98.746 Wt %
Drilling Fluid @ 100 °F.
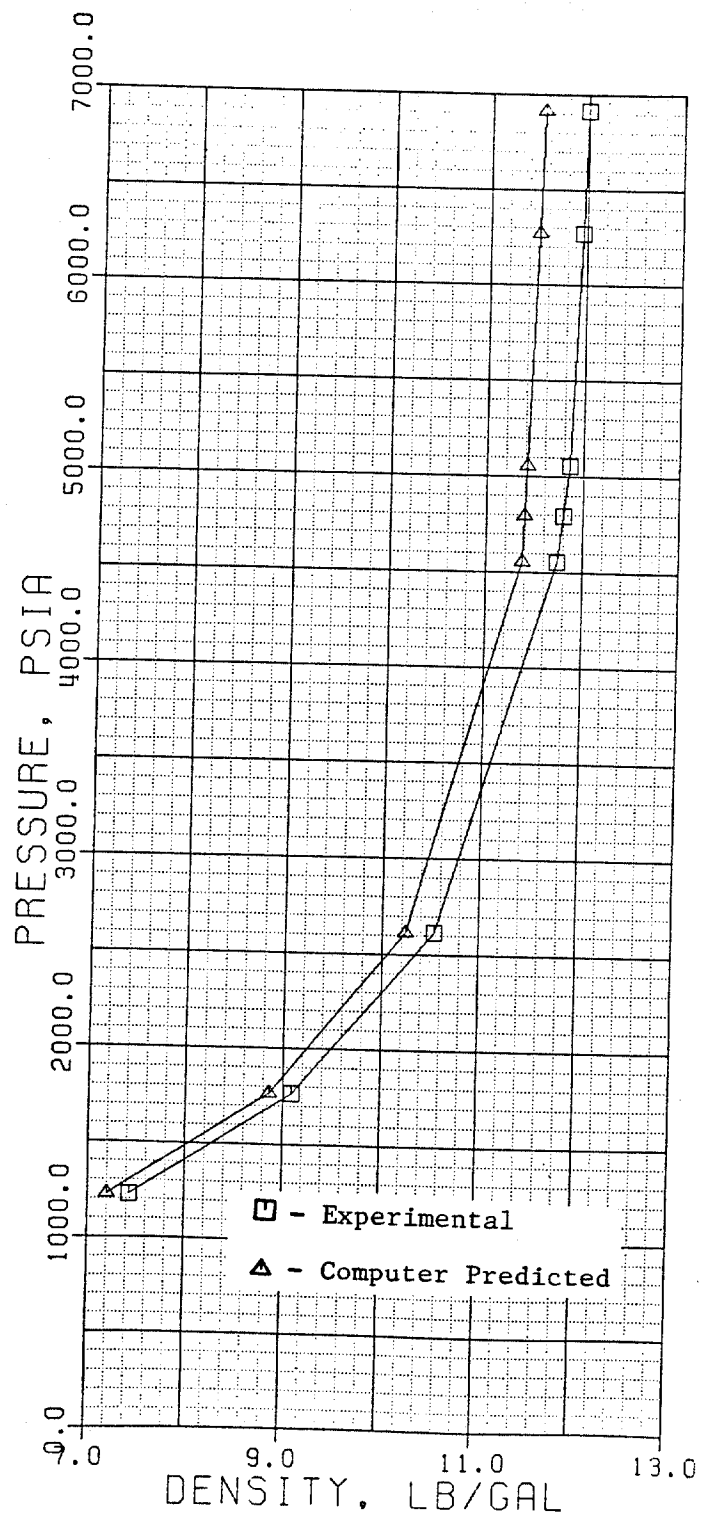
Figure 4.17: Experimental vs Predicted
Densities For 4.18 Wt % C_1
In 95.82 Wt % Drilling
Fluid @ 100 °F.

the experimental densities at low pressures is that the errors in the drilling fluid density predictions are masked by the fact that as the pressure is decreased, the volume fraction occupied by the methane in equation 4.26 is getting larger while the volume fraction occupied by the drilling fluid is getting smaller.

It is felt that the error in the predicted densities does not make the model invalid. The model will be used in a well control simulator to predict annular densities which will in turn be used to determine the bottom hole pressures during well control operations. Knowledge of the bottom hole pressure due to the column of fluid in the annulus is needed in order to determine the choke position required to maintain a constant bottom hole pressure during circulation of the gas kick out of the well. Use of the densities predicted by the current study's model will cause the well control simulator to predict over compensated choke positions. At the same time it is not felt that the densities predicted are so erroneous as to cause the simulator to predict choke positions that might cause formation break down.

CHAPTER V

CONCLUSIONS AND RECOMMENDATIONS

Presented in this chapter are the conclusions and recommendations of this study. First the conclusions and recommendations of the experimental study will be presented followed by those of the theoretical study (computer model).

5.1 Experimental Study Conclusions

1. An experimental apparatus and procedures have been developed for measuring bubble point pressures and densities for gas/oil, emulsifier, and oil-base drilling fluid systems.

2. Forty three experiments have been performed yielding bubble point pressure and density data for methane/oil, emulsifier, and oil-base drilling fluid systems.

3. Effects of base oil composition on the bubble point pressures of the methane/oil systems studied is negligible.

4. From gas chromatographic analysis, the composition of three commonly used base oils for mixing oil-base drilling fluids have been presented.

5. A generalized oil composition for use in a phase

behavior computer model has been presented for base oils.

6. Based on statistical analysis of the experimental data, it was concluded that methane will completely dissolve in the oil, brine, and emulsifier components in the drilling fluid studied.

7. From the statistical analysis, it was determined that methane was most soluble in the oil component of the drilling fluid with smaller amounts dissolving in the emulsifier and brine components.

8. Solids, brine, and emulsifier content will reduce the solubility of methane in oil-base drilling fluids by diluting the oil phase of the drilling fluid.

9. The swelling (decrease in density) of the drilling fluid due to increased dissolved methane and temperature is a function of the swelling of the oil component in the drilling fluid.

10. As temperature increases the bubble point pressure of a given methane/drilling-fluid system increases; therefore, methane solubility in oil-base drilling fluids decreases with increasing temperature.

5.2 Experimental Recommendations

1. Perform methane/drilling-fluid density experiments at 200 and 300 degree F using the new method of loading drilling fluid into the PVT cell.

2. Develop experimental procedures for measuring the volumetric behavior of oil with emulsifier under the influence of temperature and pressure.

3. Determine the molecular weight of other oils used in mixing oil-based drilling fluids for use in the computer model.

4. Perform bubble point pressure and density experiments with oil, emulsifier, and oil-base drilling fluid and other gases (ethane, carbon dioxide, hydrogen sulfide, etc.)

5.3 Theoretical Study Conclusions

1. A computer model has been developed to predict methane/drilling-fluid bubble point pressures and densities (single- and two-phase).

2. Methane/emulsifier bubble point pressures can be adequately predicted using a C45 component to represent the emulsifier.

3. Bubble point pressures of methane/oil systems were accurately determined using the generalized oil composition. The generalized oil molecular weight

could not be used because it yielded densities which did not agree with values determined experimentally, thus, molecular weights determined by gas chromatography were used in the model.

4. Density predictions were within 4 % of the experimentally determined densities for methane/drilling-fluid systems with the predicted denstities being less.

5. Density predictions of the methane/drilling fluid system in the single-phase region may be made more accurate if it is experimentally determined how the addition of emulsifier to oil effects the oil's volumetric behavior.

5.4 Theoretical Recommendations

1. Expand the computer model to predict oil-base drilling fluid phase behavior with other gases.

2. If data becomes available, determine what adjustments need to be made in the computer model to predict oil volumetric behavior with emulsifier in the oil.

3. Develop a phase behavior computer model for predicting gas solubility in water-base drilling fluids that can be incorporated in the model for

oil-base drilling fluids.

BIBLIOGRAPHY

Baker, Lee E. and Luks, Kramer D., "Critical Point and
    Saturation Pressure Calculations for Multipoint
    Systems," SPEJ, February 1980, pp 15-24.

Bennett, R. B., "New Drilling Fluid Technology-Mineral
    Oil Mud," SPE 11355, Presented at the IADC/SPE
    Drilling Conference, New Orleans, LA, February 20 -
    23, 1983.

Billingsley, J. L., Tenneco Oil Exploration and
    Production, Personal Communication.

Boyd, P. A., Whitfill, D. L., Carter, T. S., and Allamon,
    J. P., "New Base Oil Used in Low-Toxicity Oil Muds,"
    JPT, January 1985, pp 136-142.

Conrad, Patrick G. and Gravier, J. F., "Peng-Robinson
    Equation of State Checks Validity of PVT
    Experiments," Oil & Gas Journal, 21 April 1980, pp
    77, 78, 83-86.

Daubert, T. E., Graboski, M. S., and Danner, R. P., Docu-
    mentation of the Basis for Selection of the Contents
    of Chapter 8 - Vapor-Liquid Equilibrium K-Values In
    Technical Data Book - Petroleum Refining. No. 8 -
    78, American Petroleum Institute (1974).

Katz, D. L. and Firoozabadi, A., "Predicting Phase
    Behavior of Condensate/crude-oil Systems Using
    Methane Interaction Coefficients," JPT, November
    1978, pp 1649-1655.

Engineering Data Book, Gas Processsors Suppliers
    Association, Tulsa, Oklahoma (1972).

Levin, Richard I. and Rubin, David S., Applied Elementary
    Statistics, Prentice-Hall, Inc., Englewood Cliffs,
    NJ (1977).

Matthews, W. R., "How To Handle Acid Gas H2S and CO2
    Kicks," Petroleum Engineer International, 15
    November 1984, pp 22-29.

McKenzie, Michael F., Factors Affecting Surface Casing
    Pressure During Well Control Operations, M. S.
    Thesis, Louisiana State University (1974).

McCain, William D. Jr., The Properties of Petroleum
    Fluids, PennWell Publishing, Tulsa, Oklahoma (1973).

104

Monger, T. G., Louisiana State University, Personal Communication.

Mudfacts Engineering Handbook, Milchem Incorporated, Houston, TX.

Nghiem, L. X., Aziz, K., and Li, Y. K., "A Robust Iterative Method for Flash Calculations Using the Soave-Redlich-Kwong or the Peng-Robinson Equation of State," SPEJ, June 1983, pp 521-530.

O'Brien, T. B., "Handling Gas In An Oil Mud Takes Special Precautions," World Oil, January 1981, pp 83-86.

O'Sullivan, T. D. and Smith, N. O., "The Solubility and Partial Molar Volume of Nitrogen and Methane in Aqueous Sodium Chloride From 50 to 125 C and 100 to 600 atm," J. Phys. Chem., Vol. 74, 1970, pp 1460-1466.

Peng, Ding-Yu and Robinson, Donald B., "A New Two-Constant Equation of State," Ind. Eng. Chem. Fundam., Vol. 15, No. 1, 1976, pp 59-64.

Redlich, O. and Kwong, J. N. S., "On the Thermodynamics of Solution. V. An Equation of State. Fugacities of Gaseous Solutions," Chemical Reviews, 44 1949, pp 233-244.

Salisbury, D. P. and Jachnik, Richard, "Use of Low Toxicity Oils Requires Knowledge of Their Base Properties and Their Interaction With Commercial Oil Mud Additives," The Milchem Report, Milchem Incorporated, Houston, TX.

Salisbury, D. P., Milchem Incorporated, Personal Communication.

Smith, J. M. and Van Ness, H. C., Introduction To Chemical Engineering Thermodynamics, McGraw-Hill Inc., New York (1975).

Soave, Giorgio, "Equilibrium Constants From A Modified Redlich-Kwong Equation of State," Chemical Engineering Science, 1972, Vol. 27, pp 1197-1203.

Standing, M. B., Volumetric and Phase Behavior of Oil Field Hydrocarbon Systems, SPE of AIME, Dallas, TX (1977).

Thomas, D. C., Lea, J. F. Jr., and Turek, E. A., "Gas Solubility in Oil-Based Drilling Fluids: Effects on

Kick Detection," JPT, June 1984, pp 959-974.

Walas, Stanley M., Phase Equilibrium In Chemical Engineering, Butterworth Publishers, Stoneham, MA (1985).

Whitson, Curtis H., "Characterizing Hydrocarbon Plus Fractions," SPEJ, August 1983, pp 683-694.

Whitson, Curtis H., "Effect of C7+ Properties on Equation-of-State Predictions," SPEJ, December 1984, pp 685-696.

Wojtanowicz, A., Louisiana State University, Personal Communication.

Yarborough, Lyman, "Application of a Generalized Equation of State to Petroleum Reservoir Fluids," Advances in Chemistry Series, 182, K. C. Chao and R. L. Robinson, Jr., ed., American Chemical Society, Washington, D. C., pp 385-435 (1979).

APPENDIX A: Experimental Apparatus Calibration

Table A.1 is a listing of the data entered into the cell calibration program. Table A.2 is a copy of of the output obtained for the data in Table A.1 from the program. Table A.3 is a listing of the computer program used to calibrate the PVT cell, generate the cell equation, and to calibrate the raw experimental data.

The cell equation generated from the calibration program is,

$$V_c = 1015.16 + .021315T_c + P_c[15.54E-05+(-2.774E-08)T_c]$$

where T_c = cell temperature, F

P_c = cell pressure, psia

V_c = cell volume, cc

The purpose of this cell equation is for calibration of the raw experimental data in terms of mercury volume and corresponding sample volume in the PVT cell at the cell pressure and temperature.

Table A.1: Raw Data

Cell Pressure, psia	Pump Volume, cc	Temperature, Deg F
515.0	13.16	67.0
2015.0	14.64	67.0
4015.0	16.29	67.0
6015.0	17.81	67.0
515.0	13.16	67.0
515.0	21.47	100.0
2015.0	22.92	100.0
4015.0	24.47	100.0
6015.0	26.00	100.0
515.0	21.47	100.0
515.0	21.17	200.0
2015.0	25.56	200.0
4015.0	27.17	200.0
6015.0	28.71	200.0
515.0	24.17	200.0

Table A.2: Calibrated Data

CELL CALIBRATION

Cell Volume	Temp Coef	Press Coef-A	Press Coef-B
.101516E+04	.201315E-01	.165399E-03	-.277471E-07

Temperature = 200.0 Deg F

Press	Exp-Vol	Calc-vol
515.	1018.999	1019.263
1015.	1019.333	1019.503
4015.	1019.666	1019.823
6015.	1019.897	1020.143

Temperature = 100.0 Deg F

Press	Exp-Vol	Calc-Vol
515.	1017.169	1017.252
2015.	1017.498	1017.469
4015.	1017.764	1017.821
6015.	1018.035	1018.146

Temperature = 67.0 Deg F

Press	Exp-Vol	Calc-Vol
515.	1016.495	1016.588
2015.	1016.773	1016.833
4015.	1017.110	1017.160
6015.	1017.400	1016.588

```
          INTEGER C6,C3
          COMMON
          A1,A2,A3,A4,A5,A6,A7,A8,A9,B1,B2,B3,B4,B5,D1,D2,D3,
          D4,C2,
          +C3,C4,C5,C7,V1,V2,V3,V4,TF
          COMMON P,V,T,M,NT
          DIMENSION B6(66),P(99),T(99),V(99),NT(5),VS(99),
          &VCELL(99),VLIQC(99),DENS(99),Z(99),
          &AC2(99),AC3(99),AC4(99),AC5(99),AC6(99),
          &VLIQVP(99),VGASC(99),VGASVP(99),PAP(99),PAVS(99)
          READ(5,*)A1,A2,A3,A4,A5,A6,A7
          READ(5,*)AB,A9,B1,B2,B3,B4,B5
          WRITE(6,100)
          JCOM=0
          M=0
          ACUM=0
          JPM=0
          N=1
          L=0
6         READ(5,1010) B6
          READ(5,*) B7,B8,B9,C1
          1010 FORMAT(66A1)
          WRITE(6,101) B6
          WRITE(6,102) A4,A5,A6,A7
          WRITE(6,200)
          WRITE(6,103)A2,A3,A9,A8,B1
          WRITE(6,104) B7,B2,B3,B4,B5
          WRITE(6,105) B9,C1,B8
          IF(B1)1,2,3
2         B1=0 0
          D7=0
          GO TO 7
1         TF=A9
          C4=AB
          CALL CELLV
          B1=V1
3         TF=A9
          C4=A8
          D1=B1
          CALL MERC
          D7=D2
7         READ(5,*,END=9) C2,C3,C4,C5,C6
          AC2(N)=C2
          AC3(N)=C3
          AC4(N)=C4
          AC5(N)=C5
          AC6(N)=C6
8         GO TO(10,11,11,13),C6
10        CALL MANIC
          IF(JCOM)14,14,15
14        JCOM=1
          WRITE(6,107)
```

```
15      WRITE(6,108) C4,C5,C7
        GO TO 7
11      D1=0.0
        D2=A1
        TF=B7
        CALL MERC
        D4=D3-D1
        CALL COMAT
        D1=V2
        CALL MERC
        IF(C6-2)16,16,17
16      D5=D2
        GO TO 7
17      D6=D2
        D2=D5-D2
        D7=D7+D2
        D2=D7
        D5=D6
        TF=B8
        D1=0
        CALL MERC
        V4=D1
        IF(A4)18,18,19
19      CALL CELLV
        VS(N)=V1-V4
        VCELL(N)=V1
        IC2=C2
        IF(IC2. NE. 0) GO TO 21
        VLIQC(N)=0
        VGASC(N)=0.
        VLIQVP(N)=0.
        VGASVP(N)=0.
        GO TO 20
21      CALL CATH (C2,C3,V4,VLIQ)
26      VLIQC(N)=VLIQ
        VGASC(N)=VS(N)-VLIQC(N)
        VLIQVP(N)=(VLIQC(N)/VS(N)*100.
        VGASVP(N)=(VGASC(N)/VS(N)*100.
20      DENS(N)=B9/VS(N)
        IF (C1.EQ.0.0) GO TO 18
        Z(N)=(1.4935E-3*C4*VS(N))/(C1*(B8+460.))
18      V(N)=V4
        P(N)=C4
        IF(JPM)22,22,23
22      WRITE(6,109)
23      WRITE(6,110) P(N), VCELL(N),V(N),VS(N),DENS(N),Z(N),
        VLIQC(N),VLIQVP
        &(N),VGASC(N),VGASVP(N)
        N=N+1
        JPM=1
        GO TO 7
13      M=M+1
```

```
                    B1=V4
                    A9=B8
                    A8=C4
                    JPM=0
                    NT(M)=N-ACUM-1
                    T(M)=B8
                    ACUM=NT(M)+ACUM
                    GO TO 6
9                   IF (A4)24,24,25
24                  M=M+1
                    NT(M)=N-ACUM-1
                    T(M)=B8
                    CALL CALIBR
24                  CONTINUE
100                 FORMAT(/17X,'PROGRAM PVT MERCURY CALCULATIONS')
101                 FORMAT(/17X,66A1/)
102                 FORMAT(20X, C E L L   E Q U A T I O N'//16X,'CELL
                    VOL
                    ',4X,'TEM',
                    +'P-COEF',3X,'PRESS COEF-A',3X,'PRESS COEF-B'/12X,3E13.6,
                    E15.6)
103                 FORMAT(/14X,'PUMP COEF-A PUMP COEF-B START-TEMP START
                    -PRESS',
                    +'MERC-CELL'/12X,2E13.6,2(F10.3,2X),F9.3)
104                 FORMAT(/14X,'RM.TEMP REF-PRESS REF-VOL MANIFL-500
                    MANIFL',
                    +'8000'/12X,F9.3,1X,F10.4,1X,3F10.7)
105                 FORMAT(/14X,'GRAMS IN CELL MCLS IN CELL CELL
                    TEMP'/14X,3E13.6)
107                 FORMAT(/26X,'MANIFOLD CALIBRATION'//23X,'PRESS.
                    EXP-VOL',3X,
                    +'CAL.VOL')
108                 FORMAT(17X,F10.0,2F10.4)
109                 FORMAT)//8X,'PRESS. CELL-VOL CELL-HG SMPL-VOL DENSITY
                    Z-FACTOR LIG
                    &-VOL %-OIL-VOL GAS-VOL%-GAS-VOL')
110                 FORMAT(1HO,5X,F7.0,3F9.3,2F9.5,4F8.2)
200                 FORMAT(/26X,'I N I T I A L   D A T A')
                    WRITE(6,39)
39                  FORMAT(///1HO,21X,'I   N   P   U   T     D   A   T
                    A'/1HO,5X,'C2',10X,
                    &'C3',10X,'C4',10X,'C5',10X,'C6')
                    DO 1000 II=1,N
                    WRITE(6,40) AC2(II),AC3(II),AC4(II),AC5(II),AC6(II)
40                  FORMAT(1HO,5F12.4)
1000                CONTINUE
59                  STOP
                    END
                    SUBROUTINE CELLV
                    INTEGER C6,C3
                    COMMON A1,A2,A3,A4,A5,A6,A7,A8,A9,B1,B2,B3,B4,B5,
                    &D1,D2,D3,D4,C2,C3,C4,C5,C7,V1,V2,V3,V4,TF
```

```
      V1=4A+A5*TF+(A6+A7*TF)*C4
      RETURN
      END
      SUBROUTINE MANIC
      INTEGER C6,C3
      COMMON
      A1,A2,A3,A4,A5,A6,A7,A8,A9.B1,B2,B3,B4,B5,D1,D2,D3,D4,C2,
     +C3,C4,C5,C7,V1,V2,V3,V4,TF
      IF(B5-1.E-2)1,1,2
    2 B5=(B3-B5)/(B2-6015)
      B4=(B3-B4)/(B2-515.)
      C7=0
      RETURN
    1 C7=B3-((B5+((B4-B5)*1.E6)/(C4*B2))*(B2-C4))
      RETURN
      END
      SUBROUTINE MERC
      INTEGER C6,C3
      COMMON
      A1,A2,A3,A4,A5,A6,A7,A8,A9,B1,B2,B3,B4,B5,D1,D2,D3,D4,C2,
     +C3,C4,C5,C7,V1,V2,V3,V4,TF
      HG1=(.2414+2.05E-4*TF)*1.3-6
      HG2=0.5F*(.214E-6=8.88E-9*TF)*1.3-6
      HG4=1.0=1.0086E-4*(TF-60.)+2.4E-9*(TF-60.)**2
      IF(ABS(D1)-0.00001)16,16,17
   16 D3=D2*HG4
      D1=D3*EXP(-HG3)
      RETURN
   17 DE-D1*EXP(HG3)
      D2=D3/HG4
      RETURN
      END
      SUBROUTINE COMAT
      INTEGER C6,C3
      COMMON
      A1,A2,A3,A4,A5,A6,A7,A8,A9,B1,B2,B3,B4,B5,D1,D2,D3,D4,C2,
     +C3,C4,C5,C7,V1,V2,V3,V4,TF
      CALL MANIC
      V3=C7
      V3=V3-D4
      V2=A1-A2*C5-A3*C5**2+V3
      RETURN
      END
      SUBROUTINE CATH(C2,C3,V4,VLIQ)
      INTEGER C6,C3
      GOTO(1,2),C3
    1 VLIQ=(1.0446*C2-319.759)-V4
      GOTO8
    2 VLIQ=(1.0466*C2+2.129)-V4
    8 IF(VLIQ.GT.5.0)GOTO10
      VLIQ=0. 160*VLIQ
      RETURN
```

```
10      VLIQ=VLIQ-3.975
        RETURN
        END
        SUBROUTINE CALIBR
        INTEGER C6,C3
        COMMON
        A1,A2,A3,A4,A5,A6,A7,A8,A9,B1,B2,B3,B4,B5,D1,D2,D3,D4,C2,
        +C3,C4,C5,C7,V1,V2,V3,V4,TF
        COMMON P,V,T,M,NT
        DIMENSION
        B6(66),P(99),T(99),NT(5),VS(99),VCELL(99),VLIQC(99
        +),DENS(99),Z(99)
        DIMENSION
        SLOP(99),AINTER(99),AVRS(99),AVR(99),A(5),B(5),C(5),D(5)
        +,AVRI(99)
        N=0
        KMAX=0
        KMIN=1
        L=0
        K=0
        DO 1 J=1,M
        ASLOP=0
        ACINTR=0
        L=L+NT(J)-1
        DO 10 I=KMIN,L
        IF(P(I).NE.P(I+1)) GO TO 11
        K=K+1
10      CONTINUE
11      KMIN=I
        DO 12 I=KMIN,L
        IF(F(I+1).EQ.P(KMIN)) GO TO 13
        IF(I.NE.L) GO TO 12
        WRITE(6,124)
        RETURN
12      CONTINUE
13      KMAX=I-1
        DO 2 I=KMIN,KMAX
        SLOP(I)=(V(I+1)-V(I))/(P(I+1)-P(I))
        ASLOP=ASLOP+SLOP(I)
        AINTER(I)=V(I)-SLOP(I)*P(I)
        ACINTR=ACINTR+AINTER(I)
2       CONTINUE
        APOINT=NT(J)-K-2
        AVRS(J)=ASLOP/APOINT
        AVRI(J)=ACINTR/APOINT
        K=0
        KMIN=KMAX+3
        L=L+1
1       CONTINUE
        J=1
        IF(M.EQ.2) GO TO 14
        N=M-1
```

```
         DO 3 J=1,N
  14     D(J)=(AVRS(J)-AVRS(J+1))/(T(J)-T(J+1))
         C(J)=AVRS(J)-D(J)*T(J)
         B(J)=(AVRI(J)-AVRI(J+1))/(T(J)-T(J+1))
         A(J)=AVRI(J)-B(J)*T(J)
         A4=A4+A(J)
         A5=A5+B(J)
         A6=A6+C(J)
         A7=A7+D(J)
  3      CONTINUE
         A4=A4/(M-1)
         A5=A5/(M-1)
         A6=A6/(M-1)
         A7=A7/(M-1)
         WRITE(6,120) A4,A5,A6,A7
  120    FORMAT  (/26X,'C  E  L  L   C A L I  B  R  A  T  I  O
        N'//16X,'CELL VOL',4
        +X,'TEMP-COEF',3X,'PRESS       COEF-A',3X,'PR5SS      COEF-
        B',/12X,3E13.6,
        +E15.6)
         K=1
         L=0
         DO 4 J=1,M
         WRITE(6,121) T(J)
         WRITE(6,122)
         L=L+NT(J)
         DO 5 I=K,L
         VHG=A4+A5*T(J)+(A6+A7*T(J))*P(I)
         WRITE(6,123) P(I),V(I),VHG
  5      CONTINUE
         K=1+L
  4      CONTINUE
  121    FORMAT(//14X,'TEMPERATURE= ',F6.0)
  122    FORMAT(/20X,'PRESS EXP-VOL CALC-VOL')
  123    FORMAT(//18X,F7.0,F9.3,F10.3)
  124    FORMAT(/20X,'MISTAKE IN INPUT DATA')
         RETURN
         END
```

APPENDIX B: Cell Loading and Mixture Characterization

Appendix B.1: Methane/pure-oil Experiments

118 of 207

To prepare the system for loading sample into the PVT cell, the PVT cell, sample bottles, and corresponding tubing are evacuated with the vacuum pump (Refer to Figure 3.1). The experimental oil is then loaded into the burret filling it to the 500 cc mark. The stop cock and cell valve are then opened and a given amount of oil is allowed to flow into the cell. The hose connecting the burret to the cell is then disconnected and the volume of oil occupying the hose is measured and subtracted from the burret reading. This is done to take into account that initially, only air occupied the connecting hose before the stop cock and cell valve were opened. The oil volume is then recorded on the volumetric calculations sheet shown in Table B.1 and the lb-moles of oil in the cell are then determined.

To load the sample bottle with gas, the pressure regulator on the gas storage bottle is set at a desired delivery pressure and then opened allowing gas to flow into the sample bottle. Once the pressure had stabilized, the regulator and appropriate system valves are closed. Mercury is now pumped into the gas filled bottle, from the bottom, to a desired loading pressure. The loading pressure, room temperature, and pump volume are then recorded on the calculations sheet in the proper spaces. The cell valve is now opened and the gas is allowed to flow into the cell. When the pressure is

stabilized, the cell valve is closed and mercury is again pumped into the sample bottle until the initial loading pressure is reached. The pressure, room temperature, and new pump volume are recorded and the mercury displaced and corresponding gas and lb-moles of gas displaced are calculated.

Now that the lb-moles of gas and oil in the cell are known, the mole percent of each component in the cell is calculated as shown on the sheet.

When the lb-moles of gas in the cell need to be increased, the procedure just described for gas is repeated and the additional lb-moles of gas are added to the lb-moles of gas initially in the cell and the mole percentages are recalculated.

Table B.1: Methane/oil Volumetric Calculations

Gas Calculations:

Gas type = _____
Molecular weight = _____ lb/lb-mole
Critical temperature = _____ degree R
Critical pressure = _____ psia

Initial pump volume = _____ cc
Initial pressure at pump volume = _____ psia
Room temperature = _____ degree F
z – factor = _____
n/V = pressure/(z – factor x 10.73 x temperature)
    = _____/(_____ x 10.73 x _____)
    = _____ lb-mole/cubic foot

Final pump volume = _____ cc
Final pressure at pump volume = _____ psia
Room temperature = _____ degree R
z – factor = _____
n/V = pressure/(z – factor x 10.73 x temperature)
    = _____/(_____ x 10.73 x _____)
    = _____ lb-mole/cubic feet

Mercury displaced = initial volume – final volume
                  = _____ – _____
                  = _____ cc

Gas displaced = mercury displaced/28,323
              = _____/28,323
              = _____ cubic feet

lb-moles displaced = final n/V x gas displaced
                   = _____ x _____
                   = _____ lb-moles

Gas weight in cell = lb-moles x molecular weight x 453.59
                   = _____ x _____ x 453.59
                   = _____ gm

Oil Calculations:

      Oil type = _____
      Molecular weight = _____ lb/lb-mole
      Specific gravity = _____
      Density = specific gravity x 62.4
             = _____ x 62.4
             = _____ lb/cubic feet

    Volume of oil = _____ cc

    Weight of oil = (volume of oil/28,323) x oil density
             = (_____ /28,323) x _____
             = _____ lb

    lb-moles of oil = weight of oil/molecular weight of oil
             = _____ / _____
             = _____ lb-mole

Composition Calculations:

    Total lb-moles of mixture = lb-moles oil + lb-moles gas
                 = _____ + _____
                 = _____ lb-moles

    Mole % gas = lb-moles gas/total lb-moles x 100
          = _____ / _____ x 100
          = _____ %

    Mole % oil = 100 - mole percent gas
          = 100 - _____
          = _____ %

Appendix B.2:   Methane/drilling-fluid Experiments

The procedure for loading the gas into the PVT cell is the same as outlined in Appendix B.1. The method of loading the drilling fluid into the cell is also the same as outlined in Appendix B.1 but the adsorption of the drilling fluid to the sides of burret and connection hose had to be taken into account in order to reduce errors that would arise in the weight calculations. To do this a new volumetrics calculation sheet, as shown in Table B.2 was developed. The steps for determining the density of the the drilling fluid and the weight percentages of each component in the cell are shown on the sheet and are self explanatory.

When the lb-moles of gas in the PVT cell need to be increased the procedure as described in Appendix B.1 was used.

Table B.2: Methane/drilling fluid Volumetric Calculations

Experiment No._____
Date:_____

Drilling Fluid Calculations:

    1. Clean 100 cc graduated cylinder weight = _____ gm
    2. Volume of sample in graduated cylinder = _____ cc
    3. Weight of graduated cylinder + sample = _____ gm
    4. Density of mud = (3. - 1.)/2.
$$= (\underline{\hspace{2cm}} - \underline{\hspace{3cm}})/\underline{\hspace{2cm}}$$
$$= \underline{\hspace{2cm}} \text{ gm/cc}$$
    5. Weight of clean burret = _____ gm
    6. Weight of clean beaker = _____ gm
    7. Weight of sample + beaker = _____ gm
    8. Weight of sample in beaker = 7. - 6.
$$= \underline{\hspace{2cm}} - \underline{\hspace{2cm}}$$
$$= \underline{\hspace{2cm}} \text{ gm}$$
    9. Weight of beaker after pouring sample into burret =
$$\underline{\hspace{2cm}} \text{ gm}$$
  10. Weight of sample in burret = 7. - 9.
$$= \underline{\hspace{2cm}} - \underline{\hspace{2cm}}$$
$$= \underline{\hspace{2cm}} \text{ gm}$$
  11. Weight of burret after introducing sample into cell =
$$\underline{\hspace{2cm}} \text{ gm}$$
  12. Weight of sample left in burret = 11. - 5.
$$= \underline{\hspace{2cm}} - \underline{\hspace{2cm}}$$
$$= \underline{\hspace{2cm}} \text{ gm}$$
  13. Weight of sample in cell = 10. - 12.
$$= \underline{\hspace{2cm}} - \underline{\hspace{2cm}}$$
$$= \underline{\hspace{2cm}} \text{ gm}$$
  14. Volume of sample in cell = 13./4.
$$= \underline{\hspace{2cm}} / \underline{\hspace{2cm}}$$
$$= \underline{\hspace{2cm}} \text{ cc}$$

Gas Calculations:

    Gas type = _____
    Molecular weight = _____ lb/lb-mole
    Critical temperature = _____ degree R
    Critical pressure = _____ psia

    Initial pump volume = _____ cc
    Initial pressure at pump volume = _____ psia
    Room temperature = _____ degree F
    z - factor = _____
    n/V = pressure/(z - factor x 10.73 x temperature)
$$= \underline{\hspace{2cm}} / (\underline{\hspace{2cm}} \times 10.73 \times \underline{\hspace{2cm}})$$
$$= \underline{\hspace{2cm}} \text{ lb-mole/cubic foot}$$

Final pump volume = _____ cc
Final pressure at pump volume = _____ psia
Room temperature = _____ degree R
z - factor = _____
n/V = pressure/(z - factor x 10.73 x temperature)
    = _____/(_____ x 10.73 x _____)
    = _____ lb-mole/cubic feet

Mercury displaced = initial volume - final volume
                  = _____ - _____
                  = _____ cc

Gas displaced = mercury displaced/28,323
              = _____/28,323
              = _____ cubic feet

lb-moles displaced = final n/V x gas displaced
                   = _____ x _____
                   = _____ lb-moles

Gas weight in cell = lb-moles x molecular weight x 453.59
                   = _____ x _____ x 453.59
                   = _____ gm

Composition Calculations:

Total weight in cell = gas weight + drilling fluid weight
                     = _____ + _____
                     = _____ gm

Weight % gas in cell = weight gas/total weight x 100
                     = _____/_____ x 100
                     = _____ %

Weight % drilling fluid in cell = 100 - percent gas
                                = 100 - _____
                                = _____ %

APPENDIX C: Sample Experimental Procedure

Table C.1 is a listing of raw data taken during an experiment using 22.42 mole percent methane and 77.58 mole percent Mentor 28 low toxic oil. This data, along with the manifold compressibilities, is entered into the calibration program listed in Appendix A, and the calibrated data, as shown in Table C.2, is obtained. Figure C.1 shows the raw date plotted as pressure versus pump volume and the corresponding bubble point pressure. Figure C.2 shows the calibrated data plotted as pressure versus mixture volume and the corresponding bubble point pressure. The advantages of the calibrated data over the raw data is the fact that you have mixture volumes instead of a pump volume which allows calculation of both two-and single-phase densities.

Table C.1: Raw Data

Cell Pressure, psia	Pump Volume, cc	Temperature, Deg F
415.0	1.10	100.0
495.0	50.00	100.0
625.0	100.00	100.0
720.0	120.00	100.0
745.0	130.00	100.0
775.0	135.00	100.0
785.0	137.00	100.0
910.0	139.00	100.0
1280.0	140.00	100.0
1650.0	142.00	100.0
2150.0	144.00	100.0

Table C.2: Calibrated Data

Press.	Cell-Vol	Cell-HG	Smpl-Vol
415.	1017.359	517.053	500.306
495.	1017.372	566.003	451.369
625.	1017.393	616.028	401.365
720.	1017.408	636.011	381.397
745.	1017.412	646.021	371.391
775.	1017.417	651.014	366.403
785.	1017.419	653.012	364.406
910.	1017.439	654.933	362.506
1280.	1017.499	655.713	361.786
1650.	1017.560	657.515	360.044
2150.	1017.641	659.259	358.382

131
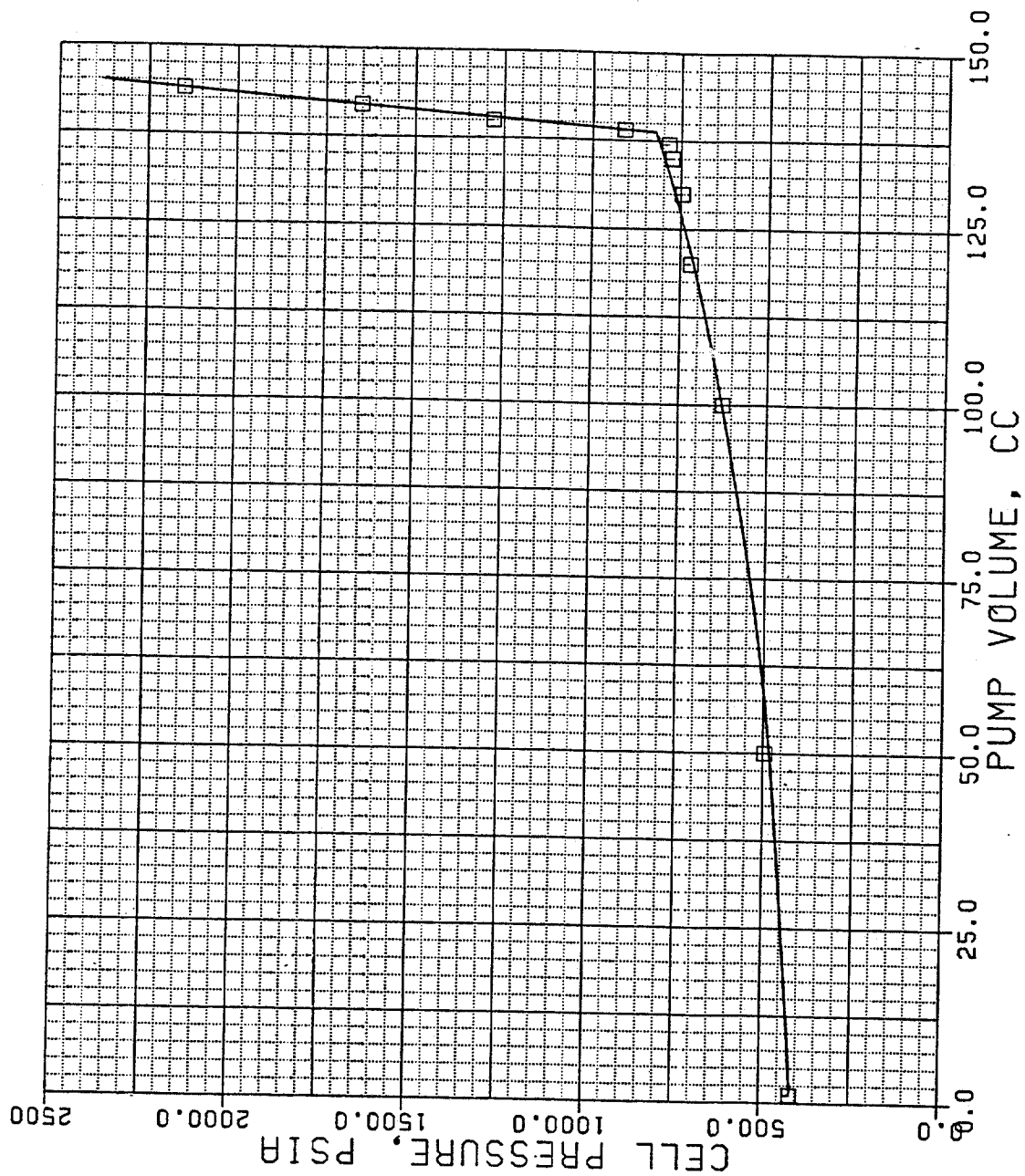
Figure C.1: Experimental Data Before Calibration.
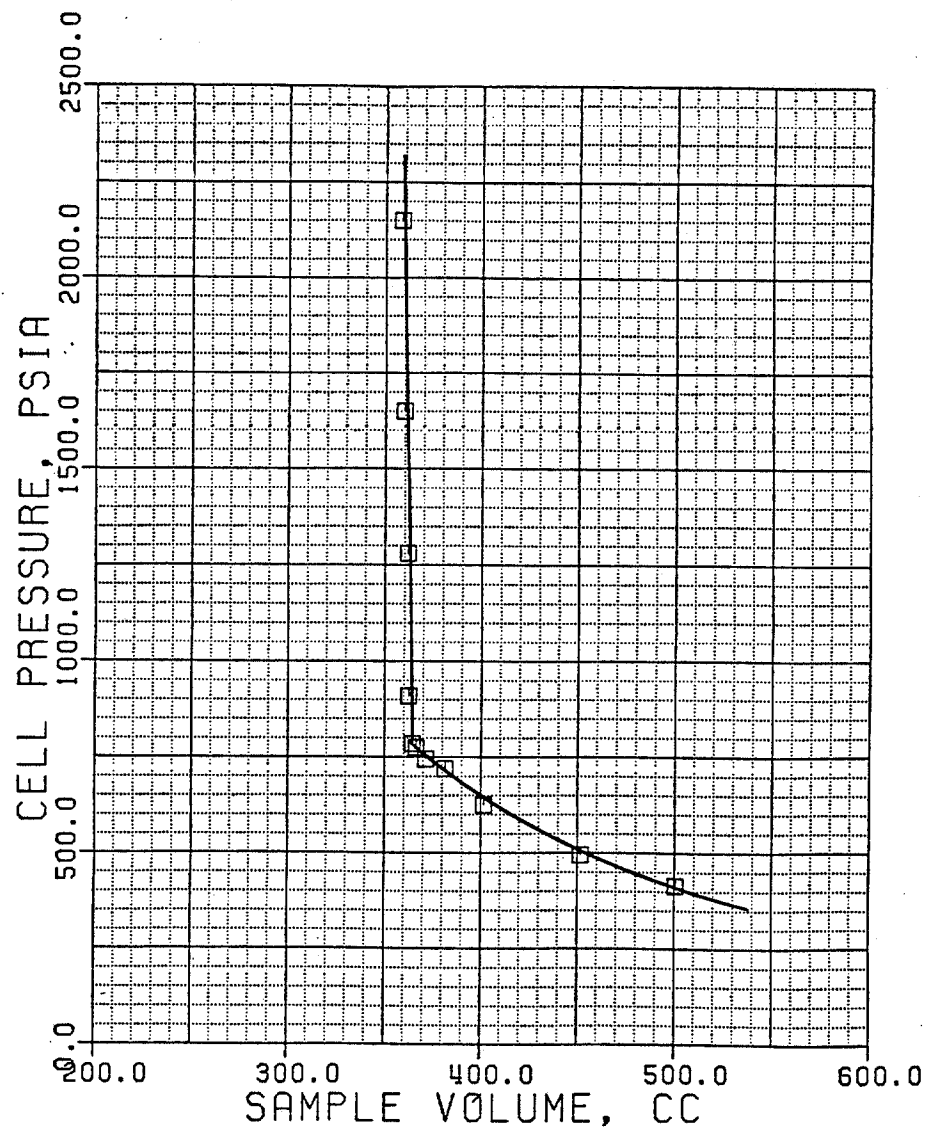
Figure C.2: Experimental Data After Calibration.

APPENDIX D: Calibrated Experimental Data

Appendix D.1: Methane/diesel Data

19.50 mole % Methane
80.50 mole % Diesel
T = 100.0 Deg F

Pressure, psia	Mixture Volume, cc
285.0	262.580
370.0	216.040
430.0	196.066
465.0	186.080
485.0	181.090
510.0	176.104
535.0	171.118
550.0	169.129
560.0	167.135
575.0	165.145
585.0	163.149
600.0	161.159
615.0	159.169
630.0	157.178
650.0	155.193
670.0	153.207
690.0	151.220
710.0	149.234
1040.0	147.529
1610.0	145.987

Bubble Point Pressure, Pbp = 720.0 psia

Bubble Point Density = 7.6587 ppg

30.26 mole % Methane
69.74 mole % Diesel
T = 100.0 Deg F

Pressure, psia	Mixture Volume, cc
490.0	262.625
645.0	216.022
755.0	196.076
830.0	186.119
915.0	176.167
1030.0	166.240
1185.0	156.342
1225.0	154.369
1585.0	152.649
2200.0	151.115

Bubble Point Pressure, Pbp = 1220.0 psia

Bubble Point Density = 7.3866 ppg

32.45 mole % Methane
67.55 mole % Diesel
T = 100.0 Deg F

Pressure, psia	Mixture Volume, cc
455.0	530.187
530.0	482.027
625.0	431.960
770.0	381.928
845.0	361.926
895.0	351.933
950.0	341.945
980.0	336.952
1015.0	331.963
1050.0	326.973
1090.0	321.987
1130.0	317.001
1180.0	312.022
1230.0	307.042
1290.0	302.070
1360.0	297.104
1450.0	292.151
2125.0	289.607
2690.0	287.979
3365.0	286.421

Bubble Point Pressure, Pbp = 1475.0 psia

Bubble Point Density = 6.595 ppg

46.46 mole % Methane
53.54 mole % Diesel
T = 100.0 Deg F

Pressure, psia	Mixture Volume, cc
945.0	481.687
1105.0	436.037
1375.0	386.080
1645.0	356.180
1835.0	341.268
2085.0	326.396
2215.0	320.468
2335.0	316.539
2410.0	313.582
2480.0	311.624
2625.0	308.715
3710.0	305.446

Bubble Point Pressure, Pbp = 2545.0 psia

Bubble Point Density = 6.2684 ppg

56.35 mole % Methane
43.65 mole % Diesel
T = 100.0 Deg F

Pressure, psia	Mixture Volume, cc
1570.0	482.561
1685.0	434.624
2170.0	384.817
2495.0	364.980
2710.0	355.097
2845.0	350.173
3000.0	345.263
3175.0	340.365
3385.0	335.491
3480.0	333.548
3590.0	331.615
3705.0	329.686
3825.0	327.760
4120.0	325.949
4660.0	324.299
5305.0	322.717

Bubble Point Pressure, P_{bp} = 3795.0 psia

Bubble Point Density = 5.9558 ppg

60.40 mole % Methane
39.60 mole % Diesel
T = 100.0 Deg F

Pressure, psia	Mixture Volume, cc
1650.0	482.417
2020.0	432.543
2620.0	386.140
3075.0	366.396
3230.0	361.487
3290.0	359.522
3360.0	357.564
3435.0	355.609
3515.0	353.657
3590.0	351.702
3735.0	348.792
3900.0	345.894
4075.0	343.004
4265.0	340.123
4490.0	337.265
5070.0	334.644

Bubble Point Pressure, Pbp = 4080.0 psia

Bubble Point Density = 5.5838 ppg

Appendix D.2:   Methane/Mentor 28 Data

22.42 mole % Methane
77.58 mole % Mentor 28
T = 100.0 Deg F

Pressure, psia	Mixture Volume, cc
415.0	500.306
495.0	451.396
625.0	401.365
720.0	381.397
745.0	371.391
775.0	366.403
785.0	364.406
910.0	362.506
1280.0	361.786
1650.0	360.044
2150.0	358.382

Bubble Point Pressure, Pbp = 775.0 psia

Bubble Point Density = 7.4032 ppg

30.24 mole % Methane
69.76 mole % Mentor 28
T = 100.0 Deg F

Pressure, psia	Mixture Volume, cc
625.0	500.448
750.0	453.614
965.0	403.654
1130.0	378.713
1180.0	373.737
1200.0	371.747
1530.0	369.983
1950.0	368.274
2440.0	366.608

Bubble Point Pressure, Pbp = 1200.0 psia

Bubble Point Density = 7.1844 ppg

41.95 mole % Methane
58.05 mole % Mentor 28
T = 100.0 Deg F

Pressure, psia	Mixture Volume, cc
1060.0	500.898
1300.0	451.911
1750.0	402.095
1895.0	392.169
1985.0	387.219
2400.0	385.501
2810.0	383.778
3295.0	382.103

Bubble Point Pressure, Pbp = 1985.0 psia

Bubble Point Density = 6.9369 ppg

45.38 mole % Methane
54.62 mole % Mentor 28
T = 100.0 Deg F

Pressure, psia	Mixture Volume, cc
1205.0	501.286
1500.0	452.309
2095.0	402.582
2185.0	397.630
2225.0	395.652
2265.0	393.674
2385.0	391.750
2800.0	390.027
3265.0	388.336

Bubble Point Pressure, Pbp = 2315.0 psia

Bubble Point Density = 6.7972 ppg

50.29 mole % Methane
49.71 mole % Mentor 28
T = 100.0 Deg F

Pressure, psia	Mixture Volume, cc
1500.0	501.849
1890.0	452.911
2315.0	423.124
2535.0	413.246
2660.0	408.318
2720.0	406.353
2785.0	404.392
2850.0	402.431
3225.0	400.678
3695.0	398.987
4235.0	397.342

Bubble Point Pressure, Pbp = 2825.0 psia

Bubble Point Density = 6.6673 ppg

16.33 mole % Methane
83.67 mole % Mentor 28
T = 200.0 Deg F

Pressure, psia	Mixture Volume, cc
400.0	513.341
490.0	463.721
570.0	433.421
640.0	413.233
660.0	408.188
670.0	406.171
780.0	404.240
965.0	403.375
1275.0	401.583

Bubble Point Pressure, Pbp = 670.0 psia

Bubble Point Density = 7.1189 ppg

28.58 mole % Methane
71.42 mole % Mentor 28
T = 200.0 Deg F

Pressure, psia	Mixture Volume, cc
820.0	513.646
1020.0	464.759
1160.0	439.548
1280.0	424.446
1295.0	422.431
1310.0	420.417
1325.0	418.403
1610.0	416.582
2070.0	414.879
2185.0	412.934

Bubble Point Pressure, Pbp = 1340.0 psia

Bubble Point Density = 6.8984 ppg

37.73 mole % Methane
62.27 mole % Mentor 28
T = 200.0 Deg F

Pressure, psia	Mixture Volume, cc
1250.0	514.173
1560.0	466.582
1755.0	446.469
1885.0	436.434
1920.0	434.434
1945.0	432.426
2035.0	430.464
2310.0	428.631
2585.0	426.796
2780.0	424.905
3355.0	423.274

Bubble Point Pressure, Pbp = 1950.0 psia

Bubble Point Density = 6.6685 ppg

42.27 mole % Methane
57.73 mole % Mentor 28
T = 200.0 Deg F

Pressure, psia	Mixture Volume, cc
1515.0	514.839
1940.0	465.448
2140.0	450.401
2175.0	448.400
2220.0	445.394
2255.0	443.394
2290.0	441.394
2325.0	439.393
2650.0	437.595
3020.0	435.827
3385.0	434.054
3800.0	432.313
4235.0	430.586

Bubble Point Pressure, Pbp = 2325.0 psia

Bubble Point Density = 6.5407 ppg

46.25 mole % Methane
53.75 mole % Mentor 28
T = 200.0 Deg F

Pressure, psia	Mixture Volume, cc
1945.0	515.587
2265.0	466.036
2345.0	461.028
2395.0	458.024
2435.0	456.027
2475.0	454.029
2510.0	452.027
2550.0	450.030
2585.0	448.028
2630.0	446.034
2950.0	444.226
3300.0	442.438
3680.0	440.669
4080.0	438.913

Bubble Point Pressure, Pbp = 2660.0 psia

Bubble Point Density = 6.4128 ppg

20.43 mole % Methane
79.57 mole % Mentor 28
T = 300.0 Deg F

Pressure, psia	Mixture Volume, cc
620.0	506.707
765.0	457.080
880.0	431.602
960.0	416.322
1085.0	414.375
1460.0	411.588
1720.0	409.733
2025.0	407.908
2285.0	406.048

Bubble Point Pressure, Pbp = 980.0 psia

Bubble Point Density = 6.9559 ppg

26.19 mole % Methane
73.81 mole % Mentor 28
T = 300.0 Deg F

Pressure, psia	Mixture Volume, cc
860.0	507.006
1070.0	457.202
1130.0	447.017
1195.0	436.835
1235.0	431.750
1250.0	429.715
1275.0	426.664
1290.0	424.629
1305.0	422.594
1485.0	420.683
1685.0	418.785
1935.0	416.921

Bubble Point Pressure, Pbp = 1315.0 psia

Bubble Point Density = 6.7509 ppg

32.73 mole % Methane
67.27 mole % Mentor 28
T = 300.0 Deg F

Pressure, psia	Mixture Volume, cc
1210.0	504.485
1440.0	468.829
1520.0	458.654
1565.0	453.570
1610.0	448.486
1655.0	443.401
1710.0	438.325
1725.0	436.289
1750.0	434.260
1775.0	432.231
1935.0	430.298
2195.0	428.435
2230.0	426.413

Bubble Point Pressure, Pbp = 1780.0 psia

Bubble Point Density = 6.628 ppg

38.39 mole % Methane
61.61 mole % Mentor 28
T = 300.0 Deg F

Pressure, psia	Mixture Volume, cc
1540.0	508.164
1945.0	459.230
2065.0	449.086
2110.0	444.003
2145.0	441.982
2180.0	439.960
2305.0	438.003
2555.0	436.134
2835.0	434.285
3140.0	432.452

Bubble Point Pressure, Pbp = 2199.0 psia

Bubble Point Density = 6.5352 ppg

Appendix D.3:   Methane/Conoco LVT Data

9.91 mole % Methane
90.09 mole % LVT
T = 100.0 Deg F

Pressure, psia	Mixture Volume, cc
185.0	250.441
290.0	181.196
345.0	164.228
360.0	159.234
510.0	157.398
870.0	155.715
1445.0	154.163
3005.0	152.320
4220.0	151.208

Bubble Point Pressure, Pbp = 395.0 psia

Bubble Point Density = 7.6294 ppg

21.49 mole % Methane
78.51 mole % LVT
T = 100.0 Deg F

Pressure, psia	Mixture Volume, cc
435.0	250.479
590.0	210.798
675.0	186.838
745.0	176.874
850.0	164.933
1375.0	162.335
1750.0	160.611
2550.0	159.191
3545.0	157.906

Bubble Point Pressure, Pbp = 875.0 psia

Bubble Point Density = 7.5501 ppg

29.88 mole % Methane
70.12 mole % LVT
T = 100.0 Deg F

Pressure, psia	Mixture Volume, cc
665.0	250.645
930.0	201.805
1015.0	191.848
1140.0	179.916
1225.0	173.967
1295.0	170.010
1685.0	168.298
2205.0	166.677
2835.0	165.132
3735.0	163.780

Bubble Point Pressure, Pbp = 1345.0 psia

Bubble Point Density = 7.3565 ppg

42.84 mole % Methane
57.16 mole % LVT
T = 100.0 Deg F

Pressure, psia	Mixture Volume, cc
965.0	266.357
1155.0	236.949
1240.0	226.971
1345.0	217.006
1475.0	207.055
1645.0	197.127
1865.0	187.228
2015.0	182.302
2085.0	180.338
2630.0	178.649
3335.0	177.053
4225.0	175.564
4690.0	174.831

Bubble Point Pressure, Pbp = 2080.0 psia

Bubble Point Density = 6.2825 ppg

Appendix D.4: Methane/oil-base-drilling-fluid Data

2.90 Weight % Methane
97.10 Weight % 13.0 ppg Drilling Fluid
T = 100.0 Deg F

Pressure, psia	Mixture Volume, cc	Mixture Density, ppg
1025.0	247.746	8.77
1490.0	199.601	10.89
1655.0	189.700	11.46
1760.0	184.767	11.77
1885.0	179.847	12.09
2030.0	174.944	12.43
2205.0	170.061	12.78
2420.0	165.208	13.16
2710.0	160.410	13.55
3105.0	155.688	13.96
3730.0	151.136	14.38
4755.0	149.883	14.50

Bubble Point Pressure, Pbp = 2925.0 psia

Bubble Point Density = 13.85 ppg

3.40 Weight % Methane
96.90 Weight % 13.0 ppg Drilling Fluid
T = 100.0 Deg F

Pressure, psia	Mixture Volume, cc	Mixture Density, ppg
1165.0	248.114	8.54
1710.0	199.936	10.59
2185.0	180.230	11.76
2590.0	170.499	12.43
2875.0	165.694	12.79
3260.0	160.960	13.16
3825.0	156.357	13.55
4135.0	154.577	13.71
4850.0	153.090	13.84
5940.0	151.873	13.95

Bubble Point Pressure, Pbp = 3605.0 psia

Bubble Point Density = 13.41 ppg

4.30 Weight % Methane
95.70 Weight % 13.0 ppg Drilling Fluid
T = 100.0 Deg F

Pressure, psia	Mixture Volume, cc	Mixture Density, ppg
1480.0	248.695	8.56
2210.0	200.865	10.60
2500.0	191.052	11.15
2920.0	181.333	11.74
3200.0	176.525	12.06
3585.0	171.793	12.39
4090.0	167.149	12.74
4825.0	162.672	13.09
5225.0	160.958	13.23
5940.0	159.473	13.35

Bubble Point Pressure, Pbp = 4425.0 psia

Bubble Point Density = 13.01 ppg

0.57 Weight % Methane
99.43 Weight % 13.0 ppg Drilling Fluid
T = 200.0 Deg F

Pressure, psia	Mixture Volume, cc	Mixture Density, ppg
335.0	242.250	10.43
525.0	192.910	13.10
635.0	177.829	14.21
685.0	172.814	14.62
745.0	167.804	15.06
845.0	164.856	15.33
1645.0	163.484	15.46
2395.0	162.035	15.59
3355.0	160.735	15.72
4495.0	159.563	15.84

Bubble Point Pressure, Pbp = 780.0 psia

Bubble Point Density = 15.31 ppg

1.70 Weight % Methane
98.30 Weight % 13.0 ppg Drilling Fluid
T = 200.0 Deg F

Pressure, psia	Mixture Volume, cc	Mixture Density, ppg
1015.0	242.814	10.41
1630.0	194.779	12.98
1900.0	184.862	13.68
2085.0	179.941	14.05
2210.0	176.999	14.28
2445.0	175.152	14.43
3170.0	173.675	14.56
4015.0	172.283	14.67
4830.0	170.866	14.79
5920.0	169.651	14.90

Bubble Point Pressure, Pbp = 2135.0 psia

Bubble Point Density = 14.14 ppg

2.32 Weight % Methane
97.68 Weight % 13.0 ppg Drilling Fluid
T = 200.0 Deg F

Pressure, psia	Mixture Volume, cc	Mixture Density, ppg
1395.0	243.414	10.34
2330.0	195.499	12.93
2540.0	190.595	13.27
2790.0	185.720	13.61
2910.0	183.785	13.76
3040.0	181.858	13.90
3415.0	180.115	14.04
4230.0	178.698	14.15
5115.0	177.330	14.26
5555.0	176.643	14.31

Bubble Point Pressure, Pbp = 2875.0 psia

Bubble Point Density = 13.89 ppg

1.07 Weight % Methane
97.93 Weight % 13.0 ppg Drilling Fluid
T = 300.0 Deg F

Pressure, psia	Mixture Volume, cc	Mixture Density, ppg
515.0	261.237	7.97
700.0	221.044	9.42
815.0	205.767	10.12
915.0	195.596	10.65
1050.0	185.448	11.23
1170.0	178.359	11.68
1285.0	173.315	12.02
1360.0	170.292	12.23
1450.0	167.278	12.45
1515.0	165.272	12.61
1595.0	163.276	12.76
1865.0	161.396	12.91
2570.0	159.787	13.04
3550.0	158.349	13.16
4770.0	157.057	13.26

Bubble Point Pressure, Pbp = 1600.0 psia

Bubble Point Density = 12.82 ppg

2.32 Weight % Methane
97.68 Weight % 13.0 ppg Drilling Fluid
T = 300.0 Deg F

Pressure, psia	Mixture Volume, cc	Mixture Density, ppg
1770.0	238.523	10.60
2345.0	210.393	12.01
2680.0	200.414	12.62
2905.0	195.469	12.94
3155.0	190.541	13.27
3600.0	188.831	13.39
4680.0	186.572	13.55
5400.0	185.063	13.66
5805.0	184.342	13.72

Bubble Point Pressure, Pbp = 3080.0 psia

Bubble Point Density = 13.12 ppg

2.52 Weight % Methane
97.48 Weight % 13.0 ppg Drilling Fluid
T = 300.0 Deg F

Pressure, psia	Mixture Volume, cc	Mixture Density, ppg
1945.0	239.269	10.77
2445.0	216.051	11.93
2765.0	206.139	12.50
2970.0	210.228	12.81
3115.0	198.303	12.99
3220.0	196.362	13.12
3330.0	194.426	13.26
3645.0	192.694	13.38
4210.0	191.210	13.48
4855.0	189.806	13.58
5525.0	188.427	13.68

Bubble Point Pressure, Pbp = 3275.0 psia

Bubble Point Density = 13.22 ppg

Appendix D.5: Methane/emulsifier Data

1.104 Weight % Methane
98.896 Weight % Emulsifier
T = 100.0 Deg F

Pressure, psia	Mixture Volume, cc
135.0	267.579
180.0	218.061
225.0	188.023
275.0	168.011
325.0	153.008
400.0	138.020
485.0	128.049
535.0	123.068
605.0	118.098
660.0	115.124
725.0	112.156
1275.0	109.475
2395.0	108.122
4045.0	107.072

Bubble Point Pressure, Pbp = 800.0 psia

2.454 Weight % Methane
97.546 Weight % Emulsifier
T = 100.0 Deg F

Pressure, psia	Mixture Volume, cc
300.0	267.568
400.0	218.076
505.0	188.071
615.0	168.091
735.0	153.128
930.0	138.209
1145.0	1128.312
1300.0	123.392
1425.0	120.458
1585.0	117.545
1890.0	114.716
2740.0	113.208
4030.0	111.953

Bubble Point Pressure, Pbp = 1840.0 psia

4.03 Weight % Methane
95.97 Weight % Emulsifier
T = 100.0 Deg F

Pressure, psia	Mixture Volume, cc
495.0	267.633
660.0	281.222
835.0	188.258
1025.0	168.325
1240.0	153.417
1455.0	143.521
1790.0	133.694
2045.0	128.832
2420.0	124.038
2905.0	120.311
3765.0	117.802
5080.0	116.556

Bubble Point Pressure, Pbp = 2590.0 psia

0.965 Weight % Methane
99.035 Weight % Emulsifier
T = 200.0 Deg F

Pressure, psia	Mixture Volume, cc
140.0	269.510
220.0	199.691
290.0	169.364
375.0	149.171
480.0	134.051
600.0	124.001
695.0	118.998
1240.0	116.297
2185.0	114.847
3650.0	113.708

Bubble Point Pressure, Pbp = 770.0 psia

2.074 Weight % Methane
97.926 Weight % Emulsifier
T = 200.0 Deg F

Pressure, psia	Mixture Volume, cc
295.0	269.490
465.0	199.283
625.0	169.009
760.0	153.905
895.0	143.863
1095.0	133.859
1240.0	128.885
1390.0	124.926
1545.0	121.982
2310.0	119.405
3445.0	118.059
4960.0	116.934

Bubble Point Pressure, Pbp = 1725.0 psia

4.03 Weight % Methane
95.97 Weight % Emulsifier
T = 200.0 Deg F

Pressure, psia	Mixture Volume, cc
575.0	269.811
780.0	220.068
915.0	199.898
1110.0	179.765
1335.0	164.713
1545.0	154.714
1685.0	149.736
1855.0	144.776
2075.0	139.846
2375.0	134.963
2715.0	131.117
3060.0	128.286
3450.0	126.495
4585.0	125.148
5255.0	124.534

Bubble Point Pressure, Pbp = 3215.0 psia

0.878 Weight % Methane
99.122 Weight % Emulsifier
T = 300.0 Deg F

Pressure, psia	Mixture Volume, cc
140.0	268.800
215.0	197.791
285.0	167.155
370.0	146.754
435.0	136.568
535.0	126.405
600.0	121.332
765.0	116.323
1195.0	114.547
2070.0	113.044
3435.0	111.837

Bubble Point Pressure, Pbp = 750.0 psia

2.074 Weight % Methane
97.926 Weight % Emulsifier
T = 300.0 Deg F

Pressure, psia	Mixture Volume, cc
340.0	271.576
505.0	210.832
675.0	180.259
880.0	159.934
1035.0	149.804
1280.0	139.729
1455.0	134.725
1695.0	129.761
2290.0	128.085
3300.0	126.663
3965.0	126.048

Bubble Point Pressure, Pbp = 1800.0 psia

3.60 Weight % Methane
96.40 Weight % Emulsifier
T = 300.0 Deg F

Pressure, psia	Mixture Volume, cc
545.0	268.966
740.0	218.461
870.0	198.087
1055.0	177.746
1260.0	162.532
1450.0	152.421
1720.0	142.360
1910.0	137.364
2150.0	132.397
2330.0	129.440
2560.0	126.512
2850.0	123.621
3645.0	122.061
4805.0	120.720
5515.0	120.126

Bubble Point Pressure, Pbp = 3200.0 psia

Appendix D.6: Supplemental Methane/drilling-fluid Data

1.25 Weight % Methane
98.75 Weight % 13.0 ppg Drilling Fluid
T = 100.0 Deg F

Pressure, psia	Mixture Volume, cc	Mixture Density, ppg
390.0	260.962	7.22
560.0	211.627	8.91
760.0	181.668	10.38
1020.0	161.772	11.65
1125.0	156.882	12.02
1250.0	151.883	12.41
1695.0	147.138	12.81
2535.0	145.636	12.94
3760.0	144.361	13.06

Bubble Point Pressure, Pbp = 1360.0 psia

Bubble Point Density = 12.74 ppg

2.95 Weight % Methane
97.05 Weight % 13.0 ppg Drilling Fluid
T = 100.0 Deg F

Pressure, psia	Mixture Volume, cc	Mixture Density, ppg
880.0	261.240	7.35
1260.0	212.243	9.04
1790.0	182.562	10.51
2675.0	163.091	11.77
2940.0	160.249	11.98
3165.0	158.383	12.12
4325.0	156.071	12.30
4910.0	155.418	12.35

Bubble Point Pressure, P_{bp} = 3050.0 psia

Bubble Point Density = 12.14 ppg

4.18 Weight % Methane
95.82 Weight % 13.0 ppg Drilling Fluid
T = 100.0 Deg F

Pressure, psia	Mixture Volume, cc	Mixture Density, ppg
1225.0	261.540	7.43
1765.0	213.896	9.09
2615.0	184.405	10.54
4555.0	165.565	11.74
4795.0	164.691	11.80
5055.0	163.864	11.86
6270.0	162.587	11.96
6915.0	161.971	12.00

Bubble Point Pressure, Pbp = 4250.0 psia

Bubble Point Density = 11.85 ppg

APPENDIX E: Linear Regression Error Analysis

To curve fit two sets of data, X and Y, by linear regression to a straight line equation, given as:

$$Y = bX \qquad\qquad (E.1)$$

where b = the slope of the line

X = value for which Y is a function of

Y = product of b and X

the slope, b, of the line will be found by,

$$b = \frac{\Sigma XY - n\bar{X}\bar{Y}}{\Sigma X^2 - nX^2} \qquad\qquad (E.2)$$

where n = number of X and Y sets

$\bar{X}$ = average of the X values

$\bar{Y}$ = average of the Y values.

The standard error of estimate of the linear regressed line is determined by,

$$S_e = \frac{\Sigma(Y - \bar{Y})^2}{n - 2} \qquad\qquad (E.3)$$

where Y = the predicted estimate using linear regressed equation

S_e = standard error of estimate.

The standard error of the regression coefficient can be found with,

$$S_b = \frac{S_e}{\Sigma X^2 - n\bar{X}^2} \qquad\qquad (E.4)$$

where S_b = standard error of the regression

coefficient.

Once the standard error of the regression coefficient has been found along with the slope of the line and the degree of freedom given as,

$$\text{degrees of freedom} = n - 2 \qquad \text{(E.5)}$$

where n = number of X and Y data sets,

the upper and lower limits of the slope for a given confidence interval can be found with,

$$\text{upper limit} = b + t(S_b) \qquad \text{(E.6)}$$

and,

$$\text{lower limit} = b - t(S_b) \qquad \text{(E.7)}$$

where b = slope of the line

S_b = standard error of the regression coefficient

t = t-distribution determined from Levin and

Rubin as a function of the degrees of free-

dom and the confidence interval.

Using the above outlined procedure, the upper and lower limits for the methane in drilling fluid, oil, and emulsifier curve fits were determined for a 90 percent confidence interval. It was felt that because methane

is so insoluble in brine that an analysis of this type
would not be meaningful and therefore was not conducted.
However Figures 3.10 and 3.11 were curve fitted for
analysis outlined in Appendix F. All the curve fitted
equations and there upper and lower limits are summarized
in Table E.1.

Table E.1: Linear Regression Fits of Experimental Data

Methane/drilling-fluid

T = 100 degree F:

Pbp(lower limit) = 959.663XC1

Pbp(upper limit) = 1110.98XC1

Pbp(mean) = 1035.32XC1

T = 200 degree F:

Pbp(lower limit) = 1195.65XC1

Pbp(upper limit) = 1354.28XC1

Pbp(mean) = 1274.97XC1

T = 300 degree F:

Pbp(lower limit) = 1215.66XC1

Pbp(upper limit) = 1808.77XC1

Pbp(mean) = 1512.21XC1

Methane/Mentor 28

T = 100 degree F:

XC1(lower limit) = 2.017E-03Pbp

XC1(upper limit) = 2.256E-03Pbp

XC1(mean) = 2.136E-03Pbp

T = 200 degree F:

XC1(lower limit) = 1.861E-03Pbp

XC1(upper limit) = 2.025E-03Pbp

XC1(mean) = 1.9427E-03Pbp

T = 300 degree F:

XC1(lower limit) = 1.652E-03Pbp

T = 300 degree F (cont.):

   XCl(upper limit) = $1.879E-03Pbp$

   XCl(mean) = $1.7652E-03Pbp$

Methane/emulsifier

T = 100 degree F:

   XCl(lower limit) = $1.189E-03Pbp$

   XCl(upper limit) = $1.368E-03Pbp$

   XCl(mean) = $1.2785E-03Pbp$

T = 200 degree F:

   XCl(lower limit) = $1.0083E-03Pbp$

   XCl(upper limit) = $1.352E-03Pbp$

   XCl(mean) = $1.18E-03Pbp$

T = 300 degree F:

   XCl(lower limit) = $7.45E-04Pbp$

   XCl(upper limit) = $1.417E-03Pbp$

   XCl(mean) = $1.081E-03Pbp$

Methane/brine

   Methane solubility = $A + BT + CT^2$

   $A = 5.5601 + 8.49E-03Pbp - 3.064E-07Pbp^2$

   $B = -0.03484 - 4.0E-05Pbp$

   $C = 6.0E-05 + 1.5102E-07Pbp$

   Salinity correction = $e^{bx(solids)}$

   $b = -.06 + 6.69E-05T$

Nomenclature

P_{bp} = Methane/drilling-fluid bubble point pressure, psia

X_{C1} = weight % methane

Methane solubility (brine) = scf methane/bbl of H_2O

$$\text{Salinity correction} = \frac{\text{scf methane soluble in brine}}{\text{scf methane soluble in water}}$$

T = temperature, degree F

APPENDIX F: Procedures For Experimental Analysis

The procedure for determining the relative amounts
of methane dissolved in each liquid phase of the oil-base
drilling fluid is outlined in Table F.1. To calculate
the weight percent methane dissolved in each component at
the bubble point pressure of the methane/drilling-fluid
system in question (lines 13, 22, and 25), the linear
regression curve fitted equations presented in Table E.1
of Appendix E were used. To determine the maximum and
minimum amounts of methane not accounted for, as shown in
Table 3.12, it was necessary to evaluate these equations
for every possible combination. Since this requires many
calculations a FORTRAN program was written to do these
calculations and is shown.

Table F.1:   Procedures For Calculating Relative
             Amounts of Cl Reacting With Drilling
             Fluid Components.

Weight % Cl = _____ %   Temperature, T = _____ °F
Weight % Drilling Fluid = _____ %

1. Volume of drilling fluid = _____ cc

2. Density of drilling fluid = a. _____ gm/cc = b. _____ ppg

3. Weight of drilling fluid = 1. x 2.
                             = _____ x _____
                             = _____ gm

4. Oil:water ratio = a. _____ :b. _____

5. Base oil density = _____ gm/cc

6. _____ ppm brine density = _____ gm/cc

7. Oil & brine density = (4a. x 5.) + (4b. x 6.)
                        = (_____ x _____) + (_____ x _____)
                        = a. _____ gm/cc = b. _____ ppg

8. Volume of oil & brine in 1. = (35. − 2b.)/(35. − 7b.) x 1.
                                = (35. − _____)/(35. − _____) x _____
                                = _____ cc

9. Volume of oil in 1. = 4a. x 8.
                        = _____ x _____
                        = _____ cc

10. Volume of brine in 1. = 8. − 9.
                          = _____ − _____
                          = _____ cc

11. Pounds of Cl dissolved in 1. = _____ lbs

12. Bubble point pressure = _____ psia

13. Weight % Cl dissolved in oil needed for 12. = _____ psia

14. Pounds of oil in 1. = (9. x 5.)/453.052
                        = (_____ x _____)/453.052
                        = _____ lbs

15. Pounds of Cl dissolved in oil at 12. = (13. x 14.)/(100 − 13.)
                                         = (_____ x _____)/(100 − _____)
                                         = _____ lbs

16. Pounds of Cl left to react with other drilling components
    = 11. - 15.
    = _____ - _____ = _____ lbs

17. Volume of drilling fluid mixed = _____ cc

18. Volume of emulsifier used in 17. = _____ cc

19. Emulsifier volume:drilling fluid volume ratio = 18./17.
    = _____/_____
    = _____

20. Volume of emulsifier in 1. = 1. x 19.
    = _____ x _____
    = _____ cc

21. Pounds of emulsifier in 1. = 20. x .925 gm/cc
    = _____ x .925 gm/cc
    = _____ gm/453.052
    = _____ lbs

22. Weight % Cl dissolved in emulsifier needed for 12. = _____ %

23. Pounds of Cl dissolved in emulsifier at 12.
    = (22. - 21.)/(100 - 22.)
    = (_____ - _____)/(100 - _____)
    = _____ lbs

24. Pounds of Cl left to react with other drilling components
    = 16. - 23.
    = _____ - _____
    = _____ lbs

25. Solubility of Cl in pure water at T = _____ scf/bbl

26. Salinity correction factor at _____ ppm = _____

27. Solubility of Cl in brine = 26. x 25.
    = _____ x _____
    = _____ scf/bbl]

28. Volume of Cl dissolved in brine = 6.2898E-06 x 10. x 27.
    = 6.2898E-06 x _____ x _____
    = _____ scf

29. Pounds of Cl dissolved in brine = (28./379.4) x 16.04
    = (_____/379.4) x 16.04
    = _____ lbs

30. Pounds of Cl left to react with other drilling components
    = 24. - 29.
    = _____ - _____
    = _____ lbs

```fortran
      PROGRAM ANALYS
C
C THIS  PROGRAM  TAKES  THE VALUES OF  THE  MAXIMUM  AND
C MINIMUM LIMITS OF THE LINEAR REGRESSION FITTED EXPERI-
C MENTAL DATA PRESENTED  IN TABLE E.1 AND  EVALUATES ALL
C POSSIBLE  COMBINATIONS  FOR A  GIVEN  WEIGHT % METHANE
C DISSOLVED IN THE DRILLING FLUID AT A GIVE TEMPERATURE.
C
C             PROGRAMMED BY PATRICK O'BRYAN
C                 LOUISIANA STATE UNIVERSITY
C
      DIMENSION BPBP(3),BOIL(3),BEML(3)
C
C THE MAXIMUM, MEAN, AND  MINIMUM VALUES OF THE  SLOPES
C FOR THE  METHANE/OIL, DRILLING FLUID, AND  EMULSIFIER
C REGRESSION FITTED CURVES ARE ENTERED HEAR IN THE FORM
C OF DATA STATEMENTS.
C
      DATA BPBP/1512.21,1808.76,1215.66/
      DATA BOIL/.0017652,.001879,.001652/
      DATA BEML/.001081,.001417,.000745/
C
C ENTER  WEIGHT  OF DRILLING  FLUID MIXED WITH METHANE,
C WEIGHT  OF  EMULSIFIER  IN GIVEN  WEIGHT  OF DRILLING
C FLUID, TEMPERATURE, AND WEIGHT % METHANE THAT WILL BE
C DISSOLVED IN THE DRILLING FLUID.
C
      WRITE(*,'(A$)') 'ENTER WEIGHT OF OIL IN MUD, LB: '
      READ(*,'(BN,F6.1)')WTOIL
      WRITE(*,'(A$)') 'ENTER WEIGHT OF EMUL IN MUD, LB: '
      READ(*,'(BN,F15.9)')WTEML
      WRITE(*,'(A$)') 'ENTER TEMPERATURE, F: '
      READ(*,'(BN,F5.1)')T
  100 WRITE(*,'(A$)') 'ENTER WEIGHT % C1 IN MUD: '
      READ(*,'(BN,F5.2)')XC1
      WRITE(*,'(A$)') 'ENTER C1 WT DISSOLVED IN MUD, LB: '
      READ(*,'(BN,F15.9)')WTC1
      OPEN(6,FILE='PRINTER:')
      WRITE(6,11)
   11 FORMAT(32X,'LINEAR REGRESSION ERROR ANALYSIS')
      WRITE(6,12)
   12 FORMAT(32X,'------ ---------- ----- --------',///)
      WRITE(6,13)XC1
   13 FORMAT('WEIGHT % C1 DISSOLVED IN MUD = ',F3.1,' %')
      WRITE(6,14)T
   14 FORMAT('TEMPERATURE = ',F5.1,' F',/)
C
C M = LINEAR REGRESSION SLOPE
C
      WRITE(6,15)
   15 FORMAT('(1)-MAX, MIN, MEAN LIN REG M (C1/MUD)')
      WRITE(6,16)
```

```
      16 FORMAT('(2)-MAX, MIN, MEAN LIN REG M (C1/OIL)')
         WRITE(6,17)
      17 FORMAT('(3)-MAX, MIN, MEAN LIN REG M (C1/EML)')
         WRITE(6,18)
      18 FORMAT('(4)-PERCENT C1 DISSOLVED IN OIL, %')
         WRITE(6,19)
      19 FORMAT('(5)-PERCENT C1 DISSOLVED IN EMULSIFIER, %')
         WRITE(6,20)
      20 FORMAT('(6)-PERCENT C1 NOT ACCOUNTED FOR, %',/)
         WRITE(6,21)
      21 FORMAT('CONFIDENCE LEVEL IS 90.0 %',///)
         WRITE(6,22)
      22 FORMAT('  (1)     (2)     (3)     (4)     (5)     (6)')
         WRITE(6,23)
      23 FORMAT('  ---     ---     ---     ---     ---     ---')
C
C THE ANALYSIS BEGINS HERE.
C
         DO 5 K=1,3
         BP=BPBP(K)
         DO 4 L=1,3
         BO=BOIL(L)
         DO 3 M=1,3
         BE=BEML(M)
         PBP=(BP*XC1)
         XC1OIL=(BO*PBP)
         WC1OIL=(((XC1OIL/100.)*WTOIL)/(1.-(XC1OIL/100.)))
         XC1EML=(BE*PBP)
         WC1EML=(((XC1EML/100.)*WTEML)/(1.-(XC1EML/100.)))
         WC1LFT=WTC1-WC1OIL-WC1EML
         PC1OIL=(WC1OIL/WTC1)*100.
         PC1EML=(WC1EML/WTC1)*100.
         PC1LFT=(WC1LFT/WTC1)*100.
         WRITE(6,1)BP,BO,BE,PC1OIL,PC1EML,PC1LFT
       1 FORMAT(F7.2,3X,F7.6,3X,F7.6,3X,F6.2,3X,F5.2,3X,F6.2)
       3 CONTINUE
       4 CONTINUE
       5 CONTINUE
         WRITE(*,'(A$)') 'ENTER 1 FOR NEW RUN: '
         READ(*,'(BN,I1)')I
         IF(I.EQ.1)THEN
          GO TO 100
         ENDIF
         END
```

VITA

Patrick Leon O'Bryan is the son of Mr. and Mrs. L.K. O'Bryan of Brandon, MS. He was born in Hattiesburg, MS on August 17, 1961. He married Pamela Elizabeth Bramlett, of Brandon, in August, 1983. He graduated from Brandon High School in 1979 and then attended Mississippi State University where he recieved a Bachelor of Science degree in Petroleum Engineering in May, 1983. In September, 1983 he began work on a Master of Science degree in Petroleum Engineering at Louisiana State University.
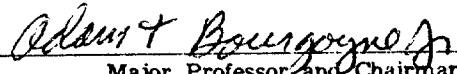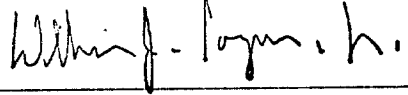
MASTER'S EXAMINATION AND THESIS REPORT

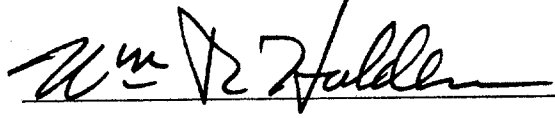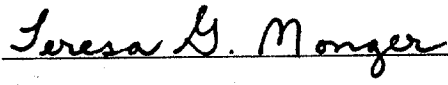**Candidate:**   Patrick Leon O'Bryan

Major Field: Petroleum Engineering

Title of Thesis: The Experimental And Theoretical Study Of Methane Solubility In An Oil-Base Drilling Fluid

Approved:

_____
Major Professor and Chairman

_____
Dean of the Graduate School

EXAMINING COMMITTEE:

_____

_____

_____

_____

_____

Date of Examination:

_____

November 21, 1985

0.965 Weight % Methane
99.035 Weight % Emulsifier
T = 200.0 Deg F

Pressure, psia	Mixture Volume, cc
140.0	269.510
220.0	199.691
290.0	169.364
375.0	149.171
480.0	134.051
600.0	124.001
695.0	118.998
1240.0	116.297
2185.0	114.847
3650.0	113.708

Bubble Point Pressure, Pbp = 770.0 psia